



PRINTABLE

Flexible
Electronic
Platforms
for NASA
Missions

S
P
A
C
E
C
R
A
F
T



Phase Two Report
Kendra Short
David Van Buren
September 2014

FINAL REPORT

EARLY STAGE INNOVATION

NASA INNOVATIVE ADVANCED CONCEPTS (NIAC)

PHASE 2

PRINTABLE SPACECRAFT:

Flexible Electronic Platforms for NASA Missions

Kendra Short, Principal Investigator
David Van Buren, Co-Investigator
Jet Propulsion Laboratory

September 10, 2014

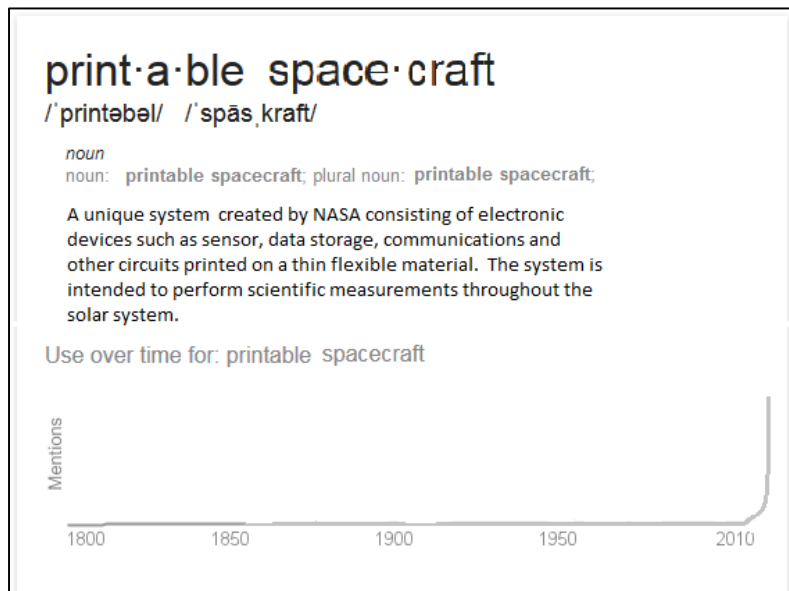
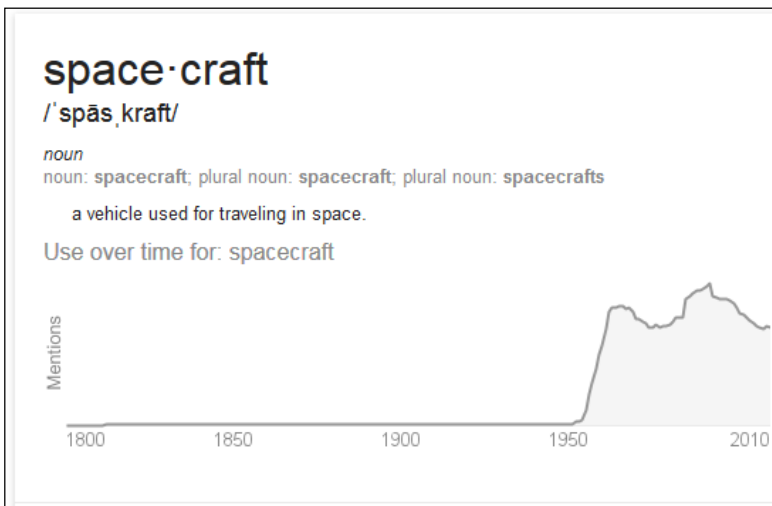
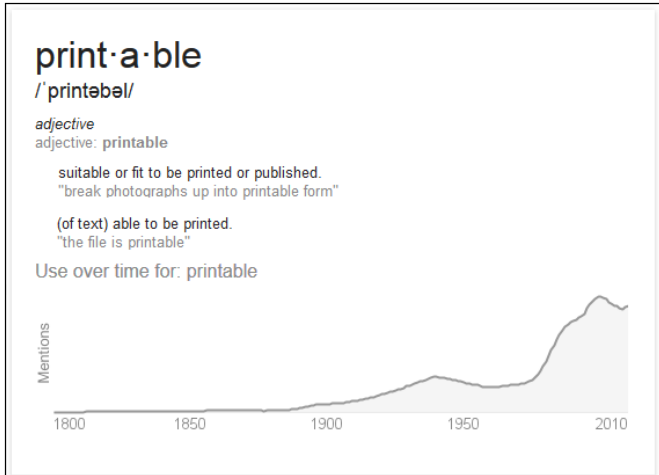
Restrictive Notice

The information (data) contained in this document may be subject to U.S. export laws and regulations. It is furnished to NASA with the understanding that it will not be made publicly available prior to full and complete review for Export Compliance.

Contents

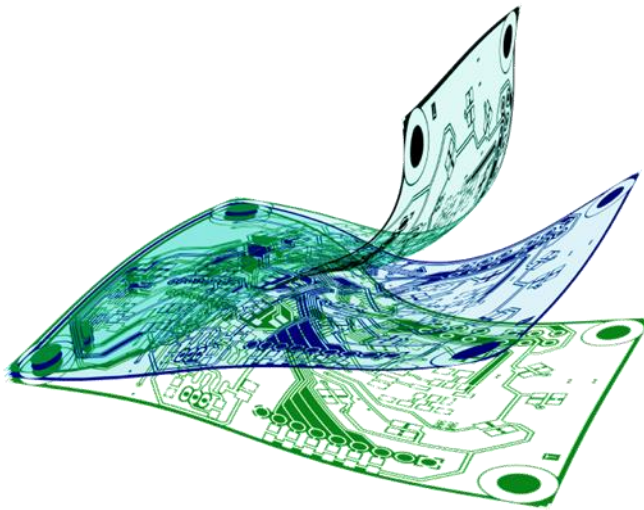
1	INTRODUCTION.....	1-5
1.1	Why Printed Electronics?	1-5
2	PHASE TWO STUDY APPROACH AND SYNOPSIS	2-7
3	TECHNOLOGY OVERVIEW	3-10
3.1	The Basic Elements.....	3-10
3.2	Hybrid and Integrated	3-11
4	BENEFITS AND APPLICATIONS	4-12
4.1	Benefits and Advantageous Characteristics.....	4-12
4.2	Applications	4-12
4.2.1	Engineering Applications:.....	4-13
4.2.2	Science Missions	4-14
5	REFERENCE MISSION.....	5-15
5.1	Introduction.....	5-15
5.2	Science Motivation	5-15
5.3	Previous Network Missions and Human Exploration Concepts.....	5-16
5.3.1	MESUR Network	5-16
5.3.2	Pascal	5-17
5.3.3	MetNet	5-18
5.3.4	Human Exploration Precursor Data	5-19
5.3.5	Human Assisted Science Missions.....	5-20
5.3.6	Summary of Previous Network Concepts	5-21
5.4	STANLE Reference Mission	5-22
5.4.1	Mission and Vehicle Overview:.....	5-24
5.4.2	Aerodynamics and distribution	5-25
5.4.3	STANLE Platform Design	5-26
5.4.4	Study Considerations.....	5-41
6	STANLE REFERENCE MISSION – SCORECARD	6-44
6.1	Overview	6-44
6.2	Technical Design Changes.....	6-45
6.3	Cost Comparison.....	6-47
6.4	Mass Comparison.....	6-50
6.5	Summary – Scorecard.....	6-51
6.6	Alternative Implementations.....	6-51
7	PROTOTYPE DEVELOPMENT AND DEMONSTRATION	7-52
8	ENVIRONMENTAL TESTING.....	8-66
8.1	Motivation for test program.....	8-66
8.2	The Test Program.....	8-66

8.3	Test Samples	8-67
8.4	Results.....	8-68
9	ROADMAPS.....	9-72
9.1	NASA Technology Roadmaps and Applications for Printed Electronics	9-72
9.2	Printed Electronics Technology Area Roadmap.....	9-72
9.3	STANLE Mission Roadmap	9-73
10	SUMMARY AND CONCLUSIONS.....	10-76
10.1	Summary	10-76
10.2	Conclusions.....	10-76
11	ACKNOWLEDGEMENTS	11-78
12	REFERENCES	12-79
13	APPENDIX A – ENVIRONMENTAL TEST REPORT	13-83



1 Introduction

1.1 Why Printed Electronics?



universal...

...impactful

...progressive

Why printed electronics? Why should NASA use printed electronics to make a spacecraft? Three words provide the answer *universal* *impactful* ... *progressive*. The technology is universal because the applications it can affect are broad and diverse from simple sensors to fully functional spacecraft. The impact of flexible, printed electronics range from straightforward mass, volume and cost savings all the way to enabling new mission concepts. The benefits of the technology will become progressively larger from what is achievable today so that investments will pay dividends tomorrow, next year and next decade.

We started off three years ago asking the question can you build an entire spacecraft out of printed electronics? In other words, can you design and fabricate a fully integrated, electronic system that performs the same end to end functions of a spacecraft - take scientific measurements, perform data processing, provide data storage, transmit the data, powers itself, orients and propels itself – all out of thin flexible sheets of printed electronics? This “Printable Spacecraft” pushes the limits of printed flexible electronics performance. So the answer is yes, more or less. In our studies for the NIAC program, we have explored this question further, to explain more completely what “more or less” means and to outline what is needed to make the answer a definitive “yes”.

Despite its appealing “Flat Stanley” like qualities, making a Printable Spacecraft is not as easy as flattening the Cassini spacecraft with a bulletin board, as was Stanley Lamchop’s fate.* But, if NASA invests in the design challenges, the materials challenges, the performance challenges of printed electronics, it might find itself with a spacecraft that can enable as many

* All references to Flat Stanley are to the original book series by Jeff Brown. This book series inspired the international Flat Stanley Project which encourages global literacy started by Dale Hubert in 1994. Please refer to their website www.flatstanley.com for further information about this highly valuable project and this beloved character.

adventures and advantages as Flat Stanley including putting it in an envelope and mailing it to the planet of your choice. You just have to let your imagination take over.

In this report we document the work of the Phase 2 Printable Spacecraft task conducted under the guidance and leadership of the NASA Innovative Advanced Concepts (NIAC) program. In Phase One of the NIAC task entitled “Printable Spacecraft”, we investigated the viability of printed electronics technologies for creating multi-functional spacecraft platforms. Mission concepts and architectures that could be enhanced or enabled with this technology were explored. In Phase 2 we tried to answer the more practical questions such as can you really build a multifunctional printed electronic spacecraft system? If you do, can it survive the space environment? Even if it can, what benefit does a printable system provide over a traditional implementation of a spacecraft?

2 Phase Two Study Approach and Synopsis

The primary goal of the Phase II effort is to study major feasibility issues associated with cost, performance, development time and key technologies. These results are aimed at providing a sound basis for NASA to consider the concept for further development and a future mission, substantiated with a description of applicable scientific and technical disciplines necessary for development. Toward that end, the proposed Phase II study must:

- Continue to assess the concept in a mission context — the main focus should be feasibility and comparing properties/performance with those of current missions/concepts. Concepts that may support multiple missions should discuss the range, but must feature detailed analysis for at least one candidate mission.*
- Assess the programmatic benefits and cost versus performance of the proposed concept — show the relationship between the concept's complexity and its benefits, cost, and performance.*
- Develop a pathway for development of a technology roadmap and identify the key enabling technologies*

This solicitation seeks concepts that could open new possibilities for NASA missions or activities, or enable revolutionary improvement in terms of performance, weight, cost, reliability, operational simplicity, or other figures of merit associated with aerospace endeavors.

- Excerpt from the NIAC Phase Two Call for Proposals

At the end of the Phase One report, we identified the “Risks and Challenges” of a printable spacecraft which intentionally laid the basis for the Phase Two scope of work. For the concept of a printable spacecraft to succeed there are both technical and programmatic concerns that must be addressed. Technical feasibility involves questions about sufficient performance to achieve desired functionality, system integration issues, and environmental compatibilities. The primary programmatic threat for a printed spacecraft is not achieving an adequate cost/benefit ratio. In other words, the implementation costs remain too high, and the science return does not justify the cost. For uniquely enabled applications, ones that cannot be achieved any other way, the benefit may be so high that performance and cost may not be significant drivers. However, for applications in which traditional platforms can do the job, then the printed platform needs to show a significant benefit (e.g. less mass, volume or cost) for similar functionality.

Our team proposed five specific tasks aimed at addressing the technical and programmatic feasibility of a printed spacecraft. These tasks were: (1) define a reference mission which exploits a printed spacecraft, (2) build a functional prototype of a printed spacecraft, (3) conduct environmental testing on materials and devices (4) perform a cost/benefit analysis within the context of the reference mission (5) prepare roadmaps for the reference mission and other applications.

Reference Mission:

We defined a Mars environmental meteorological network as our reference mission. The mission would consist of thousands of small sheets of printed electronic science stations which would flutter to the surface after being released from their entry vehicle. With an intended lifetime of one year, the science stations measure valuable environmental parameters during diurnal and annual cycles. This reference mission, named STANLE, provided a consistent benchmark and rationale for the subsequent tasks of the Phase Two effort. It provided a basis for comparison with a traditional mission against key metrics to determine programmatic benefit. It was a driver for the requirements of the point design of the prototype printed spacecraft fabrication. The reference mission also provided a focused set of environmental requirements to evaluate compatibility of materials and components in the environmental test program. The reference mission defined the end state of functionality and readiness so that a roadmap from current capabilities to desired functionality could be created. The STANLE mission concept and a description of the science station point design is described in Chapter 5.



Reference Mission Cost / Benefit Analysis:

JPL has a unique capability in the engineering design team known as Team X. This is a concurrent design environment specifically formulated to generate conceptual mission designs and perform trade studies. We leveraged the experience within Team X to study the cost, mass and risks associated with implementing the reference mission using the printed electronics landers compared with a traditional lander approach. The results of the Team X study allowed us to verify a scorecard of metrics to ascertain mission-level benefits of the printed landers. In addition, the engineers in Team X were able to augment the technical assumptions for the STANLE mission concept by designing a notional dispenser for the landers and optimize the parameters of solar illumination vs relay orbiter coverage vs surface location and dispersion. The results of the Team X analysis are contained in Chapter 6.



Figure 1 Team X Concurrent Engineering Center at JPL

Bench Top Functional Prototype

For an integrated printed spacecraft, technical feasibility issues are mostly centered on system compatibility, inter-component functionality and performance. Therefore, we focused a significant effort in Phase Two to design and fabricate a benchtop prototype of a printed spacecraft capitalizing on the expertise at Xerox PARC. We used the reference mission as a

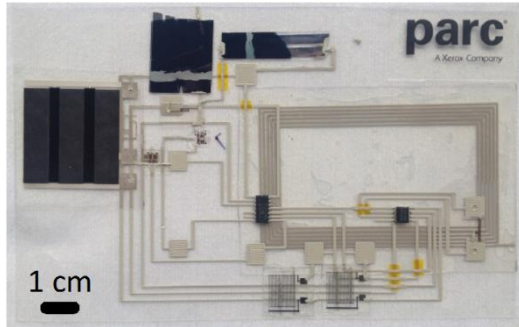


Figure 2 Xerox PARC Printable Spacecraft Prototype

guide for the functional and technical specifications for the platform. PARC successfully built a fully performing prototype of a flexible printed electronics science station. They demonstrated end to end functionality of generating multiple and continuous sensor data streams, storing the data in memory, and retrieving and transmitting the data wirelessly. This design effort is captured in Chapter 7.

Environmental Compatibility Testing

One significant aspect of technical feasibility we explored in Phase Two was the compatibility of printed electronic elements and manufacturing with the space environment. Both the materials *and* the functionality of the components need to be able to survive within the environmental challenges of space. We used our Mars lander reference mission to narrow the range of effects to be tested to vacuum, temperature cycling between -120°C to $+50^{\circ}\text{C}$, and moderate radiation doses (10-50 krad) consistent with one year on the surface. JPL has partnered with the Structures Technology Group within Boeing Research and Technology to define and execute this test program. Materials testing alone is insufficient to determine the environmental survivability of a printed spacecraft component. Therefore, we included functional elements as well as materials samples as test article coupons in the test program. The test articles included solar cells, transistor arrays, temperature sensors and materials coupons with PEEK, PEN and Kapton substrates and silver and carbon inks. After exposure, test article evaluation included electrical and mechanical integrity, such as resistance changes, functional changes, delamination, loss of tensile strength and other effects that might compromise the overall viability of the spacecraft. This test program is summarized in Chapter 8 with a full report contained in Appendix A.

Science Mission and Engineering Applications

We explored more of the engineering applications and mission concepts by developing two kinds of roadmaps. One was a generalized technology area capability roadmap. A second was focused on the specific mission development and technology needs of the STANLE mission concept. These roadmaps, described in Chapter 9, are made up of individual advancements that can enable a number of diverse applications.

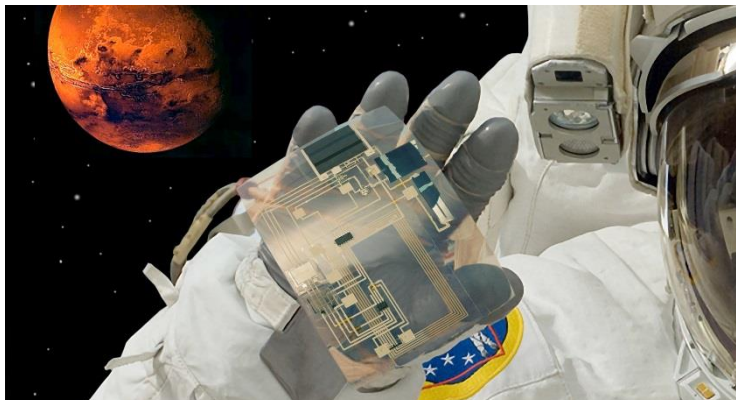


Figure 3 Artists rendering of the printed spacecraft in space (image credit: Xerox PARC)

3 Technology Overview

3.1 The Basic Elements

Printed electronics is enabled by the development of solution-processable materials and the fabrication techniques that exploit the properties of these liquid materials. The basic materials of traditional electronic circuitry (dielectrics, conductors and semiconductors) are produced in a soluble form allowing the generation of “functional inks”. Inks may contain organic or inorganic compounds or even be infused with particles such as carbon nanotubes to elicit a particular behavior. These inks are “printed” onto a variety of substrates either rigid or flexible to form thin sheets of electronic circuits. When applied in combinations and layers, these materials can produce the building blocks of electronic circuits (e.g. transistors) or more complex devices such as solar cells, CMOS circuitry, batteries and sensors. Some of these elements are shown in Figure 4 A-C below.

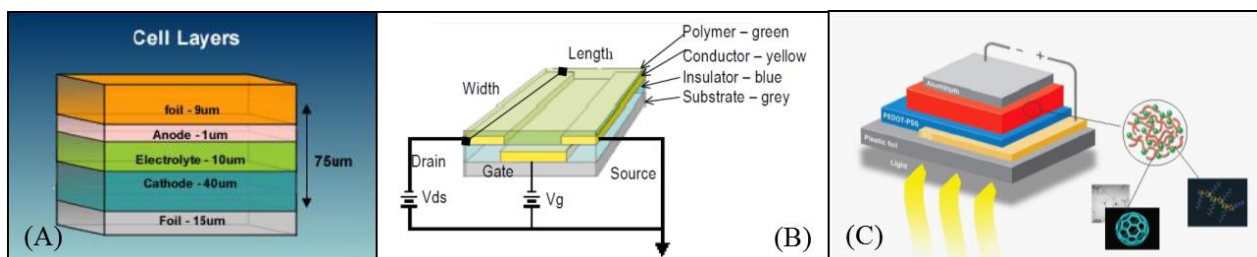


Figure 4 - Printed Elements: A– Solid State Battery Layers (image credit: Planar Energy) B –Traditional geometry for a field effect transistor (Credit: IDTechEx) C- Typical Construction of an organic solar cell (Credit: IDTechEx)

The combination of a soluble ink and a flexible substrate can be combined using several manufacturing approaches that are included under the umbrella of “printing”. Examples include inkjet printing, or drop on demand, e-jet printing, aerosol-jet, gravure, screen printing and flexography, or other more exotic means of “printing” including stamping and direct write. Some of these approaches are compatible with high-volume roll to roll processing. Some are more compatible with lower volume sheet-based fabrication.

The advantages provided by the substrate flexibility and the potential for low cost manufacturing are driving many industries to adopt printed electronics in a wide variety of applications. From large corporations and small start-ups, a wide spectrum of products from consumer electronics to healthcare to sportswear, are beginning to emerge. Biomedical, food packaging and military applications play a major role in defining the applications and technology advancements in printed electronics.

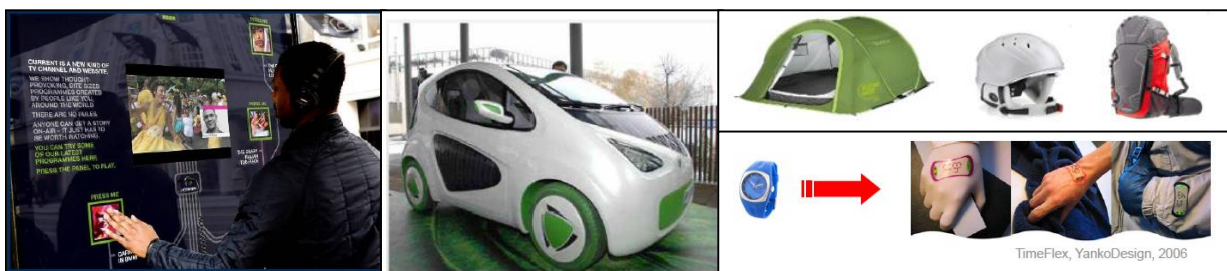


Figure 5 - Examples of consumer products envisioned with printed electronics (Credit: IDTechEx, SolarPrint, TimeFlex)

3.2 Hybrid and Integrated

Known limitations of printed electronics compared to traditional silicon electronics are the reduced electron mobility and larger feature sizes. Also, the manufacturing process has more inherent inconsistency than silicon wafer fabrication and this inconsistency can manifest itself in variations of device and circuit performance. The trend of industry to overcome these limitations is to use flexible hybrid electronic (FHE) systems – printed circuits and devices where it makes sense and discreet chips or flexible silicon circuits where higher performance is needed. Flexible hybrid electronics is moving forward at a rapid pace with significant investments. For example, in the past two years, American Semiconductor produced three new functional products in their Silicon on Polymer FleX™ line: the FleX-MCU™ microcontroller, the FleX-ADC™ analog to digital converter and the FleX-RFIC™ RF integrated circuit. These are crystalline silicon chips manufactured in the Tower Jazz foundry but thinned to a few micron and mounted on flexible polymer substrates. They are easily integrated into printed systems providing increased functionality without compromising form factor. Also indicating the future direction for investments, the topic of Flexible Hybrid Electronics is one of six technical subject areas that are candidates for a DOD investment in an Institutes for Manufacturing Innovations (IMI).⁴² If selected, this influx of government investment in manufacturing innovation facilities would benefit the advancement of flexible hybrid electronics.

The trend towards multi-functional or integrated systems is strongly apparent in the products that are being announced and partnerships being formed. By multi-functional, we mean combining the sensors, the batteries, the data processing and possible display or transmission of data. It is only a multi-functional system that can provide a complete solution to an end user's functional need. Many commercial ventures for integrated systems are beginning to emerge not just as prototypes, but as marketable products. Thin Film Electronics ASA has announced the first commercial order for a Smart Label™ system - products that will include memory, sensing, display and wireless communication - at a per unit price that allows high volume production and use. First demonstrated in December 2012, Thinfilm's proof-of-concept label for temperature monitoring of perishable goods was one of the first integrated printed systems. In less than two years, it has moved from prototype to commercial production.⁵² It's a similar story with other products entering the marketplace such as the MC10/Reebok CHECKLIGHT™ head impact detection system. Countless examples of other integrated system ideas and prototypes fill the flexible electronics conferences. The British manufacturing center for technology investments, CPI, describes many case studies from integrated displays to electronic noses. They use the clever term “printegrated” to describe multiple functions and layers being integrated through printed electronics.⁴³ It's clearly becoming a world of *go integrated or go home*.

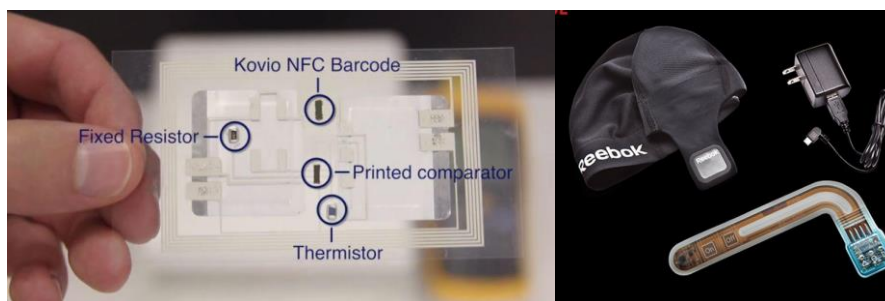


Figure 6 Integrated printed electronics systems in commercial production
(A) Thinfilm's SmartLabel™ (B) Reebok and MC10 CHECKLIGHT™

4 Benefits and Applications

4.1 Benefits and Advantageous Characteristics

The benefits to NASA of printed electronics technology are the same as what is driving industry to invest their resources in advancing this field. The market potential for products that leverage these features is large.³⁹ Some of these attributes are described below.

- **Flexibility:** The flexible substrate of a printed spacecraft provides many options for storage and deployment. Reconfiguring on orbit or after deployment enables a third dimension to be realized for additional structural rigidity, improved performance (antenna or optics shape), or even mobility. Conformability to surfaces is advantageous in many engineering applications to improve sensing or to fit with existing hardware/infrastructure designs.
- **Low recurring costs:** Depending on the specific system and manufacturing approach, the cost of recurring engineering may be less than a traditional assembled system. This makes it an attractive platform for large numbers (networks) or “disposable” applications.
- **Low mass & volume:** Because circuits are applied to light-weight thin substrates, the mass and volume of the platform is significantly reduced from a conventional printed circuit board. The thin sheets of printed electronic systems make a printed spacecraft attractive as secondary payloads. Accommodating and stowing large numbers of units is simpler when multiple platforms can be stacked together like a ream of paper.
- **Short cycle time:** For a printed platform, the design paradigm shifts away from mechanical packaging challenges to a focus on electrical layouts and fabrication flow. Circuits can be printed easily by a number of lab-scale printers allowing platform designs to be prototyped, tested, and modified quickly. Component libraries and design rules can be built up over time which will further reduce design times. Functional analysis and performance simulations can be constructed virtually on the computer prior to committing to manufacturing. Manufacturing will span days, not months due to the reduction of touch labor. Testing can be done in parallel on multiple copies, rather than serially on a qualification and flight units. All of these effects result in shorter development times which in turn help contain costs and open up flight opportunities that require fast turnaround times
- **Robustness:** The nature of the construction provides the electronic circuits a certain robustness over traditional chip on board construction. The delicate nature of solder joints and silicon chips are replaced with mechanically robust “ink stacks” making the circuitry more resilient to structural loading environments such as launch, landing, shock.

4.2 Applications

Given the numerous advantages described above, it is easy to see that the application space is diverse. From improving engineering diagnostics to enhancing or enabling mission concepts, flexible printed electronic systems have broad impact potential stretching as far as supporting future human exploration with resource efficient and adaptable in-situ manufacturing processes. Some of these applications are described further here. A more thorough description is provided in the Phase One report.⁶²

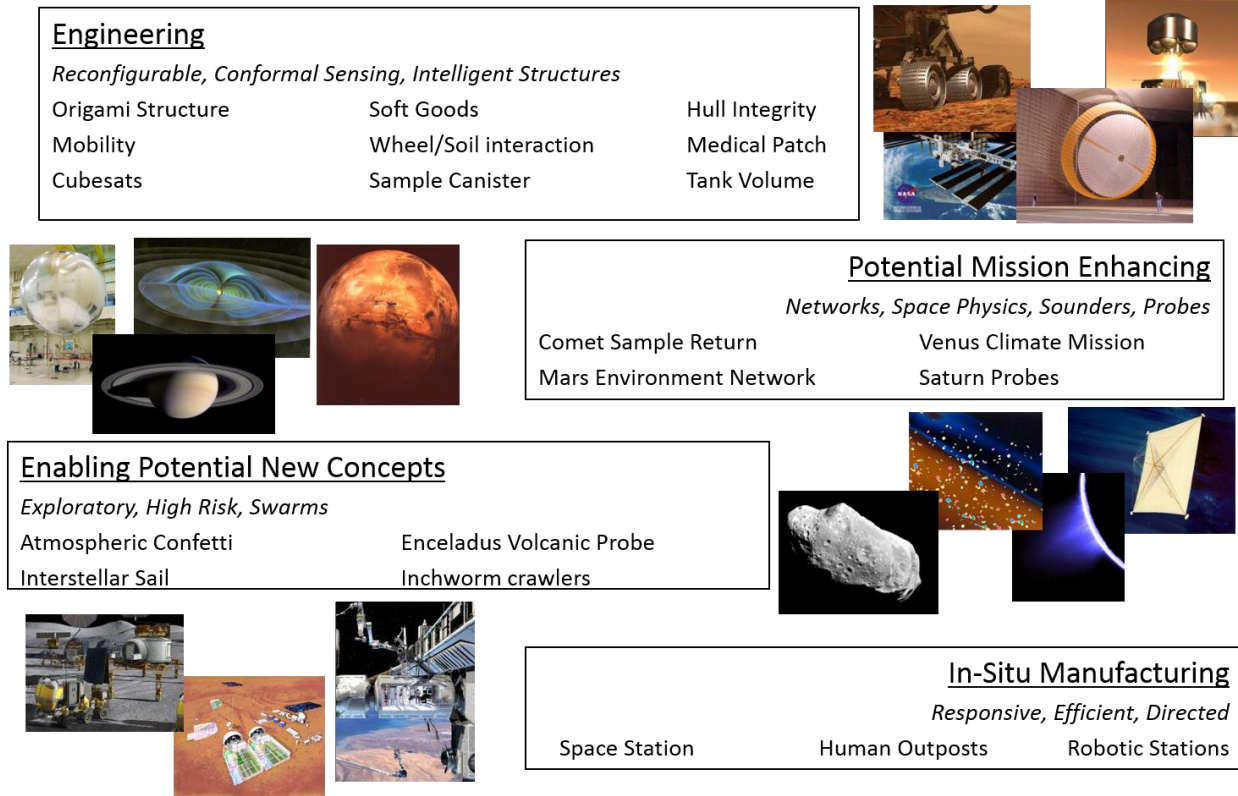


Figure 7 - NASA Applications. There are many engineering, science and human exploration applications that could benefit from the unique features of printed systems.

4.2.1 Engineering Applications:

Whether focused on singular sensing or structural aspects of the flexible printed systems, engineering functions can be augmented by the characteristics of printed electronics. Reconfigurability, conformal sensing and intelligent structures networks are just some of the engineering applications that can be imagined. Reconfigurability can be achieved with the use of printed electro-active polymer inks on thin substrates enabling functionality in systems such as origami structures and flexible mechanisms. Packaged compactly and unfolding in orbit, the usefulness of an actuated thin film for backup structures to achieve prescribed shapes for antennas or optics in situ or even perhaps assisting with mobility (erecting a sail or a sheet autonomously folding itself into a “paper airplane”) is apparent. Other forms of reconfigurable mobility are rolling/unrolling and inchworm motions. Where inherent contact and conformability to the surface is critical to the measurement (e.g. strain gauges), printed sensors offer great advantages. Some structures may be curved, soft-goods, stretchable or even extremely large areas in which discrete sensor arrays and the wiring for them would be impractical. Embedding sensing and knowledge into a structure (intelligent structures) is a goal of many applications. Strain, damage detection, applied loads, temperature are all pieces of data that if known throughout the structure could be used to intelligently adjust parameters or understand the margin to failure such in a pressurized tank or space station module hull integrity. Terrestrial applications for structural health monitoring of building infrastructure and bridges are driving a recent focus on complete sensor systems for these intelligent networks.

4.2.2 Science Missions

The space science community knows all too well that the unlimited thirst for knowledge and data is fettered by the reality of limited resources and limited launch opportunities. A printed spacecraft can supplement an already existing mission by providing a low resource, low cost sensor system that can fly as a secondary payload. The table below appeared in the Phase One report offering possibilities for how printed technologies can enrich the currently envisioned NASA science objectives through enhancements for several Decadal Missions.

Table 1 - How the Decadal Missions could be enhanced by a printable payload

Decadal Mission	Potential Printed Enhancement
Mars Trace Gas Orbiter	Aeroshell drops printed passive CH ₄ surface sensors capable of nanomolar detection that are subsequently observable by a high resolution imager. These would be dropped over a site showing detection of CH ₄ from orbit and would map the origin of the gas.
Comet Surface Sample Return	"Leaves" are dropped over the surface of the comet to assess organic content to provide a statistical representation of surface composition rather than a single point and guide site selection for gathering the return sample.
Lunar Geophysical Network	Deploy sensor nets around landers to perform seismic, ground-penetrating radar, mineralogical, and heat-flow measurements.
Lunar South Pole Aitken Basin Sample Return	Simple precursor lander sends out printed "crawlers" which perform large area surface reconnaissance to identify the optimal site for main lander to gather return samples.
Saturn Probe, Uranus Orbiter and Probe, Venus Climate Mission	Main probes eject printed atmospheric sensors which perform nearby multi-point/multi-path sensing to give 3-D distributions of atmospheric parameters. Also possible are printed balloons which provide persistent measurements along their paths as carried by the winds.
Mars Astrobiology Explorer-Cacher	A printed film records data within the sample return canister to document the sample environment from collection to return.

Because of the distinctive features of a printable spacecraft, it becomes possible to think of implementing uncommon mission concepts such as threshold sensing missions, swarm missions, passive platforms, or large area sensing sheets. Simplistic detection of chemical species to confirm the existence of or detect a concentration threshold can be done with a sensor platform the size of a postage stamp. Adopting a threshold sensing strategy for a mission would allow very simple sensors and minimizes the data processing and return. These may be an affordable intermediate step to improve our knowledge of uncharacterized targets before committing significant resources. Swarm missions use optimized individual platforms that either distribute or divide the job based on specific functionality or when data is taken in combination represents a more powerful data set than singular measurements. This concept has been proposed using other nanosatellite platforms and has a lot of merit for multi-point systems. A printed spacecraft offers another platform option to consider for swarm missions. A third idea is a purely passive platform that responds with data only when interrogated by a receiving device. This is the basis of the RFID tag industry.

5 Reference Mission

5.1 Introduction

The theme of *mission context* runs consistently through the goals of the NIAC program. A candidate mission was defined to provide the comparative context for the application of printed electronics. While there are many valuable candidate missions, we selected a recognizable science mission in which the vision of implementing the mission with a printed spacecraft platform was well-defined. We chose a surface environmental network for Mars as a realistic balance between science value, reasonable technology advancements and a potentially enabling use of printed electronics. Other missions that were considered had notable drawbacks for the purposes of this reference mission. Titan or Europa surface probes, while addressing high value science objectives, ran the risk of being too large a step for materials compatibility and survivability. Solar sail missions presented packaging challenges not planned to be addressed in this task. Atmospheric confetti has alternate technologies that could achieve the same objectives and therefore was potentially not *enabled* by printed electronics. The Mars environmental surface network represents an optimum balance of:

- Environmental requirements (temperature, radiation) that are within reach of the state of the art within the time frame considered.
- Functional requirements that push the current state of the art but can be met through practical extrapolation of technology advancements.
- System challenges, the solution to which are possible but not obvious
- A unique application that provides an enabling twist on an existing concept.
- Feasible alternate implementations such as technology demonstration payloads or Mission of Opportunity flights if a dedicated mission is not desirable.

5.2 Science Motivation

The National Academies Decadal Report “Vision and Voyages for Planetary Science in the Decade 2013-2022” defines the science priorities for planetary exploration. Climate and atmospheric science is among the top three science priorities within the Mars community. In addition, a solid understanding of Martian atmospheric processes substantiated by accurate climate models is a critical piece of planning for potential future human exploration at the surface, and is a beneficial even for robotic mission operations. The desire for global characterization of the Martian atmosphere including surface measurements is expressed in the following passage:

*“Fundamental advances in our understanding of modern climate would come from a complete determination of the three-dimensional structure of the Martian atmosphere from the surface boundary layer to the exosphere. This should be **performed globally**, ideally by combining wind, surface pressure and accurate temperature measurements from landed and orbital payloads. **Surface measurements are required** to complement these measurements and to characterize the boundary layer and monitor accurately the long -term evolution of the atmospheric mass. On a global scale, a network of at least 16 meteorological stations would be ideal and carrying a capable meteorological payload to measure surface pressure, temperature, electrical fields, and winds on all future landed missions would provide an excellent start to developing such a network.”²*

While many of the recent orbiters (Odyssey, MRO, MGS) have been able to observe the weather and climate of Mars from space, meteorology measurements on the surface have been more sparse and localized. Key interactive processes between the surface and the atmosphere are controlled within the Planetary Boundary Layer such as dust lifting, weathering and water vapor exchange with the surface/subsurface. Observations within this boundary layer are critical for accurate climate and atmospheric models.¹ Numerical models of the Martian atmosphere have been constructed on various scales to simulate the different atmospheric processes. Examples includes low-resolution (≈ 300 km) General Circulation Models (GCM), higher resolution limited area mesoscale models (≈ 10 – 100 km) and microscale or Large Eddy Simulation (LES) models.⁴⁰ Unfortunately, on the smallest scales and in the crucial region of the surface-atmosphere interface, the models are not well supported by current data. In situ surface measurements of near surface wind, temperature, moisture, and pressure from a set of dedicated meteorological sensors are necessary to improve these models. Measurements from a global network to bolster the Global Circulation Models are important as are increased fidelity of measurements within the smaller scale areas to support the meso- and microscale models.

5.3 Previous Network Missions and Human Exploration Concepts

Mars network missions have been studied and proposed numerous times. Each mission concept is different in the details of the implementation but most have some common characteristics and challenges that we tried to capture and address in our reference mission. Broad area coverage is one important characteristic. Global coverage is desired but poses the challenge of multiple entry probes with sufficient time spacing to allow the planet's rotation and access to all longitudes. Areas of 100 km^2 to 1000 km^2 for the distribution of measurements is more easily achieved with a single entry vehicle which can deploy multiple landers. The quantity of measurement sites on the surface is also a debatable parameter. The quantity of a traditional "lander" concept (even small systems) is limited by the volume and mass available in a practical and qualified aeroshell design. Quantities as low as four have been proposed as a minimum, but most global network concepts consist of 12-16 sites. There is variability in the sensor packages proposed in previous mission concepts, but a common core set of measurements can be extracted: temperature, pressure, wind speed, humidity. Additional measurements of atmospheric opacity, wind direction, seismometry, imaging and chemical sensing have sometime been combined to address both meteorological and geophysical objectives with one surface platform.

Some recent and more notable proposals of Mars meteorological networks are summarized in this Section as a means of illustrating the variety of implementation options, science objectives and measurements and technical challenges and limitations. In addition, there are some examples of how the meteorological networks can support the Human Exploration goals by providing critical environmental information needed to plan the human missions and ensure the safety of the astronauts. Network missions represent a key example of potential human-assisted science missions that could be performed on Mars.

5.3.1 *MESUR Network*

The original mission concept proposed (circa 1990) was the Mars Environmental Survey (MESUR) which was to establish a global network of small science stations on the surface of Mars to operate concurrently over a minimum of one Martian year.²⁸ The full network was

envisioned to consist of a complement of 16 or more landers providing pole-to-pole coverage of the planet. The broad science objectives of the MESUR Network mission were to characterize the Martian environment in terms of atmospheric structure, internal structure, global atmospheric circulation, surface chemistry, and surface morphology. The strawman science payload for the MESUR Network mission included an atmospheric structure package (pressure, temperature, and acceleration measurements during descent), cameras for descent and surface imaging, 3-axis seismometer, meteorology package, Alpha/Proton/X-Ray spectrometer (APXS), Thermal Analyzer/Evolved Gas Analyzer (TEGA), and radio science experiments.

The engineering challenge was how to deliver multiple landers safely to the surface – a feat not attempted since Viking. An engineering precursor mission was devised to “path find” a novel new entry, descent and airbag landing system by landing one demonstration vehicle on the surface. Due to budget constraints, this demonstration vehicle eventually became the only lander, was augmented with a rover technology demonstration payload and was named the Mars Pathfinder mission which was launched in 1996.

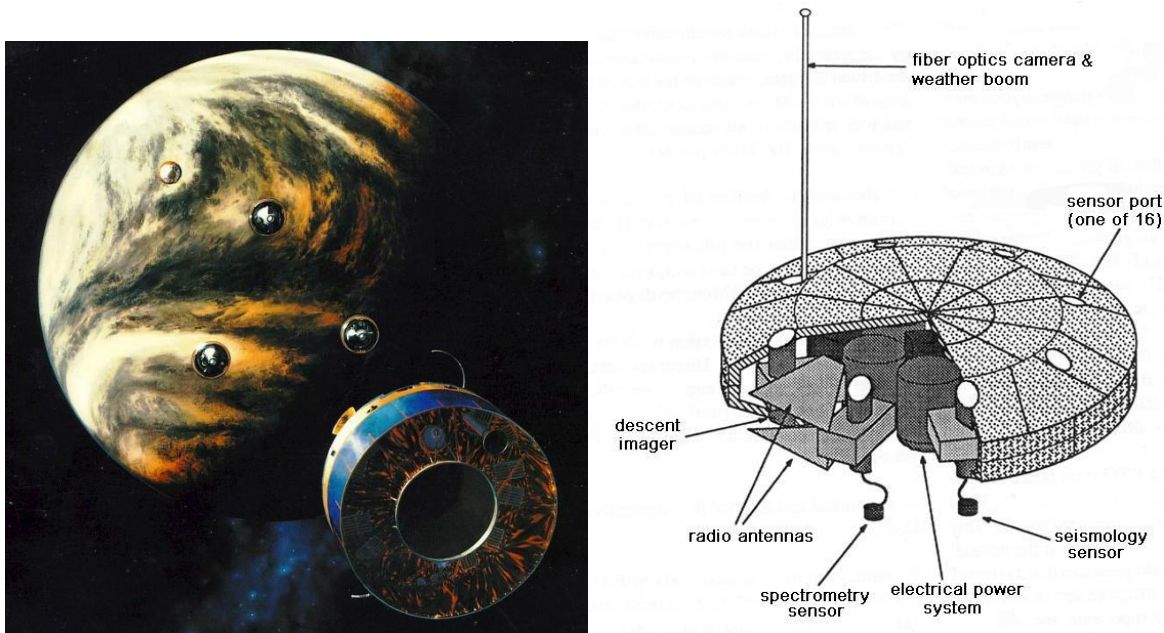


Figure 8 - MESUR Network early concepts (image credit: NASA)

5.3.2 *Pascal*

Pascal was Discovery mission proposed in 2000. The principal investigator of this mission concept was Dr. Robert Haberle from NASA/Ames. The mission as proposed would place 24 science stations on the surface of Mars to measure pressure, temperature and optical depth for two years. The stations were delivered by a carrier that entered orbit and served as the relay satellite. The probes used an aeroshell, parachute and crushable material to reach to surface and were powered by a micro-thermal power source.⁴⁴ Later the concept was modified to be 18 probes to Mars aboard a Delta-II heavy launch vehicle. The probes were deployed on approach from a flyby carrier using a propulsive time-of-arrival adjustment to achieve global coverage.

The entry, descent, and landing of each probe would utilize an ablative aeroshell, a parachute, and an airbag to reduce the impact shock. On the surface, each lander would take daily measurements of pressure, opacity, temperature, wind speed, and water vapor concentration, plus occasional panoramic imaging over the three year lifetime. The data would be relayed to an orbiter through a UHF link and then transmitted to Earth. The power was assumed to be supplied by a RHU power converter.²⁹ These two versions of the Pascal missions were more ambitious than an earlier concept that Dr. Haberle had considered. The previous mission was called “Micro-Met” which delivered 16 stations to the surface that measured pressure only for up to one year in conjunction with orbital measurements made by a spacecraft from a separate mission. The “lander stations” weighed less than 4 grams and were purely battery powered vehicles. Each was packaged in its own aeroshell deployed from a carrier vehicle, using a parachute and crushable material to decelerate.⁴⁵

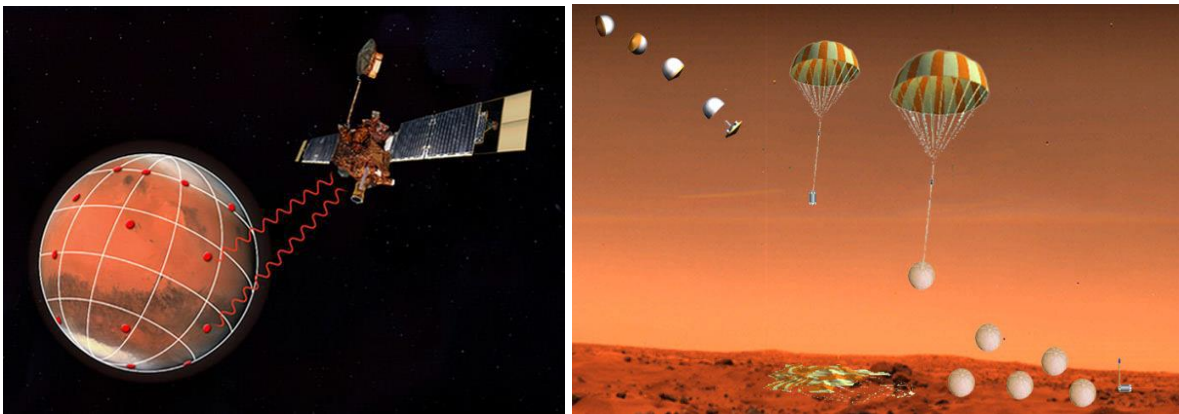


Figure 9 - Pascal Mission Concepts (image credit: NASA)

5.3.3 *MetNet*

The MetNet mission is an on-going program sponsored by the Finnish Meteorological Institute, and the Lavochkin Association in Russia. The main idea behind the MetNet landing vehicles is to use a state-of-the-art inflatable entry and descent system instead of rigid heat shields and parachutes as earlier semi-hard landing devices have used. The vehicle decelerates its entry speed using the inflatable structure and the final landing sequence includes a cone headed body penetrating the Martian soil. It is planned to deploy several tens of metnet landers (MNLs) on the Martian surface operating at least partly at the same time to allow meteorological network science. This is a technology demonstration mission utilizing one lander planned for launch in the near future (note: at press time the launch date previously quoted as 2014 was uncertain). The atmospheric payload includes: a pressure device, humidity and temperature sensors, optical devices, panoramic camera, a solar irradiance sensor (MetSIS), two solar incidence angle detectors, and a dust sensor. In addition there is a composition and structure device and a magnetometer (MOURA).³⁰

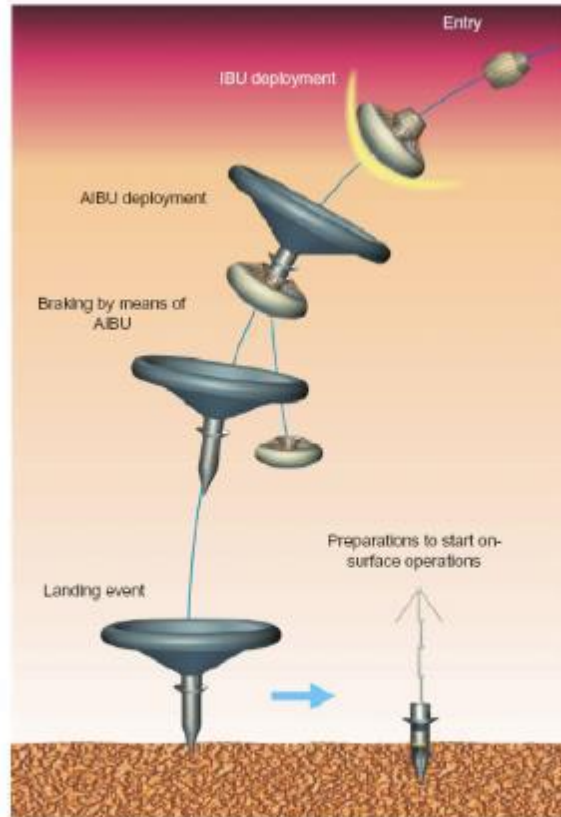


Figure 10 - Entry, Descent and Landing Sequence for the Met Net Landers

5.3.4 Human Exploration Precursor Data

Data from meteorological networks can play a valuable part in planning for Human Exploration missions. A critical piece of knowledge needed includes the atmospheric and environmental conditions on the surface. This data would need to be obtained from robotic precursor missions which would characterize atmospheric processes for future Human Exploration missions. The Mars Exploration Planning Group (MEPAG) endorsed such synergy between the robotic missions and the Human Exploration program:

*“Other landed missions will be needed to mitigate atmospheric risk. For example, to confront atmospheric risks, **the most effective approach is a network mission**, in which simultaneous measurements of the Martian atmosphere are made at multiple locations distributed over the planet. Data from a meteorology network would constitute particularly valuable input into a Martian atmospheric model for human landings and operations.”¹*

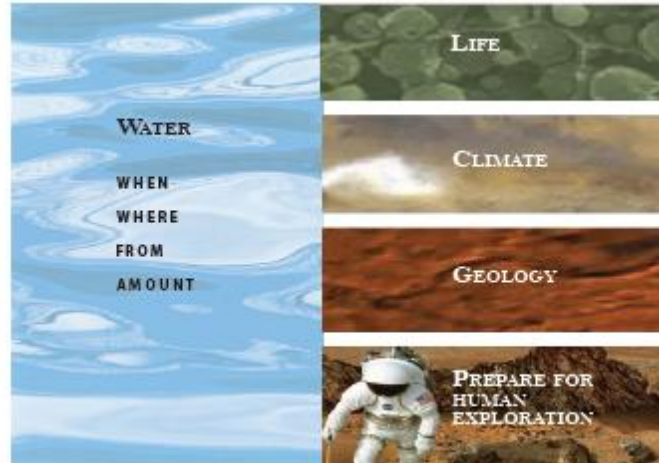


Figure 11 - Goals of the Mars Exploration Program

5.3.5 **Human Assisted Science Missions**

In 2008, a report was drafted that devised a collection of notional mission concepts called “human science reference missions (HSRMs) to illustrate potential objectives and requirements for surface operation missions of humans on Mars.³¹ This report was generated by a group called the Human Exploration Mission – Science Advisory Group (HEM-SAG). Their report identified two nominal reference missions, one of which was for humans to deploy and operate a network of meteorological stations to study Planetary Boundary Layer phenomena.

Nominal Atmospheric Human Science Reference Mission (HSRM)

...two nominal reference missions are identified: an atmospheric reference mission and a reference mission to the north polar dome for deep drilling, in order to define the more site-specific human-enabled mission activities necessary to sample the critical volatile records contained within the polar ice caps. Atmospheric reference mission activities are anticipated to be included in all human missions.³¹

A printed meteorological lander station could significantly enhance the implementation of the envisioned mission for human-assisted atmospheric studies by reducing the size and the weight of the stations to be distributed and installed. If the human explorers could print the lander stations in-situ using table top electronics printers, it would allow the real-time reaction to discoveries by allowing the fabrication of new sensor platforms and quantities as needed.



Figure 12 - Artists Concept for Human Exploration of Mars (image credit: NASA)

5.3.6 Summary of Previous Network Concepts

The diversity of implementation approaches to an environmental network mission was illustrated through the previous examples. However, these examples shared common challenges that have persisted since the first proposed concepts in the 1990s. These common challenges of the robotic network missions was captured in the graphic below from a 2006 publication from the Mars Advanced Planning Group.¹ Eight years later, the issues of lander dispersion, quantity of landers, lander impact qualification, and EDL risks and complexity largely remain as the top challenges for any landed network mission. What is needed is an architecture for the mission and the lander which can reach a broad distribution with a simple deployment scheme, can eliminate the issue of the hardware structural qualification for landing impact, can dramatically increase the number of landers brought to the surface and does not require high-risk EDL subsystems such as retro rockets, landing radars, impact attenuation, bridle deployments, and vehicle unpacking. We believe the application of printed electronics to create a thin, flexible, low cost integrated science platform offers promise to address many of these challenges.

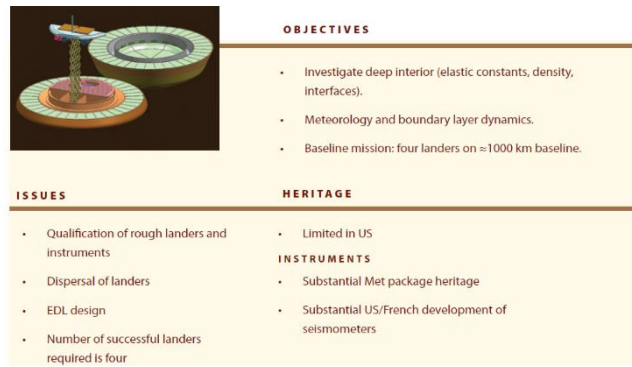


Figure 13 - Mars Network Lander mission concepts (image credit: NASA)

5.4 STANLE Reference Mission

Disclaimer: The reference mission described in this section does not represent a mission concept specifically recommended or endorsed by the Mars science community or advisory groups. It is a mission concept that was derived by the Printable Spacecraft team in order to establish requirements so that the engineering design reaches sufficient maturity to enable the technical and programmatic comparisons desired for this NIAC Phase 2 study.

The mission envisioned for the Printable Spacecraft flutter landers is called Structure of the Atmosphere - Network Lander Experiment (STANLE) which will deliver a network of thousands of meteorological stations to the surface of Mars covering an area of hundreds of square kilometers to support the measurement of moderate scale atmospheric phenomenon. It will record temperature, pressure, wind speed, atmospheric opacity, radiation, and humidity once every hour for a Martian year. A traditional cruise stage and entry system is used which releases the printed electronic platforms into the atmosphere after heatshield separation, allowing them to flutter to the surface and begin their mission. A graphical summary is provided in the “STANLE Fact Sheet” (Figure 15).

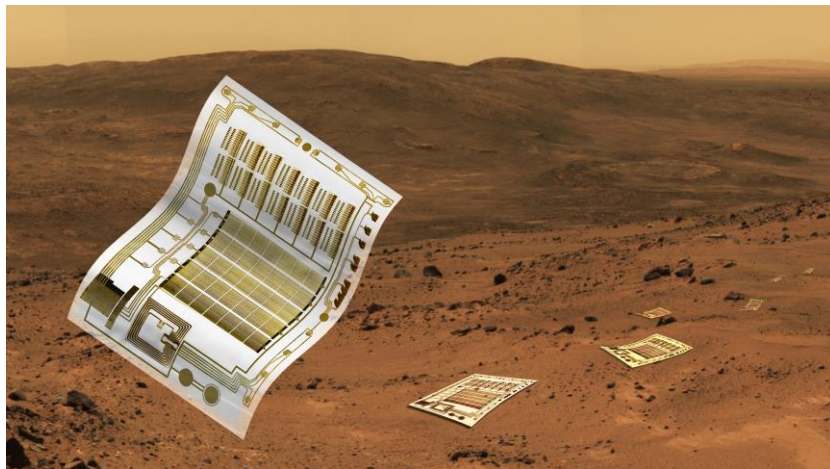
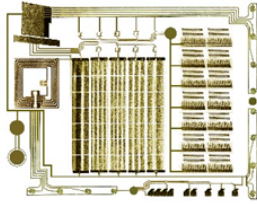


Figure 14 - Artist Conception of the STANLE Flutter Landers (Image credit: Joseph Harris, JPL)

The STANLE mission would be targeted for a launch year around 2024 which establishes a technology readiness date around 2020. This date is consistent with the NIAC ten year infusion horizon and was used as a guide for projecting necessary technology advancements. The Mission Class target would be Class C in line with a Discovery Class mission or smaller. The flight system makes maximum use of inheritance from previous medium class missions like MER, MPL, and Phoenix for the elements that are unaffected by the technology (e.g. cruise stage, entry vehicle, parachute). It is assumed that there would be an orbital relay asset similar to the UHF relay links that exist today through MRO and Odyssey.

STANLE: Structure of the Atmosphere - Network Lander Experiment



A novel flat sheet flutter lander made from flexible electronics –requires no landing hardware - creates a thousand node environmental network

Mission Objectives

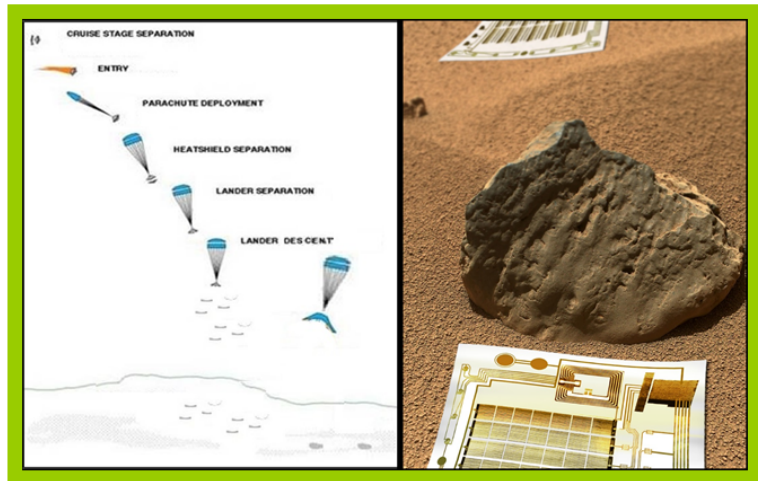
The STANLE mission will deliver thousands of environmental science platforms to the surface of Mars. Dispersed over large areas these meteorological stations will create a high density sensing network, measuring critical environmental parameters once every hour for a year.

This revolutionary new scientific platform – a printed spacecraft - is a thin flexible sheet with printed flexible electronic circuits to provide all functions from sensing to data downlink.

This novel science station provides power via solar cells and batteries. It can store up to five days worth of data from each sensor on board. When interrogated by a relay orbiter, the station downloads its data via UHF link.

Lander Technical Facts

- Weight less than 13 grams
- Sheet thickness ~125 μm .
- Sheet area 25 x 25 mm
- 10 kbits of data storage
- 8 bit A/D conversion.
- 35 mAh rechargeable battery.
- 100 mW solar cell.
- UHF data link to relay satellite.
- Six meteorological sensors:
 - Atmospheric temperature
 - Surface pressure
 - Wind speed
 - Light Intensity
 - Humidity
 - Radiation



Flight System Architecture

The STANLE flight system architecture consists of a cruise stage, which is jettisoned before entry, and an aeroshell which houses the landers and dispensers. After parachute release and heatshield separation, the landers are ejected from the backshell and flutter to the surface with no additional descent or landing infrastructure. The flutter lander enables a very simple, low risk EDL mission, reducing cost and mass from that of traditional landers.

Figure 15 Graphic Fact Sheet for the STANLE mission concept

The landed platform design was devised by the NIAC Printable Spacecraft team. JPL's Team X organization was instrumental in rounding out some of the mission design parameters including the surface operations constraints of solar illumination and communications coverage. The Team X mechanical team designed the conceptual dispenser system and layout within the backshell. The Team X communications chair redefined the link budget consistent with the revised parameters for orbital coverage, time and relay system parameters.

5.4.1 *Mission and Vehicle Overview:*

The objective of the STANLE mission architecture is to deliver many thousands of meteorological stations to the surface Mars to support the characterization of the Martian climate system and how it is controlled by near-surface circulation and atmospheric conditions. The STANLE mission would start with a launch from KSC aboard a medium class launch vehicle on a direct trajectory to Mars. The flight system consists of a cruise stage and a single 2.5m entry vehicle. The cruise stage would provide all data systems, navigation, control and communication systems for the vehicle during the Earth-to-Mars transit including a simple cold gas propulsion system to perform TCMs and final targeting maneuvers on approach. Inside the entry vehicle are the systems necessary to support the descent sequencing after separation from the cruise stage. The backshell/entry system would have simple and straightforward electronics and thermal batteries to control the functions of the entry and descent. Mounted inside the backshell is an array of dispensers which house the stacks of printed landers and the mechanisms to deploy them. The system is sized to hold roughly 7000 landers in a series of 13 dispensers. The landers inside the aeroshell would not be active during cruise. The thermal control of the cruise stage and entry vehicle hardware would be traditional heaters and radiators, and would not require a pumped fluid system.

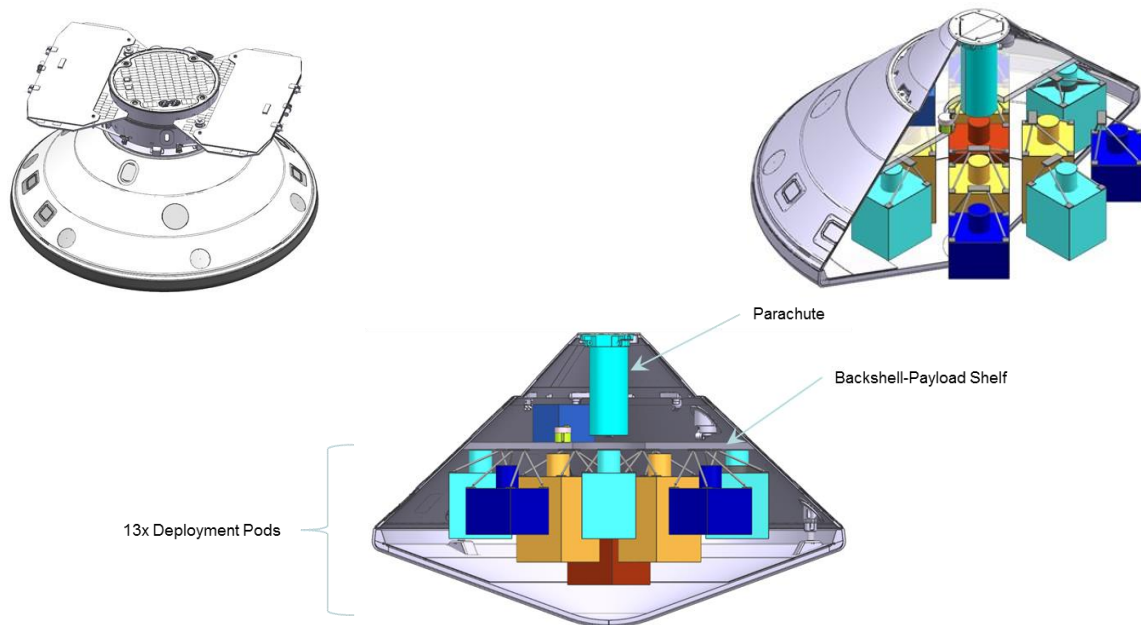


Figure 16 - STANLE Cruise Configuration and Entry Vehicle Cut-aways (image credit: Jaime Piacentine, JPL Team X)

The cruise stage would initiate separation from the entry vehicle the after final orientation. Entry would be a ballistic entry with heritage thermal protection system (TPS) systems and a parachute deployment initiated as a timed sequence from the peak deceleration to match the appropriate Mach number. Thermal batteries provide power and pyro firings. Heatshield release is initiated sufficiently after parachute deploy to ensure safe jettison and flyaway at an altitude high enough to support the largest distribution ellipse. There is no terminal decent radar, propulsion or landing system required. Once the heatshield is deployed, the various lander dispensers are opened and deployed in series. The landers are pushed out of the storage boxes with a simple spring loaded system. The spring provides enough energy to force the landers past the lip of the backshell and into the free flow of the atmosphere. The deployments would occur over the roughly 100 seconds of remaining descent time. The sequenced deployments aid in the along track distribution of the landers providing tens of kilometers of dispersion. The landers are powered on after separation from the backshell via a simple breakwire trigger. Once free of the backshell the landers flutter through the atmosphere, eventually coming to rest on the surface of Mars. Orientation is influenced by the weight distribution to increase the probability of landing right side up. Once powered on, the lander would proceed with a simple execution script which would sequence through each of the sensors once per hour and recording the data in the on board memory. A relay orbiter would initiate communication as it cycles through the cluster of landers. Surface lifetime is planned for one Martian year.

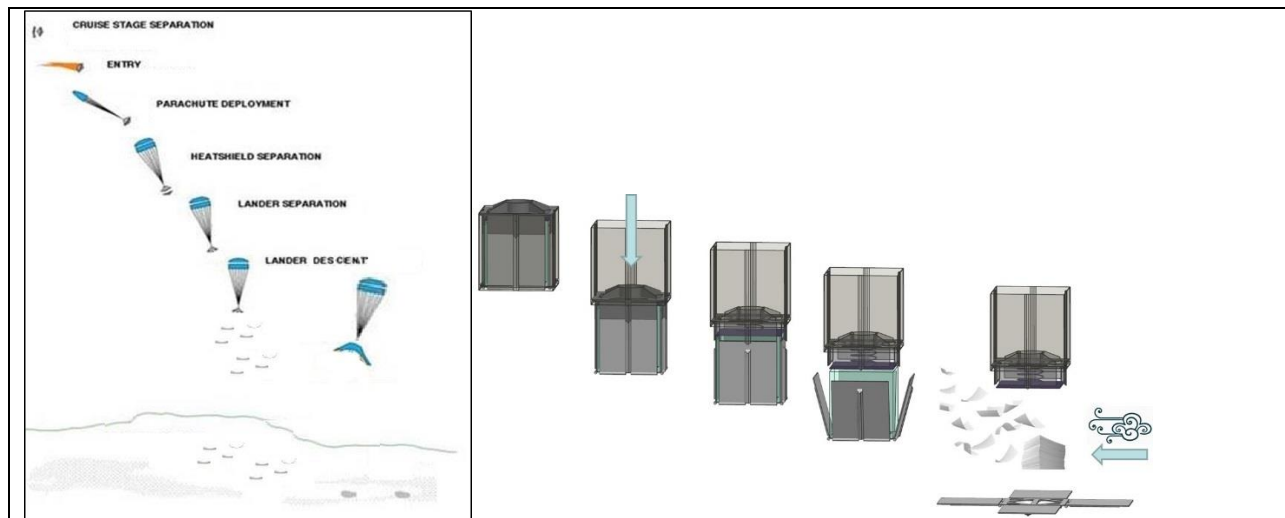


Figure 17 STANLE Entry, Descent and Deployment Sequence

5.4.2 Aerodynamics and distribution

The STANLE mission was used as the motivation for the Senior Thesis project of Kathleen Riesing and Margaret Tam, aerospace engineering majors at Princeton University.⁴⁶ They studied the aerodynamic behavior of the proposed flutter landers using MATLAB simulations and drop tests. Using data from the Mars-GRAM atmospheric model and lander release parameters derived from previous Mars missions, the students calculated the expected down range and cross range distribution of the landers. Above and beyond the flat sheet, they studied various shapes including V-fold, cones, gliders and auto-rotators. The influence of platform shapes and mass distribution on stability and landing dispersions was evaluated.

The results indicated that the geographic dispersions were in the range of 10 km (lower than desired) if the landers were to be released simultaneous from one event. Considering the horizontal velocity during the descent event, it implied that a staggered release at a higher altitude is essential for a wider area distribution. This is the baseline approach assumed in STANLE. Lifting bodies such as auto-rotators and gliders reached wider distributions but have the added complexity due to the shape and the packaging inefficiency.

Another notable result was that the shape and mass distributions can be used as a means of increasing the probability of a desired landing orientation. Cones and weighted sheets had a higher predictability of landing orientation without the shape and packaging complexity of the more aerodynamic gliders. A cone shape may even provide some benefit to the engineering and sensors on board, and is worth considering in a future study.

5.4.3 STANLE Platform Design

A complete point design of the STANLE platform has been performed in order to align mission requirements with capabilities and perform basic sizing of the functional elements and subsystems. The implementation of those elements uses a range of assumptions from today’s technology to a reasonable extrapolation of the technology up to the Technology Readiness target date of 2020 derived from a typical project timeline. The result is a self-consistent technical baseline for the STANLE platform design.

5.4.3.1 System Design Overview

The STANLE lander platform is a self-contained flat sheet approximately 125 microns thick that houses all the scientific sensors, the data collection and conversion circuits, data storage (memory), power production and control circuits, and the communications systems. The overall configuration is shown in Figure 19. The approximate dimensions are 25x25 cm, the weight is less than 13grams and the peak power produced on board is only 100 mW.

System Mass		System Power		
Element	Mass (gms)	Operational Element	Power (mW)	
			Sampling Mode	Standby Mode
Solar cells	0.06	Memory	1.0	
Batteries	1	Processor	1.0	1.0
Memory	0.05	ADC	1.0	
Processor	0.05	Clock	1.0	1.0
ADC	0.05	Temperature Sensor	0.5	
Temperature Sensor	0.05	Pressure Sensor	0.5	
Pressure Sensor	0.05	Wind Speed Sensor	0.5	
Wind Speed Sensor	0.05	Radiation Sensor	0.5	
Radiation Sensor	0.05	Humidity Sensor	0.5	
Humidity Sensor	0.05	Atmospheric opacity Sensor	0.5	
Atmospheric opacity Sensor	0.05	Additional inter connect circuitry	1.0	1.0
Antenna	0.01	Contingency (30%)	2.4	0.9
Communications Circuit	0.1	Total System Power (mW)	10.4	3.9
Additional inter connect circuitry	0.2			
Substrate	10.2			
Encapsulation	0.625			
Total Sheet Mass (gms)	12.60			

Figure 18 - System Resource Estimates for the STANLE Platform

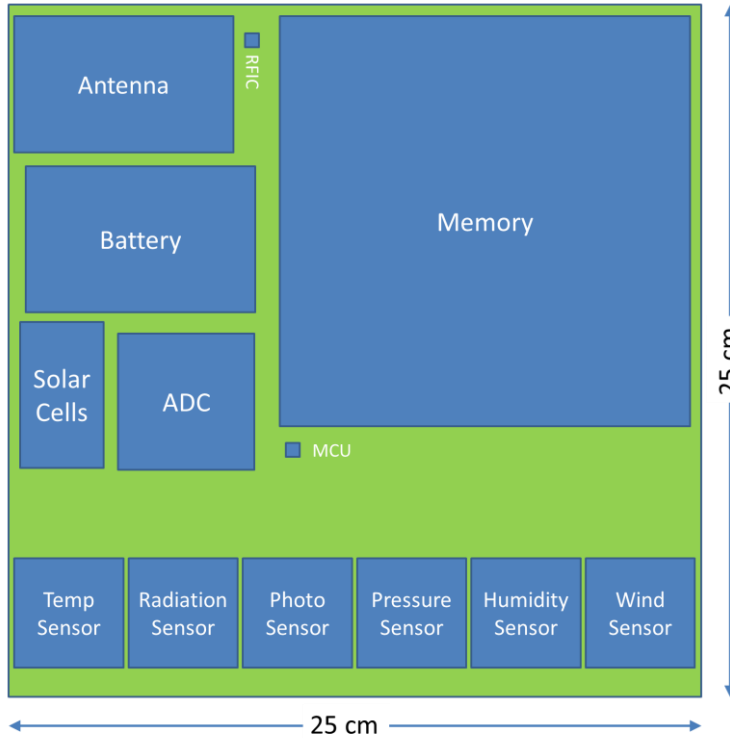


Figure 19 - Notional Layout of STANLE lander based on area required for each element.

The scientific sensor suite carried on the platform consists of six primary sensors to measure key parameters of the surface boundary layer meteorological behavior. Those measurements include: temperature, humidity, pressure, wind speed, light intensity/UV radiation, gamma radiation/total dose. Table 2 below describes the desired measurement ranges and accuracies for each sensor type. The REMS suite carried on the Mars Science Laboratory rover can be considered the state of the art environmental monitoring systems. Many of the measurement requirements, accuracies and resolution are based on what is achievable on the REMS suite.⁴⁰

Table 2 - Sensor Requirements

Sensor	Range	Accuracy/Resolution	Comment
Temperature	-120 to +20 deg C	5 deg / 0.1 deg	Depends on latitude and season
Humidity	0% to 100%	10% / 1 %	100% when ice is sublimating
Pressure	30 Pa to 1150 Pa (daily variations ~100Pa)	10 Pa / 0.5 Pa	Depends on altitude and season
Light Intensity (UV radiation)	44.7 W/m ² (210-360 nm)	5% / 0.5%	6 UV radiation bands desired. Total average is shown.
Radiation	20 mrad/day	10 mrad / 5 mrad	Total accumulated dose
Wind Speed (horiz)	0-70 m/s	1 m/s / 0.5 m/sec	Wind direction and vertical wind speed desirable

The operational scenario is a key driver for many of the engineering subsystem of the platform. The baseline design assumes one measurement per hour from each of the six sensors is recorded. The measurements are converted from analog voltage measurements to a digital value which is marked with header data to identify the sensor and the time tag. This data is stored in the memory until the supporting orbital relay spacecraft initiates the communication sequence. At that time the data is uplinked to the relay satellite. The platform has a dual mode power architecture. During the sunlight hours, the solar cell provides power to the platform as well as recharges the battery. During darkness, the battery supplies operation power to the platform. All communication passes are powered by the battery, not the solar cell. The power on board supports the microcontroller and clock functions, energizes the sensors, supports the ADC and the memory read/write functions. During a sampling period (once per hour), power is supplied to the entire platform. The rest of the hour is a “standby mode” in which power is only supplied to the microcontroller and clock. During a communication pass, power is supplied to the memory read/write circuit and the RF system. The basic engineering requirements and assumptions are captured in Table 3.

Table 3 - Engineering Operational Requirements and Assumptions

<i>Requirement</i>	<i>Subsystem</i>
Solar power supplies operational power during day and recharges battery	Power
Battery provide operational power during night and all comm passes (day or night)	Power, Comm
Power is applied continuously to the microcontroller and clock	Power, Data
Power is cycled to sensors, ADC, memory (15 minutes per hour)	Data, Sensors
Power is sized to provide one comm link per day	Comm, Power
Memory is sized to hold 5 days of data	Data
Memory is size to record one measurement per sensor per hour plus time tags and sensor ID	Data
Sensor measurements are provided in 8 bit resolution ADC	Data
Communication is via UHF relay link to orbital asset (assume MRO, ODY parameters, 5-20 deg elevation)	Comm
3.0 V circuits	All
Thermal System is passive	Thermal

Each of the functional elements of the platform are described one by one in the following sections. These sections attempt to provide the basis for the functional feasibility and technology advancements needed to achieve the desired functionality. Some design details and calculations used for sizing the engineering subsystems are provided as well.

5.4.3.2 Temperature Sensor

The current state of the art in printed temperature sensors can already meet the required range of operation and sensitivity. The state of the art is represented by a company called PST which produces a patented silicon nanoparticle negative thermal coefficient (NTC) thermistor. A spinoff of the University of Cape Town in South Africa, PST utilizes silicon nanoparticle ink which is screen printed into a resistive element which changes resistance with temperature in a

precisely calibrated way. The contacts into the system circuitry are silver ink. The nanoparticle ink is extremely stable and long lived. They produce multiple sensors, depending on the temperature range of interest. The PST “cryogenic sensor” has an active range between -263 deg C and +27 deg C with an achievable precision of 0.1 deg C.



Figure 20 - PST Thermistor

5.4.3.3 Humidity Sensor

Two sensor architectures seem to be most common for humidity sensors. There is a capacitive design in which the device is charged to a fixed potential and the discharge time is measured. The moisture content changes the capacitance of a humidity sensitive material and therefore the discharge time. There is also a resistive architecture in which the resistance of a material changes with moisture content which is directly measured. The resistive architecture is favored in higher relative humidity (RH) environments whereas the capacitive change sensors typically show good response in the lower RH environments. The parameters that can be adjusted in the design of a humidity sensors are the humidity sensitive material itself, the thickness of the sensitive layer, the precision and spacing of the interdigitized fingers. Some of the shortcomings of the current sensors with respect to the STANLE requirements include adequate sensitivity over the full range of RH 0-100%, notable hysteresis behavior, sensitivity to temperature of the humidity sensitive layer. Each of these shortcomings are essentially challenges for the device design rather than a fundamental barrier. Technology advances would be needed in further characterizing the phenomenon that affect sensitivity over range and the hysteresis behavior in order to optimize the sensor design or devise a tiered architecture. Printed humidity sensors are critical to the food management industry and environmental monitoring for building infrastructure and facilities and are receiving quite a bit of attention from industry.

To provide a sense of the current design state for printed humidity sensors, several examples are described here. A sensor demonstrated by the University of Dresden in 2011 was a capacitive design with silver nandectotante finger electrodes ink jet printed onto a polyimide substrate with a polymer particle based ink humidity sensitive layer printed over top of the electrodes. The sensor also consists of a matching “control” sensor in which a humidity insensitive layer is printed over the electrodes to provide a nulling values for changes in temperature and the humidity effects of the substrate. The sensor was characterized over 12% to 90% RH for various thicknesses of humidity sensitive layers. The sensor showed response to humidity most strongly in the 20% to 90% humidity range with hysteresis less than 5%.⁵

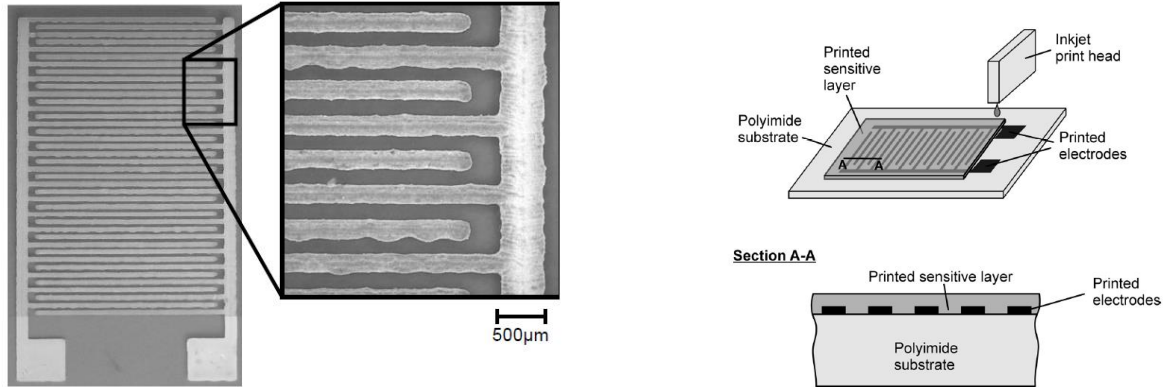


Figure 21 - University of Dresden humidity sensor design (finger electrodes and general construction)

Alternate concepts for printed humidity sensors were investigated by Tomas Unander at the Mid Sweden University. He investigated five types of sensors optimized for low or high humidity. For one particular sensor design, he measured the moisture content of the substrate itself and was able to demonstrate a sensitivity of 0.22% through a capacitive type sensor. This construction showed good stability over a range of temperatures (0.36% variation) but suffered from hysteresis and limited range of RH. This sensor was ultimately included in an integrated system including power and RFID communication.⁶

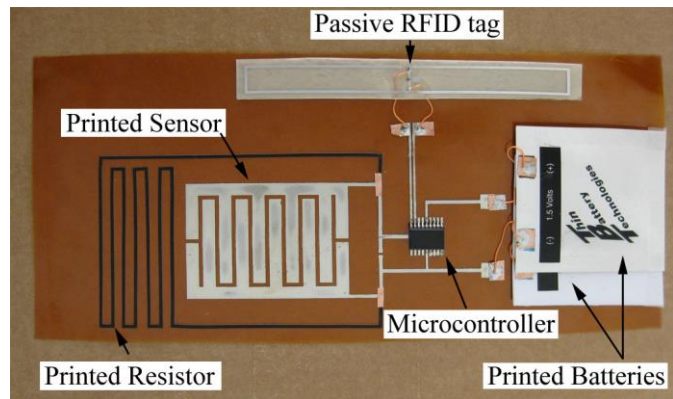
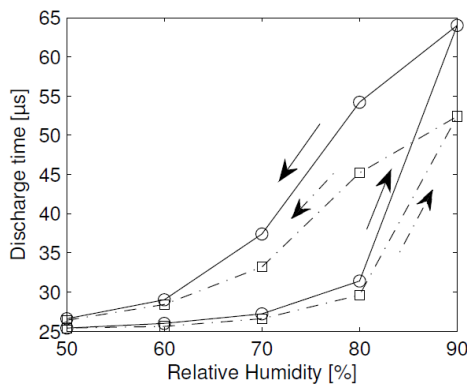


Figure 22 Capacitive Humidity Sensor (Mid Sweden University) measurements and example of a lab set-up for a fully integrated sensor system.

A third example comes from researchers at Western Michigan University who fabricated an interdigitated capacitive humidity sensor using two different thickness of a humidity layer (1 µm and 500 µm of Hydrophilic polymer pHEMA). These were tested over a range of 30% to 80% Relative Humidity. The sensors showed significant variation in the capacitance of the humidity sensing material over the higher end of the RH range tested. The measurements were affected by temperature showing a much higher sensitivity with increasing temperature.⁹

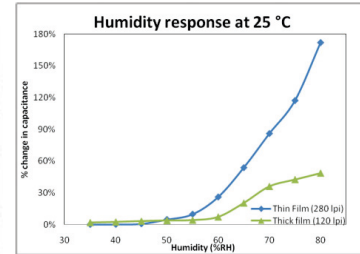
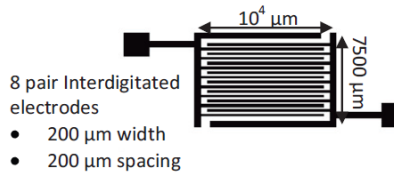


Figure 23 - Western Michigan University Printed Humidity Sensor

5.4.3.4 Pressure Sensors

The hydrostatic atmospheric pressure on Mars averages about 600Pa, but can range from as low as 30 Pa to as high as 1150 Pa (0.004 to 0.167 psi), depending on location, season and time of day. Daily variations can be on the order of 110 Pa. These are extremely low pressures compared to the static pressure levels that current printed pressure sensors are designed to measure. Most terrestrial hydrostatic printed pressure sensors are designed to operate in ranges from 35 kPa to 700 kPa (5 psi to 100 psi). The challenge in developing a sensor for Mars conditions is to lower the sensitivity range into this extremely low pressure regime. Other technology advancements include the charge amplifier circuits needed to increased voltage response range.

There are several common architectures for pressure sensors: resistive, capacitive, piezo or electro active. The resistive approach, where a material changes its resistance due to the pressure placed upon it, has poor sensitivity in the low pressure regime. It also suffers from high hysteresis. A capacitive device or piezo electric device relies on the deformation of a small cavity to register a change in the electrical behavior of the circuit (see Figure 24). The output current is directly related to the dielectric capacitance which enables the sensing of an applied pressure. These devices are more challenging to manufacture and they also have inadequate sensitivity in the low pressure regimes.



Figure 24 Piezoelectric sensor construction (image credit: Xerox PARC)

The emerging developments that support realistic sensing in “artificial skin” are promising in terms of range of detection. The goal of the artificial skin is to sense the dynamic application of a “light touch” pressure but then also continue to detect the static application and subtle changes in that pressure. One example comes from Dr. Bao at Stanford University. She has developed a micro-structured rubber based capacitive sensor that has demonstrated sensitivity down to 3 Pa. The 6 μm sized pyramidal structure is molded in PDMS which acts as the dielectric layer in the sensor. The unique shape and size of the structured PDMS allows it to deflect elastically under small pressures with increased sensitivity over an unstructured layer and exhibits none of the viscoelastic creep of other designs.¹¹ While this device is not “printed” per se, it is compatible with the thin flexible form factor of the science platform.

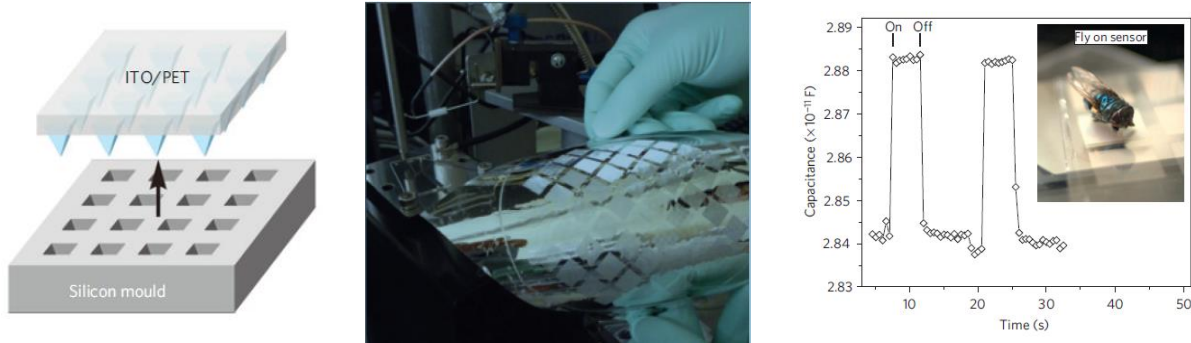


Figure 25 Microstructure PDMS, fabricated pressure sensors, demonstrated results

5.4.3.5 Light Intensity

The light intensity on the surface of Mars is a useful measurement for detecting the opacity of the atmosphere or even measuring the accumulation of dust on the sensor. The range of wavelengths is broad and measurements in multiple wavelengths provide valuable data for determining atmospheric constituents, dust, and scattering properties. With a printed photosensor, the sensing layer can be engineered to be responsive to different wavelengths and therefore multiple sensors can work in concert to cover a range of wavelength. Large area sensors utilizing carbon nano-powders with organic transistors, have been designed for infra-red detection. Various other optically sensitive materials have been used from PVDF to multi-walled Carbon Nano-tubes. Zinc oxide nanoparticles have been reported as a sensing layer for the ultraviolet light.³⁹ Sensitivities ($1 \mu\text{W}$) well in excess of the requirements expressed in Table 2 have been established in the IR wavelengths with printed photosensors.⁴¹

The UV band is of most interest at Mars to answer questions of habitability. Acreo, an element of the Swedish ICT Research Institutes, has developed a UV sensor that uses an innovative new type of ink that detects and measures UV-light directly on the printed sensor platform. A fully functional prototype was developed and demonstrated this year.⁶³ The UV-detector contains a printed area that is sensitive to UV light. The radiation is converted to an electronic signal which is proportional to UV light intensity. The result of the measurement is read directly on the display. It also gives the total dose of UV light exposure.



Figure 26 Acreo low-cost, printed, UV sensor system

5.4.3.6 Radiation

Recording the total ionizing dose of gamma radiation throughout the life of the mission is desirable to investigate habitability, microbial survival and the preservation of organic chemicals. The average dose per day on the surface is 20 mrad with peaks up to 1000mrad/day during solar proton events as measured by the recent RAD instrument on the Mars Science Laboratory mission.⁴⁹ Radiation dosimeters are not a challenge to create in a printed system. Radiation sensors are simple resistive devices in which a screen printed active layer changes its electrical resistance based on absorbed radiation. There are several materials, such as TiO₂, CuO, ZnO, CdO, MnPc, which have been characterized for electrical behavior upon exposure to radiation.^{50, 51} An alternate approach to radiation sensor is based on the response of a standard thin film a-Si solar cell as a detector for total dose.¹⁷ Testing was performed to show a detectable response in an array for standard cells up to 500 Gy/50krad.

One resistive device was recently tested by the University of Limerick, Ireland using a Nickel-Oxide sandwiched in silver contacts. This device was formulated using thick film pastes. A NiO polymer paste and a silver paste were used to fabricate the radiation sensitive material and contacts respectively. Pastes were screen printed on glass substrates to form a sandwich Metal-Semiconductor-Metal structure with an active area of 1cm² and a film thickness of 70μm.¹⁵ As the radiation sensitive material was exposed to gamma radiation (up to 720 Gy/72krad), the electrical behavior of the NiO paste was measured showing a noticeable change in the current voltage characteristics. The permittivity of the device decreased by a factor of two over the radiation range tested.¹⁵

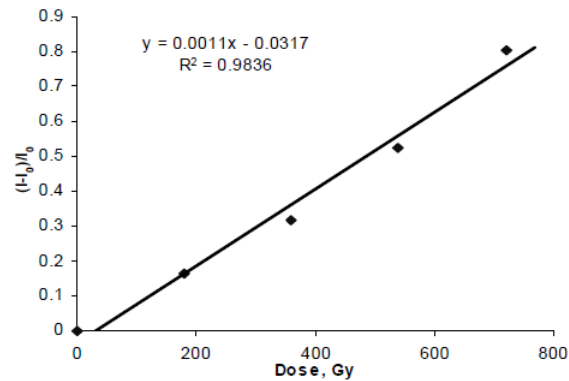


Figure 27 - Dependence of normalized current $(I-I_0)/I_0$ with radiation dose under an applied voltage of 3V. (image credit: University of Limerick).

5.4.3.7 Wind Speed

The typical method for calculating wind speed is a hot wire or hot film anemometer. The wire or film is heated above the ambient conditions and as the wind blows the atmosphere past the wire it produces a signal proportional to the heat transfer between the atmosphere and the element. Commercial hot film anemometers are already somewhat compatible with printed electronics techniques and the thin, flexible form factor. They are low voltage, low current devices and are already fabricated in thin film constructions.¹⁸ Power to heat above ambient can be a few milliwatts depending on the convective and radiation losses. The bigger challenge for the flat landers is providing the physical orientation and exposure to wind speed directions.

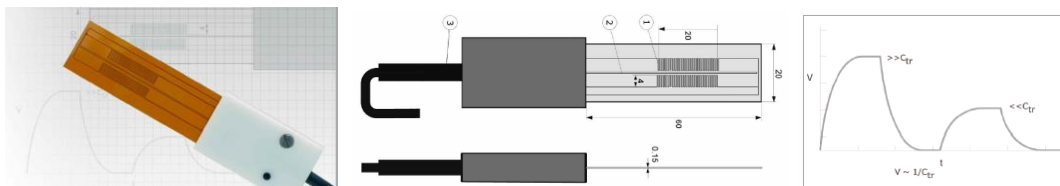


Figure 28 Commercially available thin film anemometer (image credit: Hukseflux USA Thermal Sensors)

5.4.3.8 Data Storage

Based on the engineering and operational assumptions described in the design overview, the data storage volume needs to be sized to hold one measurement per sensor per hour plus time stamps and sensors identification for five days. Each sensor measurement is 8 bits resolution from the ADC. Making some efficient assumptions as to the header information, these requirements calculate out to be just over 8.5 kbits of data volume for 5 days.

Day (9 bits)						
Hour (5 bits)		Sensor ID (3 bits)	Measurement (8 bits)			
1713 bits per day		71 bits per hour				
71 x 24 hours + 9 bits for day ID		(3+8) x 6 sensors + 5 bits for hour ID				

Figure 29 Data Volume Calculation

The design of the data storage/memory is based on the ferroelectric printed memory that Thinfilm products initially released in 2009. As described in the Thinfilm’s product release documentation, the basic design of Thinfilm Memory is a ferroelectric film sandwiched between two electrodes. When voltage is applied, the dielectric dipoles within the polymer layer align in one of two directions, depending on whether the voltage is applied to the top or bottom electrode. When the voltage is removed, the material remains pinned in the same state, and can be read as a one or a zero – a non-volatile memory cell.⁵²

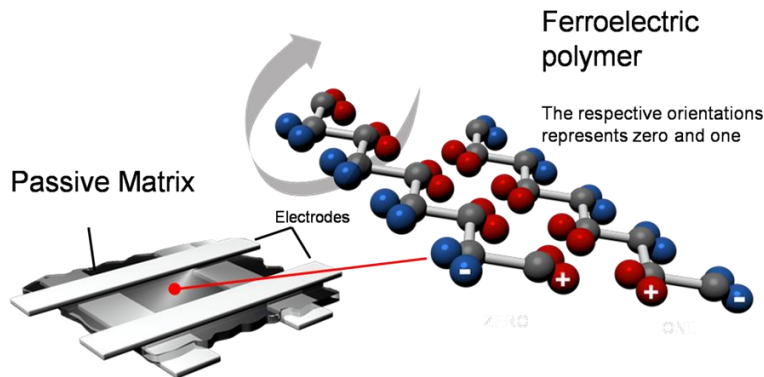


Figure 30 ThinFilm Ferroelectric Memory (image credit: Thin Film, Inc.)

The memory cells have been demonstrated to have long lifetime and degradation rates less than silicon. The product is also compatible with high volume production on roll-to-roll printing presses. In 2010, Thinfilm and Xerox PARC teamed up to add logic functionality to the memory using TFTs. The partnership released Thinfilm Addressable Memory™, the first printed rewritable memory addressed by organic logic. The logic shares several layers with the ferroelectric memory and was designed synergistically from a materials and construction perspective. This Thinfilm Addressable Memory™ is now incorporated in many products from food packaging labels to inventory management tags.



Figure 31 Xerox PARC and ThinFilm addressable memory and its application in a temperature sensing tag.

The physical size of the memory on the STANLE platform was determined by the ThinFilm construction. The current assembly of the memory includes a small area for the polymer matrix and electrodes of the memory itself as well as a large “pad” for interconnects and connection to logic TFT for the read/write circuits. The current data density is about 3.2 bits/cm². We have assumed that the design and technology will advance by the technology readiness date of 2020, to include a more integrated design between memory and logic which will reduce the number and size of the contact pads through a more integrated design. A tenfold increase in bits/cm² was assumed providing a calculated area of 15cmx15cm for the memory on the STANLE platform.

5.4.3.9 Analog to Digital Data Conversion

The data conversion from analog to digital is assumed to be done by a printed analog-to-digital converter (ADC). Recently, a fully printed analog to digital conversion circuit was produced and demonstrated. The ADC circuits printed by CEA-Liten includes more than 100 n and p type transistors and a resistive layer on a transparent plastic sheet. The ADC circuit offers a resolution of 4bits, and has a speed of 2Hz. The ADC was designed by Eindhoven University of Technology, ST Microelectronics and University of Catania, in the framework of the EU project COSMIC (Complementary Organic Semiconductors and Metal Integrated Circuits).²⁰ The size of the current device is 24cm². The technology extrapolation for this device is to achieve an 8 bit resolution in the same area. The developers of this first version anticipate being able to reduce the area significantly through their continuing developments.

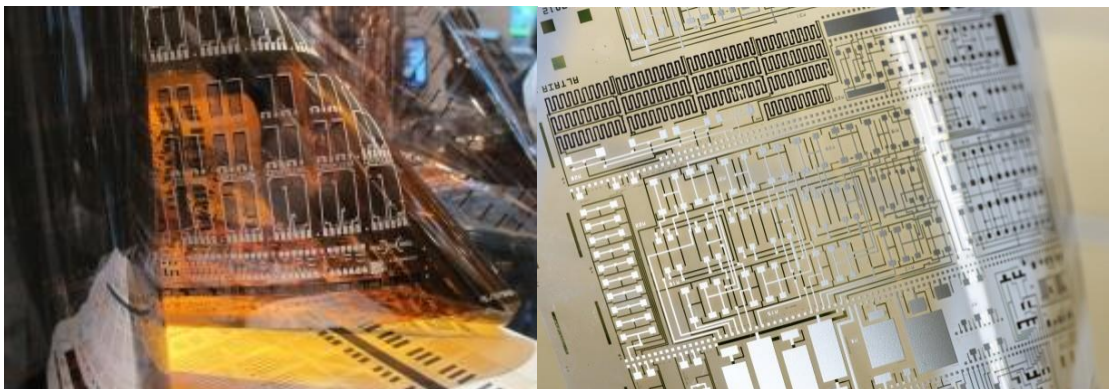


Figure 32 Printed ADC developed through the EU COSMIC project (image credit: CEA-Liten)

5.4.3.10 Microcontroller

The one functional subsystem of the STANLE platform that is difficult to extrapolate into a fully printed system is the microprocessor. A printed microprocessor to manage the functions of the STANLE platform is the biggest push for the technology advancement. The fundamental limitations of being able to produce the logical circuits needed to execute commands and programs is the circuit speed allowed by the materials and feature size, as well as the variability in the manufacturing process and the effect that has on the performance of the circuit. The current state of the art for the printed logic circuits is not capable of formulating the equivalent of a microprocessor in a reliable and cost effective way. One mitigation for the limitation is to reduce the functionality required to the execution of fixed sequences that do not require fast execution speeds. In 2011, a partnership of IMEC/TNO/Polymer Vision presented the closest thing to a printed “processor” fabricated on a flexible plastic substrate with organic transistors using a variety of application methods including spin coating and etching to create a matrix of transistors to execute a fixed program. The processor can run only one simple program of 16 instructions. The commands are hardcoded into a second foil etched with plastic circuits that can be connected to the processor to “load” the program. This program allows the processor to calculate a running average of an incoming signal. The chip runs at a speed of six hertz and can only process information in eight-bit chunks.²²

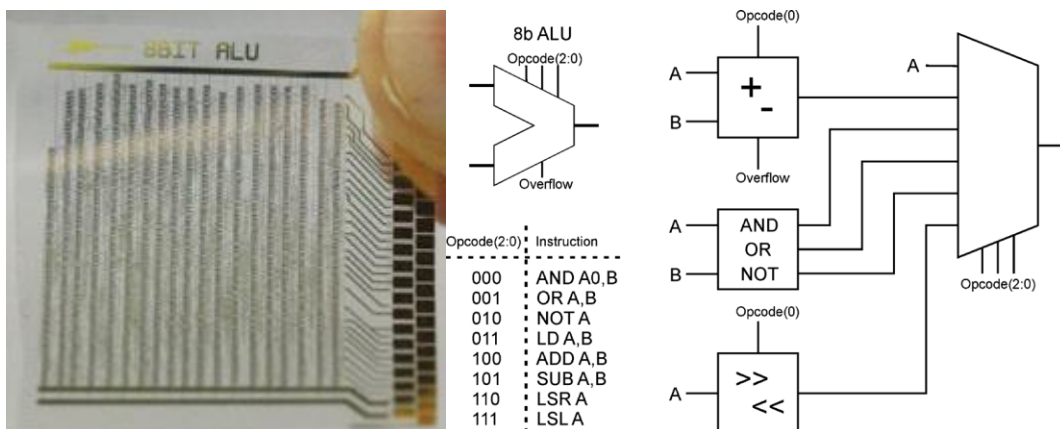


Figure 33 Plastic processor foil (left) and the symbol, instruction set, and architecture of the main building block of the processor (right). Image credit: IMEC/TNO/Polymer Vision.²⁴

The processor starts with a 25 μ m thick sheet of flexible plastic, a layer of gold electrodes are deposited on top, followed by an insulating layer of plastic, another layer of gold electrodes and the plastic semiconductors. Those transistors were made by spinning the plastic foil to spread a drop of organic liquid into a thin, even layer. When the foil is heated gently the liquid converts into solid pentacene, a commonly used organic semiconductor. The different layers were then etched using photolithography to make the final pattern for transistors. This plastic single program “processor” is approximately 2 cm x 2 cm containing approximately 4000 transistors. It operates between 10-20 volts with a power consumption of 92 μ W.²⁴

The functions required by the STANLE processor are much more elaborate than what can be accomplished with something like the first flexible plastic processor. Required functions include clock synchronization, execution script for polling the sensors, controlling the write/read

sequencing of the memory, and power regulation. Extrapolating the advances needed in designing a fabricating a printed microprocessor was not attempted. Manufacturing consistency, feature size, mobility and circuit speed, voltage level, and device density are all facets of the device that would need to be advanced. Instead, the STANLE platform assumes a “hybrid” approach of including a silicon microcontroller while maintaining the flexible and thin form factor and low voltage architecture. The microcontroller is assumed to be based on a novel Silicon on Polymer (SOP)TM thin film microprocessor device developed by American Semiconductor.²⁵ This device will control the sequencing for the sensor readings, and manage the time stamp/header information and control the logic for memory read write. It is an 8-bit RISC microprocessor operating at 20 Mhz, and low voltage (<3 V). It provides a real time clock and timer and allows for 8KB of program/data RAM, 1 KB of program ROM.²⁵ The entire microprocessor is packaged into a 5mm x 5mm area on a 14-25 micron thick polymer substrate. It is the perfect device to leverage the increased functionality of a silicon device without losing the low voltage, thin, flexible form factor desired with Flexible Hybrid electronics (FHE). The device as designed today will meet the functional requirements of the STANLE platform and does not necessarily require significant technology advancements. The challenge is with the integration of the device into the printed platform as the manufacturing of the FlexTM devices is done in a traditional foundry and the interconnects are extremely small.

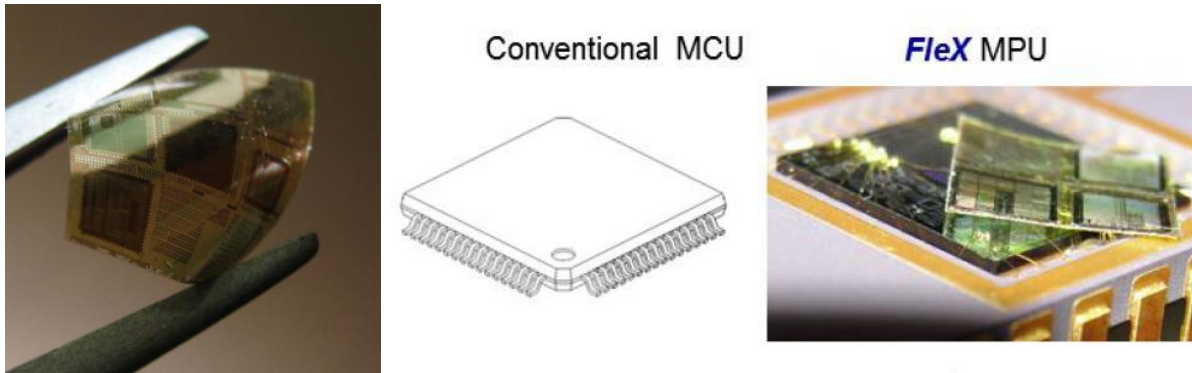


Figure 34 American Semiconductor Flex microcontroller (image credit: ASI)

5.4.3.11 Solar Cells

The power system is architected to ensure continuous operation of the STANLE platform regardless of solar illumination. The platform contains solar cells to provide the operational power of the lander as well as recharge the battery during the day. According to the power budget provided in 5.4.3.1, the solar cells are required to produce approximately 50 mW (we have allocated space and mass for 100 mW) and are strung together to provide the 3 V to the platform. The solar cells are sized to recharge the 35 mAhr of battery capacity in approximately 5 hours.

Solar Cell Peak Power:

Sampling Mode (mW)	10.4
Battery Charging (mW)	20.64
Duration (hr)	5
Voltage (V)	3
Capacity (mAhr)	34.40
Margin (50%)	15.52
Total Solar Cell Peak Output (mW)	46.6

(powers day ops plus battery charge)

Terrestrial applications have driven the printed solar cell technology to a very mature state. The materials and device fabrication technology has been optimized for manufacturing efficiency and low mass. For the STANLE platform, we have made two assumptions with respect the solar cells. The first is that the materials choices, packaging and encapsulation approach are revamped to be optimized for the space environment. The second is that the cell level performance metrics, (e.g. conversion efficiency and W/gm²) will continue to advance until 2020 as they have over the past decade. Below in Table 4 are the estimates of the technology advancement for cell efficiency, and specific weight. The “panel” specific weight for the STANLE application was pushed higher than a terrestrial application because of the limited number of cells on the STANLE platform and the lack of any structural framing mass required. Based on the performance metrics assumed below, the area required to produce the 100 mW needed for the system design was calculated to be ~4 cm x 4 cm assuming the solar irradiance at Mars.

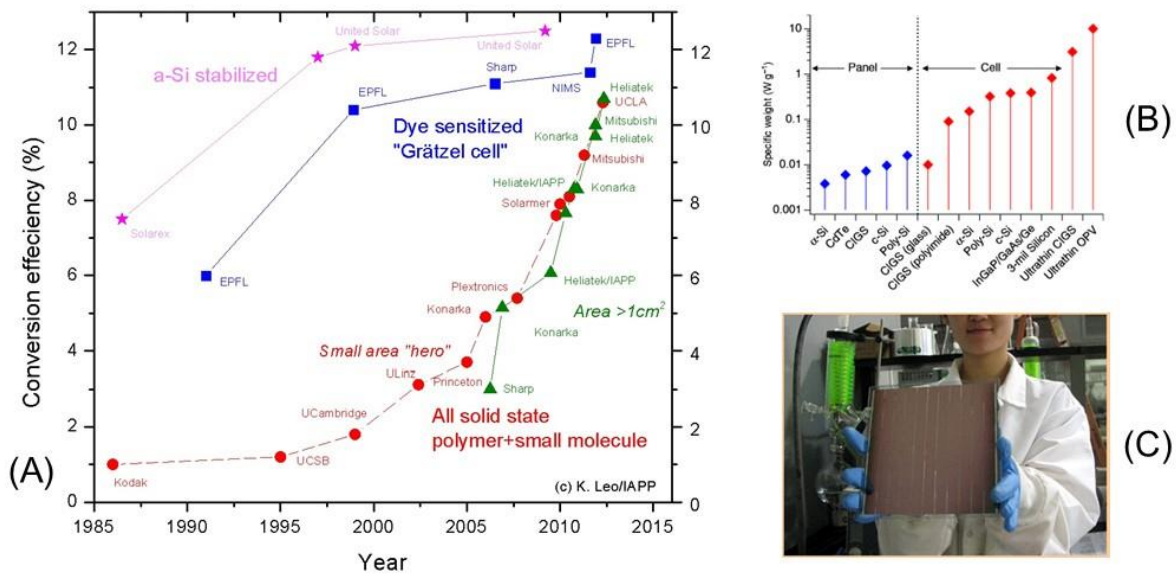


Figure 35 (A) OPV cell efficiency (image credit: IAPP) (B) Cell and Panel Specific Weight (image credit: Nature⁵⁵) (C) Solarmir OPV champion cell (image credit: Solarmir)

Table 4 Performance Advancements assumed for STANLE solar cells

Solar Cell Technology Projections	Printed TODAY ⁵⁴	Printed 2020
Cell Efficiency	9%	14%
Panel/System Efficiency	5%	10%
Cell Specific Weight (W/gm)	0.3 to 10	3 to 20
Panel/System Specific Weight (W/gm)	0.02	3

5.4.3.12 Battery

The battery is sized to provide power for night time operations and communication passes. Using the power modes from the system design table (Figure 18), the battery capacity required is approximately 35 mAh. There are currently commercially available printed thin film batteries that can readily provide that capacity at the 3-4 V level. However, those batteries are not rechargeable and have a current discharge limitation of only a few milliamps.⁵⁶ The communication burst would draw current at almost 0.5 Amps for a few seconds. Alternate choices for energy storage would include super capacitors or thin solid state energy cells. A printed super capacitor can be recharged but also is limited in its discharge current.^{33,34} A solid state cell such as Thinegy MEC 200 series could discharge at a higher current closer to what is required for the communications system but has a more limited capacity (few mAh).⁵⁷

Battery Capacity:

Nighttime duration (hrs)	12	
Duty Cycle - Sampling	25%	
Duty Cycle - Standby	75%	
Operating Voltage (V)	3	
Operations Capacity (mAh)		22
Communications Power (mW)	1500	
Comm Duration (sec)	6	
Comm Capacity (mAh)		1
Margin (50%)		11
Total Battery Capacity (mAh)		34

(powers nighttime ops plus comm)

Therefore, the desired technology advancements are to increase the discharge current, increase the capacity and add the ability to recharge. On this last point, Imprint Energy has recently announced the success of its ZincPoly™ rechargeable printed flexible battery and has received significant funding to bring the product to market.⁶⁰ So this technological advancement may not be that far off. Technology advancements are also needed to expand the operating temperature range for the materials and to provide vacuum compatible packaging for space applications. Power management circuitry would be needed including power switching, regulation and shunting.



Figure 36 Imprint Energy ZincPoly™ printed rechargeable battery

5.4.3.13 Communications

The STANLE platform assumes a UHF relay link to a Mars orbiter. The Team X study session was able to analyze the MRO and Odyssey coverage for various zones on the planet and could confirm that the majority of the time, there is a contact opportunity once every sol, assuming a reasonable elevation angle (see Figure 37). That conclusion starts to break down when you factor in higher latitude landing sites (above 60 deg), and the practical limit of how many landers the orbiter can sequence through in the pass duration. Assuming the downlink event is powered by the battery removes the additional constraint for solar illumination during the communication pass. Assuming three lander dispersion zones less than 500km long, the current communication scheme can support a 24 minute pass each day by each of two relay orbiters for each zone. In order to support roughly 2500 landers per zone in a 5 sol window, each lander would be allocated about 6 seconds for its comm pass. The assumption is that the orbiter initiates each lander’s downlink with a ping and cycles through the various landers when in view. Allocating some time within the six seconds for the initiation sequence, each lander must support a downlink rate of roughly 2 kbps.

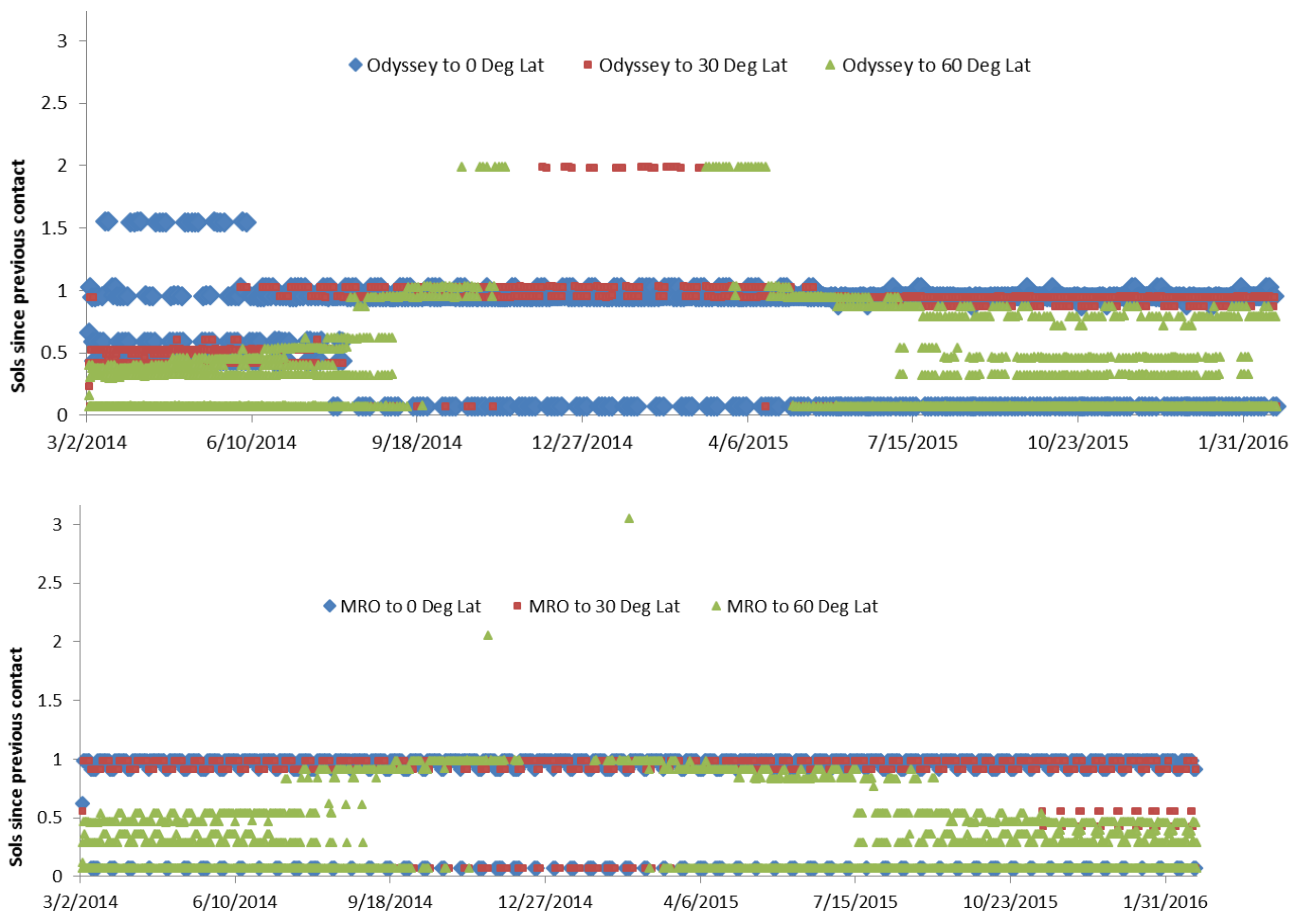


Figure 37 Communications coverage for MRO and ODY

The MRO and ODY orbiter’s UHF links operate between 400-435Mhz at fixed integral data rates (1,2,4,8,16,kbps up to 2048 kbps). These parameters and others defined for the relay links were used in the link analysis tools.⁵⁹ The STANLE on board communication system consists

of a modulator, transmitter and antenna. The antenna design assumed a gain of -5dBic at 5° degree elevation. The modulator imparted a simple convolutional code. To sustain a rate of 2 kbps , the on board transmitter was assumed to be 1.5 W . The telecommunications link between the STANLE platform and the relay orbiter with these parameters closed with a margin greater than 3 dB .

As far as implementing the RF system in a printed form factor, there are challenges similar to those described for the microcontroller. The antenna is assumed to be a simple flat antenna in a printed form factor. The antenna is not the technology challenge and in fact several printed UHF antenna designs have been fabricated, tested and data published.^{35,36} The RF circuitry (modulator and transmitter) is a larger challenge. Several commercial companies have produced near field RFID systems at 13 Mhz with fully printed RF electronics. Faster circuit speeds are required to support the higher frequency band. In addition, to boost the signal for the longer range compared to the near field systems, a higher RF power output is needed. Just as the flexible hybrid electronics approach was the solution for the microprocessor, a similar solution can exist for the RF system. The American Semiconductor FleX RFICTM SOP chip has recently become available.²⁶ The frequency band is 915 Mhz UHF but is still only a low power solution. However, there is the possibility of extrapolating this technology more readily into the needs of a mars relay UHF system.

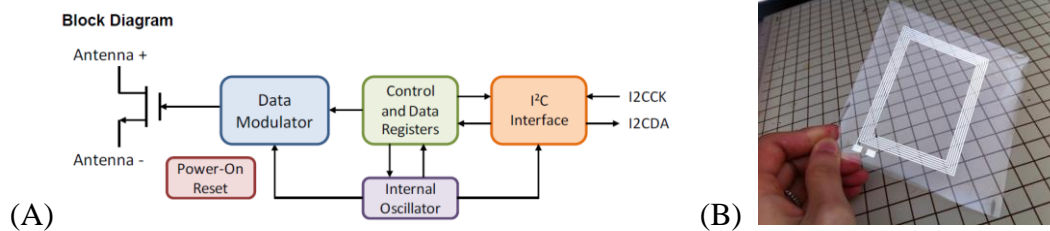


Figure 38 (A) FleX SOPTM RFIC block diagram (image credit: American Semiconductor)
(B) Printed antenna for STANLE prototype (image credit: PARC)

5.4.3.14 Thermal Design

The thermal design of the STANLE platform is purely passive. It is assumed that the platform and all the elements on it are cycling along with the environmental conditions. There are no provisions in the current design and sizing to provide any power for heating the platform or maintaining thermal stability. The sensors must be designed to be stable or calibrated vs temperature. The materials and construction is assumed to survive the thermal cycling between the range of -120 to $+20\text{ deg C}$.

5.4.4 Study Considerations

5.4.4.1 Technology Gap Assessment

After the discussion of the state of the technology with respect to each of the functional areas, it is helpful to summarize the overall state of readiness today for the STANLE platform design. For some areas, a printed system is not the only solution that will preserve the platform

characteristics of a thin flexible sheet. Integrating flexible hybrid electronics into the solution space can dramatically change the outlook of functionality. Table 5 below illustrates the gap remaining and development necessary to bring each area up to a state of readiness. The programmatic assumptions outlined a Technology Readiness date of 2020. With an additional six years of investment it seems likely that the engineering functional elements will close the gap if not with a printed solution then a flexible hybrid solution. Each of the sensor areas has commercial applications and the capabilities are also likely to continue to advance with respect to sensitivity, accuracy, stability and range. The tallest tent pole would be the reliability of the measurement under the varying conditions of Mars.

Table 5 State of Readiness of STANLE Functional Elements

Functional Element	State of Technology Today		Necessary Advancements	TRL Estimate
	Printed	Flex Hybrid		
Sensors				
Temperature Sensor	Green	Green	fully characterize and calibrate over in flight environment	4
Humidity Sensor	Yellow	Yellow	Increased sensitivity of materials; printing resolution; material hysteresis; single material for broad range	3
Pressure Sensor	Red	Red	integrate basic sensing mechanism into full device; characterize influence on environment; would pursue traditional sensor compatibility with platform	2
Light Sensor	Yellow	Yellow	sensitivity and characterization in multiple wavelengths; investigate "array" approach	3
Radiation	Yellow	Yellow	functionality and form factor exist; characterize materials and performance for environments	4
Wind Speed	Yellow	Yellow	sensitivity and performance in Mars atmospheric conditions, calibration over environments.	4
Engineering Systems				
Memory	Yellow	Green	sufficient memory exists on FHE solutions; if printed then advances needed in printing resolution; higher density form factor	3 to 4
ADC	Yellow	Green	increased resolution 4bit to 8 bit; alternate exists to use FHE solution.	3
Processing	Red	Green	Only green for FHE solution with flexible silicon chip; for printed significant increase in circuit speed, manufacturing consistency; printing resolution,	4 FHE 2 Printed
Solar Cells	Green	Green	optimization of materials for conditions, longevity testing.	4
Energy Storage	Yellow	Yellow	printed secondary batteries, high current discharge; vacuum compatible materials / packaging; investigate power regulation circuits and dual mode solutions	2 to 3
Antenna	Green	Green	design and demonstrate for frequency and gain.	6
RF Electronics	Red	Yellow	FHE solution shows promise but not designed for frequency, power and rate.	2 FHE 2 Printed
Interconnects	Green	Green	benefits from materials and manufacturing advances but no critical advances needed.	6

5.4.4.2 System Design and Mission Trades

As with any mission concept, it takes many iterations to optimize the overall approach, and vehicle design. In this study we have managed to do about one-and-a half passes through the overall mission design and flight system approach. As the concept was developing there were many trades that were identified to either improve performance/design, address a concern or get closer to the desired data return. Several of those areas are described below. Given more time and resources these would be pursued as part of mission concept maturation.

- Aerodynamics and Global Coverage of Landers: The concept pursued in this study was a single large entry vehicle with many landers for the ease of comparing to an existing traditional concept. The single aeroshell allows distribution over a moderate area which can support intermediate scale modeling goals. However, it does not meet the highly desirable global coverage. That would certainly require multiple entry probes targeted to different longitudes and latitudes.
- Simplify the descent sequence. Other possibilities can be considered that could even further simplify the descent and lander release. The dispensers could be mounted to the heatshield and be released backward into the airstream rather than down and away from the backshell. The parachute could be eliminated and a high altitude, high speed mortar deployment of the landers could be envisioned. Eliminating the parachute would further reduce the cost and risk of EDL.
- Lander configuration: Questions arise about whether the lander is biased to land “face up”. We did not embark on a trade between a double sided lander or a biased configuration. The flight testing by the Princeton students did show that weighting the bottom of the lander increased the probability of landing face up. Some evaluation of alternate shapes for the flutter landers (cones, autorotators, etc) was done by the Princeton students and showed promise for wider dispersion and oriented landing. Because flexible printed electronics could easily be compatible with these simple shapes, it is worth considering. A “raised” shape may enhance the science for some of the sensors and engineering systems (wind, temperature, solar cells and communications).

5.4.4.3 Top Technical Risks

Every mission concept has features or characteristics that pose risk to mission success. To have a fully vetted mission concept, each one must be pursued and mitigated to ensure it does not pose a fatal flaw. This task is usually tackled in the conceptual design phase. This STANLE mission concept is no different. There are several architectural and “operational” issues, as well as advances in support systems that must be considered before endorsing this mission concept. These were not tackled in the scope of the NIAC task, but were identified through the course of defining the reference mission. They should certainly be addressed during any subsequent concept maturation activity. Some risks are mission architecture risks that would exist for any large quantity of small, lightweight landers on the surface.

- Positional stability of the landers on the surface in the presence of strong winds
- Dust accumulation on low flat surfaces and the impact on solar power and sensor measurements.
- Communication switching architecture with existing orbital assets: fast cycling and re-initializing with a new lander every few seconds plus differentiation of signal.
- Perception of too many landers as “litter” on the surface and ensuring the planetary protection sterilization requirements can be met.

Some risks are unique to the printed electronics construction

- Characterization of performance changes with temperature and elongation/strain in the platform substrate
- Stacking abrasion with high density packaging.
- Aerodynamic interaction with the backshell and/or heatshield during deployment of the flutter landers.

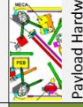

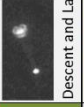






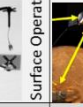
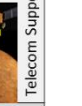
6 STANLE Reference Mission – Scorecard

6.1 Overview

Any technology needs to be evaluated on its value proposition. Does incorporating the technology into a mission bring value to that mission... a reduction in cost, risk, schedule, or an increase in science return or capability? In order to make that evaluation for printed electronics, specifically the printed network lander, we used the JPL Team X organization to evaluate the differences in mass, cost, schedule and risk for a Mars lander mission using a traditional lander and using the printed lander. The expectation was that the simplicity of the printed landers along with the unique flutter lander architecture would reduce the cost, complexity and risk associated with hardware development costs, system I&T and the entry descent and landing support hardware.

Team X is a highly sophisticated interactive, real-time design environment specifically formulated to do early trade studies and subsystem-level design work. The Team X environment condenses a design team effort that would normally be performed over several months into several hours perfecting this process through over 1100 studies. Team X is composed of about 20 discipline experts, taken from the ranks of the organizations responsible for that work at JPL, using tools designed and approved by these same organizations. Studies are conducted in a dedicated room with networked workstations sharing data on a common server. The team’s work can range from simple mass or cost estimation of existing designs to more complex optimization trades. Team X is an integral part of JPL’s concept development process.

Our approach to evaluate the benefit of infusing the printed lander was to assess the changes in key metrics for each of the major project hardware and development phases. We created a “scorecard” of the key metrics by each hardware development and functional mission phase that we expected to be influenced by the introduction of the printed lander (see Figure 39). Our predictions were that introducing the printed lander into the mission would offer a higher value for these important metrics in the majority of the key phases. In order to focus the comparison, we intentionally assumed some elements remained invariant: launch mass, cruise stage, entry conditions and parachute.

	 Payload Hardware Development	 CS /EV Hardware Development	 Descent and Landing HW Dev.	 System I&T	 Launch Operations	 Cruise Operations	 Entry Phase thru HS separation	 Descent and Release	 Landing	 Surface Operations	 Telecom Support Assets
Mass	P	S to T	P ✓	NA	S	NA	S	P ✓	P ✓	NA	NA
Cost	P	S to T	P ✓	P ✓	S	S	S	P ✓	P ✓	P ✓	P to T
Schedule	P	S to T	P ✓	P ✓	S	S	NA	NA	NA	S	NA
Risk	T	S	P ✓	T to P	S	S	S	P ✓	P ✓	T ✓	T

Printed

Traditional

Same

Figure 39 Project-level Benefits Scorecard. Check marks indicate predictions validated by Team X. Two predictions were overturned by the Team X results.

By using the Team X processes, databases, and personnel, we were able to access information from a complete study of a moderate class (~\$400M) traditional Mars lander mission. This traditional mission assumed the classic architecture of a separable cruise stage, aeroshell entry, parachute, and propulsive descent and soft touchdown of a stationary lander. The Team X study contained mission design, trajectories, flight system design including subsystem component details, operational scenarios and full mass/power list and cost down to the box level. The study also included cost estimates for the entire project with flight system details internal to the subsystems and separated by vehicle (cruise stage, entry vehicle, etc). These detailed elements were then manipulated (moved or deleted) as needed to accommodate the requirements of the printed lander mission which formed the basis of the comparison of the two mission implementations.

The Team X study validated most of the predictions – indicated with a “checkmark” in Figure 39. In a few places, the results of the Team X study indicated a change to the prediction – indicated with a change in color. The change in the “same to traditional” in cruise stage and entry vehicle development was due to shifting functions normally provided by the traditional lander into the backshell or cruise stage. This is explained further in the “Technical Design Changes” paragraph below. In several places, such as the payload development (e.g. the printed landers), Team X did not assess a comparison.

This Chapter will discuss the technical changes that were needed in the “traditional mission” flight system to accommodate the printed landers. We then present the resulting comparison of cost and mass. Schedule was not investigated in a detailed manner, but a qualitative comparison was made by the Team X system leadership.

6.2 Technical Design Changes

The architecture of the Flight System for the traditional mission is shown in the block diagram in Figure 40. A common trait of the traditional Mars lander missions is to utilize the capability of the lander to provide many of the higher order functions for the Cruise Stage and Entry Vehicle such as command and data handling, telecommunication transceivers, and attitude control algorithms. When a highly functional traditional lander is replaced with the simplicity of the printed lander, many of those functions/systems need to be added either to the entry vehicle or the cruise stage. The Team X study systematically identified the subsystem elements that needed to be “moved” from the lander. Many of the lander elements are completely eliminated from the design when the printed landers are included. Likewise, there is some unique “new” hardware that needs to be added specifically for the printed lander implementation. Most notable is the dispensers for the landers. The three kinds of modifications are shown graphically in the revised block diagram Figure 41 and itemized in Table 6.

The new dispenser hardware and structural changes needed in the backshell were designed and evaluated by the Team X mechanical and configuration leads. They assessed the ability to package and support the additional hardware. They performed conceptual designs of several dispenser ideas, settling on the collection of spring loaded boxes shown in the reference mission section Figure 16. A mass and cost estimate for these new elements was generated by those technical leads.

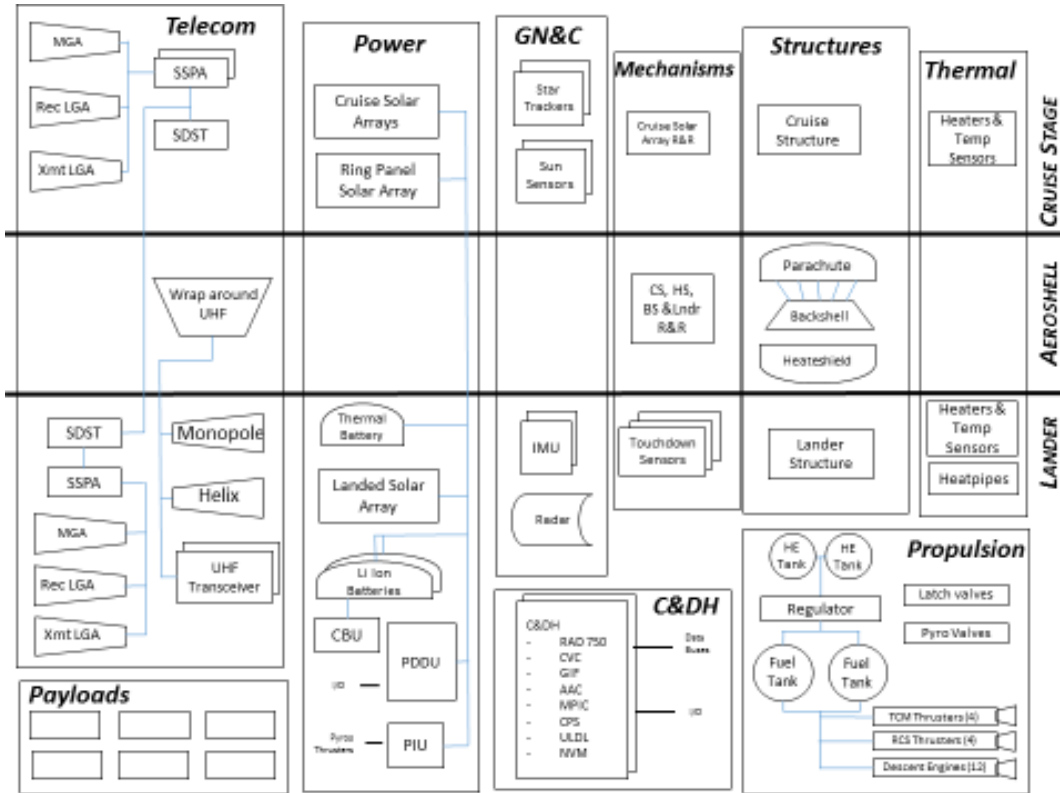


Figure 40 Traditional Mars Lander Flight System Block Diagram

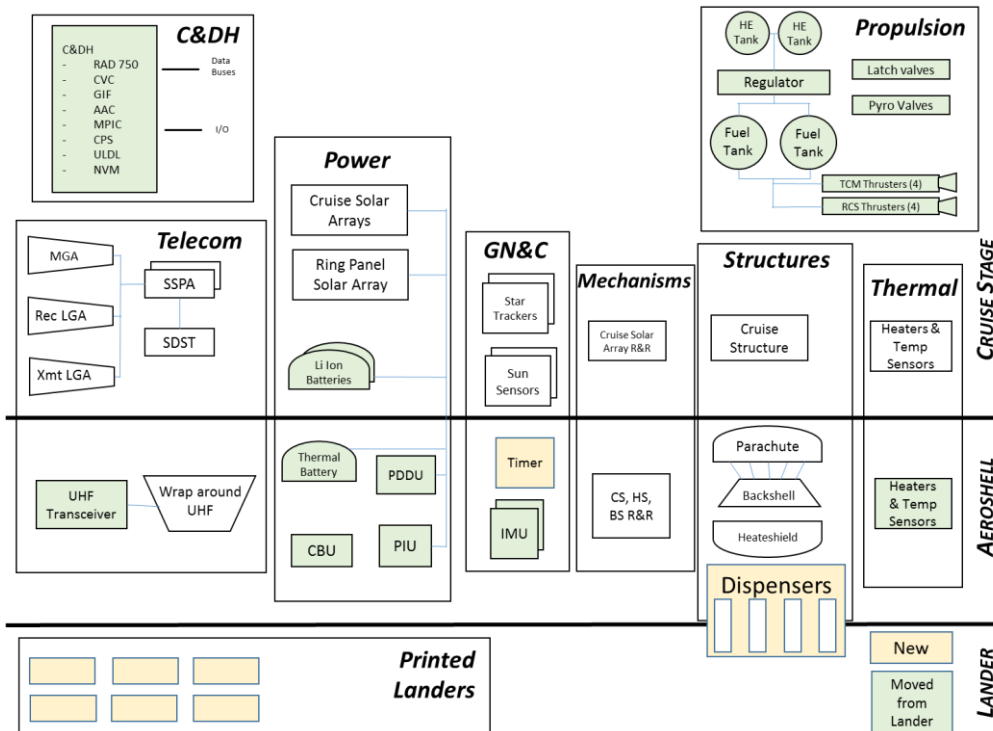


Figure 41 Printed Lander Flight System block diagram

Table 6 Design modifications made to flight system

Delete from Design		Moved to BS or CS	Add as NEW for Printed
UHF monopole	Thermal Battery	UHF Transceivers	Dispensers and mechanisms
UHF Helix	RADAR	Li Ion Battery	Structural mods to backshell
Lander SSPA	Touch Down Sensors	PDU	
Lander SDST	Descent Engines	PIU	
Lander MGA	Descent Prop System	C&DH	
Lander Rec LGA	Lander TCS system	CBU (aka BCB)	
Lander Xmit LGA	Lander Solar Arrays	IMU	

6.3 Cost Comparison

The cost structure for the two mission implementations follows the standard JPL Work Breakdown Structure (WBS) with the additional elements of aerothermal testing and landing radar unique to entry/landing missions. In addition, in the Team X database the flight subsystem costs were broken down between cruise stage, entry vehicle and lander down to the element box level for each subsystem. That allowed us to readily assess the cost adjustments needed to account for the deleted or moved items described earlier.

WBS Elements	
1.0 Project Management	
2.0 Project System Engineering	
3.0 Mission Assurance	
4.0 Science	
5.0 Payload System	
6.0 Flight System	
6.01	Flight System Management
6.02	Flight System System Engineering
6.04	Power
6.05	C&DH
6.06	Telecommunication
6.07	Structures
6.08	Thermal
6.09	Propulsion
6.10	ACS
6.11	Harness
6.12	S/C Software
6.13	M&P
6.14	Testbeds
NA	Radar
NA	Aerothermal testing
7.0 Mission Operations Preparation	
9.0 Ground Data System	
10.0 ATLO	
11.0 Education and Public Outreach	
12.0 Mission and Navigation Design	
Reserves	

In our cost comparison, we focused mainly on the hardware related WBS elements. A common feature of cost models is that the non-hardware, level of effort tasks, such as Mission Assurance, Material and Processes, are scaled as a percentage of the hardware element costs or mass. We did not take any of those cost adjustments into account. More precisely, we only compared WBS elements 5.0, 6.0 and 10.0.

The cost comparison for the Flight System estimates generated a “conservative” number and an “aggressive” number. The conservative cost numbers presented for the printed mission implementation are derived purely from the removal or addition of a box cost. Within a subsystem, we did not adjust the level of effort tasks such as management, systems engineering, or contract oversight. We did not make any changes to the software estimates or system testbeds. With the exception of one item, we did not take credit for any potential savings associated with a reduction in the level of complexity of the elements that were moved from the lander to the backshell. The one exception was the C&DH system from the traditional lander. The design from the traditional lander was fully redundant to meet requirements of the surface mission lifetime. When we moved the data system to the cruise stage for the printed mission, its function was reduced to supporting cruise and the initial entry sequence which seemed appropriate for a single string design. We removed the recurring engineering cost and the mass of the redundant cards. It was assessed by the Team X subsystem leads that several elements in the thermal design, CDH, and power subsystem (batteries, power distribution and pyro electronics) would have reduced requirements and could be simplified. However, without a design for those reduced requirements, any savings would be speculative. The potential for additional cost savings for the anticipated reductions described here is high - on the order of \$20-25M based on engineering judgment. However, this number is unverified without a certified cost model run on a complete point design for the entire printed mission flight system elements. Therefore we have included it in an “aggressive” cost comparison.

The two implementations (traditional vs printed) for the Flight System WBS (6.0) are compared side by side in Table 7. The overall cost reduction in the Flight System element by introducing the printable lander is \$34M, using the conservative assumptions.

Table 7 Flight System WBS Cost Comparison Traditional vs Printed

<i>Traditional Mission</i>							<i>Printed Mission</i>						
6.0 Flight System (\$M)						6.0 Flight System (\$M)							
6.01 Flight System Mgmt	2					6.01 Flight System Mgmt	2						
6.02 Flight System Sys Eng	18					6.02 Flight System Sys Eng	18						
Flight System	141	30	26	85	Total	Flight System	113	44	70	0	Total		
		Cruise Stage	Entry	Lander				Cruise Stage	Entry	Lander			
6.04 Power		2	0	10	12	6.04 Power		2	8	0	10		
6.05 C&DH		0	0	14	14	6.05 C&DH		9	1	0	10		
6.06 Telecommunication		8	2	21	31	6.06 Telecommunication		8	20	0	28		
6.07 Structures		8	17	10	35	6.07 Structures		8	25	0	33		
6.08 Thermal		5	7	6	17	6.08 Thermal		5	5	0	10		
6.09 Propulsion		0	0	11	11	6.09 Propulsion		5	0	0	5		
6.10 ACS		5	0	4	9	6.10 ACS		5	4	0	9		
6.11 Harness		2	1	3	6	6.11 Harness		2	1	0	3		
6.12 S/C Software		0	0	7	7	6.12 S/C Software		0	7	0	7		
NA Radar	6					NA Radar	0						
NA Aerothermal testing	3					NA Aerothermal testing	3						
6.13 M&P	1					6.13 M&P	1						
6.14 Testbeds	5					6.14 Testbeds	5						

There are two other Project WBS elements that we compared to get the overall cost comparison: ATLO (WBS10.0) and Payload development (WBS 5.0). The Assembly Test and Launch Operations (ATLO) are the costs associated with the final integration and test of the overall flight vehicle. Note that subsystem I&T is included in the subsystem costs under WBS 6.0. For the traditional lander mission, the ATLO costs were estimated at approximately \$18M. This was split into \$5M to support the cruise stage and entry vehicle integration and test and \$13M for the lander activities. We did not do a grass roots estimate for the ATLO scope of work or schedule. However, assuming all other efforts are equal, a few key elements can be deleted from the scope: lander mechanical assembly and integration (a sizable portion would be shifted to the backshell assembly), surface operations software and sequence testing, lander only thermal vacuum / vibration / mass properties testing. Based on this we took credit for a 30% reduction in the ATLO costs and estimated the printed mission WBS 10.0 at \$12M for the conservative number. A more aggressive approach would be to assume very little assembly and test time at the launch site is needed due to the simplicity of the lander payload and reduce the ATLO costs even further.

The Payload Development costs are extremely hard to estimate for such a new approach to the science platform. There are so many unknown forecasts such as the degree of manufacturing integration, fabrication infrastructure, test and verification requirements. Assumptions of technology readiness and maturity of the lander platform elements also has a high degree of uncertainty. The conservative approach, of course, would be to assume no reductions in payload costs and carry the same development costs for the instrument suite on the traditional lander which was estimated at \$30M. A “back of the envelope” estimate confirms that a printed lander development and fabrication of the many flight units could fit in that. The development costs (up through prototype development) of integrated systems with less complexity than the proposed STANLE lander have ranged from less than one million to several million dollars.² Assuming all technology is at or beyond TRL 6, and we set aside \$7M for the non-recurring design and development of the integrated STANLE lander design up through manufacturing readiness, that would leave \$23M for the fabrication and test costs of the flight units. If we assumed the maximum capacity of the Team X design (7000 lander sheets), that would give a price point of about \$3,000 for each sheet. This price point is extremely conservative and is consistent with hand assembly of each individual lander including sheet-level testing on each unit. The intent would be to optimize the design for manufacturing and test efficiencies and drive the costs per unit well below the \$3000 bogey, possibly as low as a few hundred dollars, resulting in significant reductions in payload costs. This was used in the aggressive estimate. Commercial applications of integrated sensors platforms (sensor, power, memory/logic, RFID) range from a few cents for food labels and inventory control to a few dollars per platform for building and health monitoring systems.

² Based on various integrated multifunctional platforms such as the PARC blast dosimeter, EU Cholesterol sensor, FlexTech funded projects.

The two ranges of cost savings, conservative and aggressive, are summarized in Table 8. The key finding from the Team X cost assessment study was that replacing a traditional hard lander with a collection of simple, autonomous flutter landers could result in a substantial cost savings of approximately 18% to 37% of the element compared depending on the degree of conservatism in the cost assumptions. The difference between the conservative and the aggressive numbers are taking into account the additional reductions in the flight system due to complexity components and level of effort, reducing the unit cost of the lander to a few hundred dollars, and taking additional reductions in ATLO for more streamlined launch site I&T operations.

Table 8 - Cost Comparison Summary

	<i>Traditional</i>	<i>Printed Conservative</i>	<i>Printed Aggressive</i>
<i>5.0 Payload Cost</i>	\$30 M	\$ 30 M	\$ 15 M
<i>6.0 Flight System Cost</i>	\$176 M	\$ 142 M	\$ 117 M
<i>10.0 ATLO Cost</i>	\$18 M	\$ 12 M	\$ 10 M
<i>Total Cost of Compared Elements</i>	\$224 M	\$184 M	\$142 M
<i>Cost Saving over Traditional</i>	--	18%	37%

6.4 Mass Comparison

The mass comparison is backed out in a slightly different way. We defined as an assumption of commonality that the entry mass would be the same. Essentially the mass comparison came down to whether the contents of the printed mission's entry system would fit in the same mass allocation. The traditional mission had an entry mass of approximately 564 kg (note all masses are the CBE + contingency masses from the Team X study). The accounting of the printed mission's entry system would need to include all the entry hardware from the traditional entry vehicle plus the equipment moved from the lander, the new dispensers, printed landers and any structural modifications and additions necessary to support the additional hardware. The accounting spreadsheet is shown in Table 9. As you can see, the assumption holds true and the Printed Mission's entry system does fit within the allocation.

Table 9 - Entry Mass Comparison

Entry Mass (Traditional Mission)	564	kg
Entry Mass (Printed Mission)	561	kg
<i>Existing entry system</i>	182	kg
<i>Items retained from lander</i>	56	kg
Descent communication	5	kg
C&DH elements	7	kg
Thermal hardware	6	kg
Power systems	22	kg

ACS	8	kg
Harness	8	kg
<i>New printed unique hw</i>	<i>324</i>	<i>kg</i>
Dispensers & mechanisms	156	kg
Structural Modifications	80	kg
Landers	88	kg

6.5 Summary – Scorecard

The baseline printed mission used for comparison purposes would place 7000 environmental network stations in an area of approximately 1,000 x 1000 km. This was compared to a traditional mission which would place one lander station, with a traditional payload suite, at one site. The “printed” landers would fit into the assumed aeroshell size and weight. The EDL sequence represents a lower technical risk for the printed mission by substituting a timer-based dispenser deployments and eliminating the landing radar, descent propulsion and GNC, and lander touchdown hardware of a traditional system. The overall project costs saving are estimated to be at least 18% compared to the traditional mission, but could as high as 40%. The 7000 landers represent the maximum capacity of the aeroshell for equivalent entry mass. However, if that number comes down due to science needs, the cost and mass savings will of course increase.

6.6 Alternative Implementations

Alternate architectures at a mission level are certainly possible and could potentially increase the science value or reduce the cost to get the same science return. Obviously the preferred approach for a full scale dedicated mission would be to have multiple probes with a time of arrival separation to allow global longitudinal coverage as well as entry trajectories to allow wide spread of latitudinal coverage as well. This would dramatically increase the science value of the mission by achieving global coverage. A moderate increase in complexity of the cruise stage would be required to allow multiple releases, but the entry vehicles could be much smaller and more simplistic each carrying a few hundred or a thousand landers to a region.

A second approach to the mission would be to fly the landers as a secondary payload to another mission. One dispenser could be added as a passive payload element requiring only a mechanical attachment and a release signal in the backshell. It could be designed to fit in the available space inside the aeroshell of another mission and would be opened to release the landers only after the prime payload (rover or lander) was safely released. The landers could use the primary rover or lander as a relay station as well.

7 Prototype Development and Demonstration

For an integrated platform, like a spacecraft, the feasibility issues are mostly centered on compatibility and performance. The inter-component functionality can be challenging in light of voltage requirements, thermal influence, EMI/EMC – these are issues that arise only through a “system” platform design. Therefore, we intended to focus a significant effort in Phase 2 designing and fabricating a bench top demonstration of an integrated printed spacecraft capitalizing on the expertise at Xerox PARC, a key participant in Phase One of the Printable Spacecraft task. PARC is a leading R&D organization for printed electronics. They provide design services and development of high-tech solutions for a multitude of customers. They provide custom R&D services, technology, expertise, best practices, and IP to large companies, startups, and government agency partners. As a company, they are on the leading edge of multi-functional printed systems.

We used the STANLE reference mission to guide the functional specifications and requirements for the platform. Overall the objective was to demonstrate the end to end functionality of generating continuous sensor data, storing it in memory, retrieving and transmitting the data wirelessly off a self-contained platform. PARC was asked to include at least two of the six sensors planned for the STANLE platform, demonstrate continuous operation of both sensor measurements and record a time history of each measurement, provide wireless transmission of the data off the platform, and maximize the use of printed elements using discreet components only when necessary without jeopardizing the overall thin and flexible form factor.

PARC successfully developed the benchtop prototype system and demonstrated full functionality from the sensors through the wireless transmission. Their final report is included here in Chapter 7 which describes the details of the design and construction and the system compatibility challenges they were able to overcome. The prototype spacecraft was delivered to JPL and functionality was independently verified in the lab at JPL.

Under separate funding from JPL, but as a direct follow-on to the NIAC project, PARC fabricated a second unit of the STANLE platform to fly on a student payload for a sounding rocket flight test demonstration. Demonstrating the programmatic flexibility of the digitally printed spacecraft, PARC made some layout modifications to the existing design to fit into the space allocated on the sounding rocket payload. Within weeks and at low cost, they were able to revise the design, fabricate, test and deliver a second unit. That unit is now mounted aboard the Rocksats-X student sounding rocket payload at Northwest Nazarene University awaiting launch.

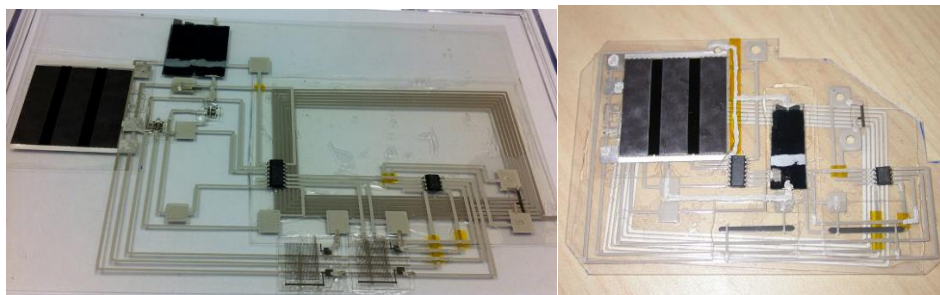


Figure 42 STANLE prototype platform NIAC version (left) Student Flight Demo version (right)

Final Report

NIAC Phase II Printed Spacecraft Project (for JPL)

Palo Alto Research Center (PARC)

6/5/14

Gregory Whiting, Brent Krusor, David Schwarz, Bob Krivacic, Tse Nga Ng, Sasha Tuganov

Introduction

For the NIAC phase II task, PARC designed, developed, fabricated, and validated a printed environmental sensor system on a flexible substrate. This approach to manufacturing such systems provides a number of benefits including low-cost, low-mass, and facile customization.

Electronics printed completely from solution readily provide these benefits, however, due to the relatively large minimum features sizes attainable with typical print techniques (typically 10s of microns) and the reduced performance of electronic materials deposited from solution, printed systems are often not currently capable of reliably delivering complex functionalities such as RF communication, general processing, or high-resolution analog-to-digital conversion.

In order to address these shortcomings, this project followed a hybrid approach that integrated prefabricated microelectronic Si-CMOS devices with printed electronic devices. This approach has the benefit of producing complex functionality without significantly sacrificing the cost, mechanical flexibility, or customizability benefits of printed electronics.

Through discussion with JPL parameters for the demonstration sensor system were determined; major requirements for the system were as follows: 1) Measurement of both temperature and irradiance 2) Maximize the number of printed components, using pre-fabricated components only when necessary 3) Wireless communication of the data 4) Mechanical flexibility of the device 5) Continuous, rather than threshold measurement.

Design

In order to achieve these requirements a system was designed to read data from a printed photosensor and a printed thermistor (organized in a resistive divider with printed resistors), and multiplexed using printed field-effect transistors. Analog-to-digital conversion and signal processing was carried out using a pre-fabricated microprocessor and wireless communication achieved through the use of an RF chip, a printed antenna and a printed network (capacitor). All components were integrated onto a mechanically flexible polyethylene naphthalate (PEN) substrate and connected using printed interconnects and other printed ancillary passive components (pull-up resistors). A schematic design of the demonstrator device is shown in Figure 43.

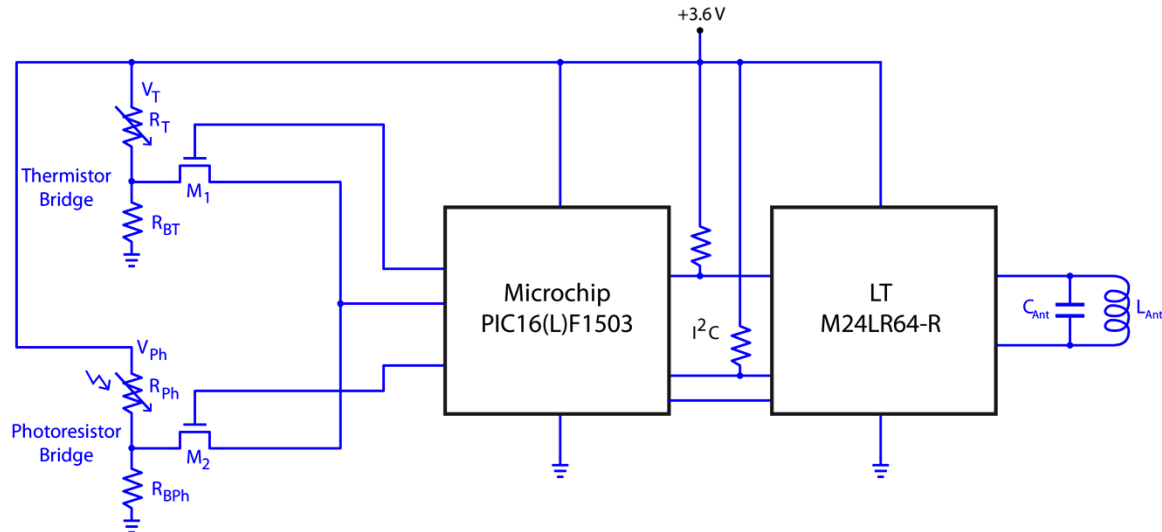


Figure 43 Schematic diagram showing the layout of the sensor system. Blue color indicates printed components, black indicates pre-fabricated components.

Other designs were also evaluated, in particular those which included a flexible microcontroller (FleX-MCU) from American Semiconductor, Inc. (ASI) (as shown in Figure 44). The clear benefit of this design is that it would include a light-weight, mechanically flexible chip (the circuitry is transferred from the Si wafer to a thin, flexible polyimide substrate). However, the functionality of the ASI chip is not sufficient for it to completely replace the PIC so it would need to be added as an additional component, with the PIC providing non-volatile memory to store the program for the FleX-MCU as well as analog-to-digital conversion. Ultimately, it was determined that incorporating the FleX-MCU into the demonstrator was outside of the scope of the project and the design shown in Figure 43 was used.

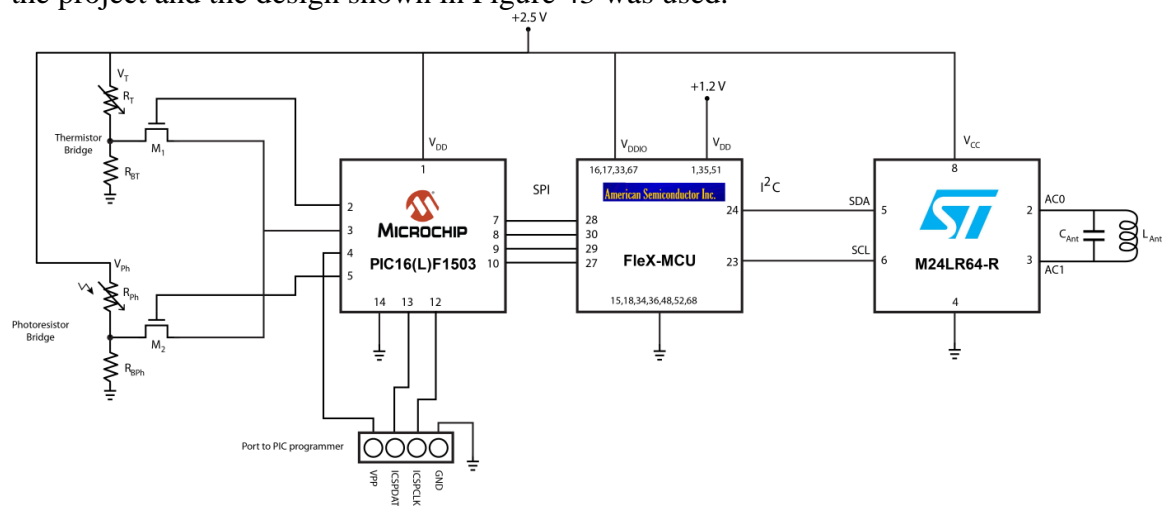


Figure 44 Schematic diagram showing a possible system layout incorporating a mechanically flexible microcontroller.

Another possible design would be to use a single chip for both ADC, processing and RF communication. We decided on this 2 chip approach as it broadened the number of readily available components, as well as allowing us to more easily debug the signals at different stages.

Important considerations for this design include electrical and mechanical integration of the chips with the printed components. For example, mechanical integration requires adhesives need

to be used that allow the substrate to flex somewhat without delamination of the rigid chips. For electrical integration a potential concern was the ADC input expecting sources of $< 10 \text{ k}\Omega$, where our sources typically are in the range of 1-10 $\text{M}\Omega$. Options to deal with this issue include using op-amps or a sample and hold chip at the input, or adding capacitors (which would increase RC time constant, and could cause leakage issues). Through device testing it was found that despite this concern it was in fact possible to provide a direct connection from the multiplexed sensors to the ADC input without the need for the suggested ancillary components.

Another significant electrical integration issue is operating voltage. Ideally we would like to use as simple a circuit as possible, requiring all components to operate at the supply voltage. Due to the low capacitance dielectrics that are typically used in printed transistors operating voltages on the order of 10-20 V are typically required. However, the supply voltage for this design is 3.6 V, necessitating printed TFTs that can be used at this supply voltage. As will be described below, a thick dielectric with higher capacitance was developed, and provided the necessary switching characteristics at the supply voltage.

Si-CMOS Components

The PIC from Microchip [PIC16(L)F1503] was chosen as it provides both a 10-bit ADC as well as a microcontroller and an I²C interface in a relatively small form factor packaged chip. The ST Microelectronics RF chip (M24LR64-R) provides for near field communication (NFC) at 13.56 MHz, a 64-Kbit EEPROM memory and an I²C bus again in a relatively small form factor packaged chip. Both chips are easily programmed and the RF chip has a further benefit of having an associated developer kit (DEMOKIT-M24LR-A) that includes a reader and corresponding software for wirelessly transferring stored data from the chip's memory. Some images of these components are shown in Figure 45.

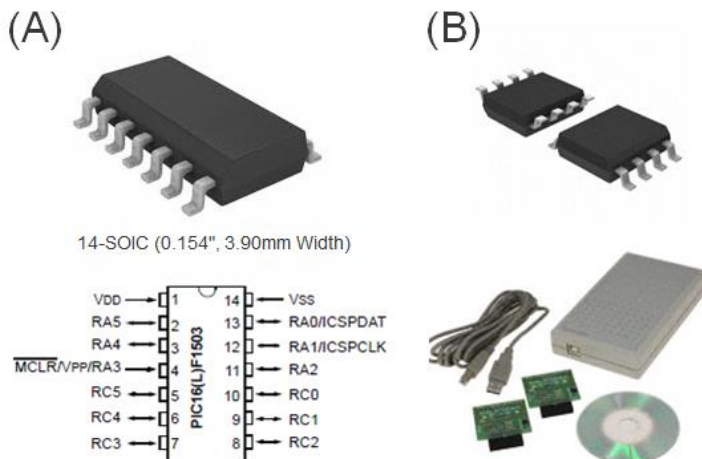


Figure 45 Si-CMOS components (A) PIC (B) RF chip and development kit including reader.

Temperature Sensor

The temperature sensor used for the system was sourced from PST Sensors. This is a resistive sensor that is fabricated by screen-printing a silicon nanoparticle ink onto screen printed silver contacts on a polyester substrate. This silver nanoparticle thermistor displays a negative temperature coefficient (NTC) -decreasing resistance with increasing temperature. On the same substrate a carbon resistor was also screen-printed to form a resistive divider. From device-to-device the resistance varies somewhat, but both the carbon resistor and the thermistor (at room temperature) show a resistance of about 1 M Ω . Characterization of the PST temperature sensor is displayed in Figure 46, showing output of both the thermistor and the divider.

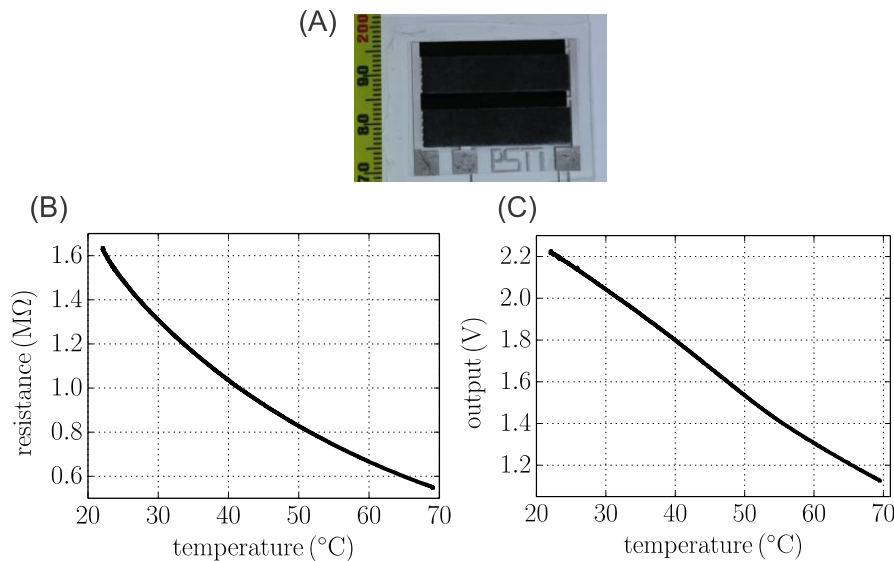


Figure 46 PST temperature sensor (A) Image of temperature sensor (B) Resistance versus temperature for the thermistor (C) Output of the resistive divider (3.6 V input).

Photosensor

Two different options were evaluated for the photosensor. Initial experimentation used a simple photoresistor fabricated by ink-jet printing a p-type organic semiconductor over ink-jet printed silver interdigitated contacts. While this device is photoresponsive, and benefits from being a very simple design, it shows quite low sensitivity. Furthermore, the response is slow [likely due to the charge transport mobility of the semiconductor and the large gaps between electrodes (~35 μ m)] causing the sensor response to drift over time. Saturation, in some cases, could take on the order of minutes, which significantly limits the utility of the photosensor. The response of this photoresistor as well as a resistive divider incorporating the photoresistor and a printed carbon resistor is shown in Figure 47.

Ultimately it was found that this simple photoresistor architecture was not suitable for the sensor system due to low sensitivity. In order to improve the performance of the photosensor we moved to a vertical bulk heterojunction (BHJ) device which is a diode structure that uses a printed blend of electron donating and accepting materials between a reflecting and transparent electrode. The BHJ structure separates the electron and hole from light induced excitons at the distributed acceptor/donor interface. These separated charges are then transported to and collected at the

electrodes. This system is very well known for organic solar cells and organic photodiodes. The photodiode used for this project was supplied by the Arias group at UC Berkeley and is based on a stencil printed polymer:fullerene (PTB7:PC₇₀BM) blend, sandwiched between a printed PEDOT:PSS anode and an evaporated aluminum cathode. These photodiodes show suitably low dark currents (~10 nA/cm² at -1.5 V) and a predictable sensitive response over many orders of magnitude of irradiance (Figure 48). This photodiode had an active area of about 3 mm² leading to resistances in the MΩ range at irradiance values of interest. The photodiode was combined with an ink-jet printed carbon resistor (~1.5 MΩ) to form the final resistive divider photosensor.

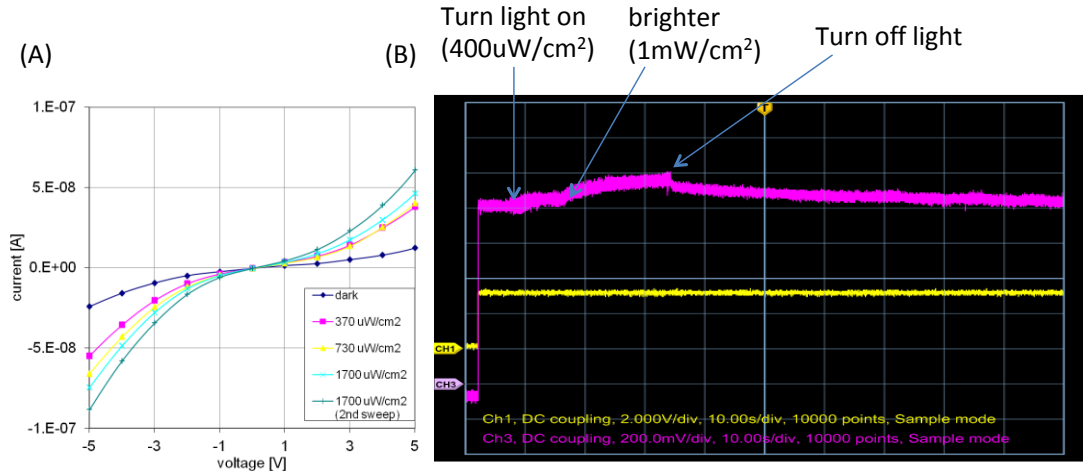


Figure 47 Photoresistor-based photosensor (A) Photoresistor response (B) Response of resistive divider with photoresistor and a printed carbon resistor (pink line is the divider output and yellow line is the supply voltage (3 V)).

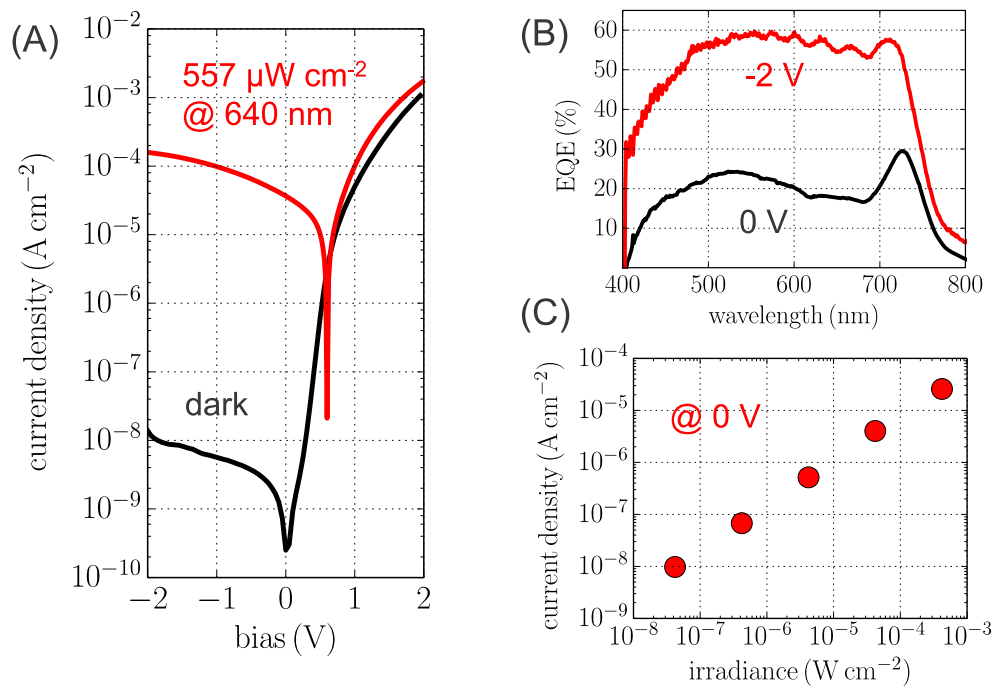


Figure 48 UC Berkeley BHJ photodiode. (A) JV curve for the sensor in the dark and illuminated by 640 nm light at 557 μW cm⁻². (B) Photodiode action spectra at short circuit and in photodiode mode at -2 V. (C) Current density versus irradiance response taken at 0 V and 640 nm illuminance.

Multiplexing Transistors

Printed field-effect transistors were used to multiplex the signal from the two sensors. The TFTs were ink-jet printed and were based on a p-type organic semiconductor. Since they should operate at the supply voltage for the sensor system (3.6 V), it was necessary to use a dielectric that provided reliable gate isolation, a low-energy interface to ensure good charge-transport properties and a capacitance high enough to allow operation at these voltages. Typically, dielectrics for printed TFTs have a thickness on the order of 0.5-1 μm to ensure isolation of the gate and a low k to reduce dielectric disorder at the interface, preventing charge trapping. Perfluoropolymers are often used as a dielectric for top-gate organic transistors as they provide a low energy interface and solvent orthogonality with most solution processed semiconductors. However, at the thicknesses typically used, these materials give areal capacitances on the order of 3-5 nF cm^{-2} , requiring operating voltages typically from 10-20 V.

In order to reduce the operating voltage, we used a bilayer fluoropolymer dielectric stack with a thin low- k interfacial layer and a thicker high- k layer making up the bulk of the dielectric. The total thickness for this dielectric was $\sim 1 \mu\text{m}$ with an areal capacitance of $\sim 25 \text{ nF cm}^{-2}$, providing effective switching at the system supply voltage (Figure 49).

The ability of these TFTs to switch the sensor signal at 3.6 V was tested (Figure 50), showing that by modulating the gate at the supply voltage the sensor signal could either be passed or blocked, suggesting that these TFTs are suitable for multiplexing the sensor signals.

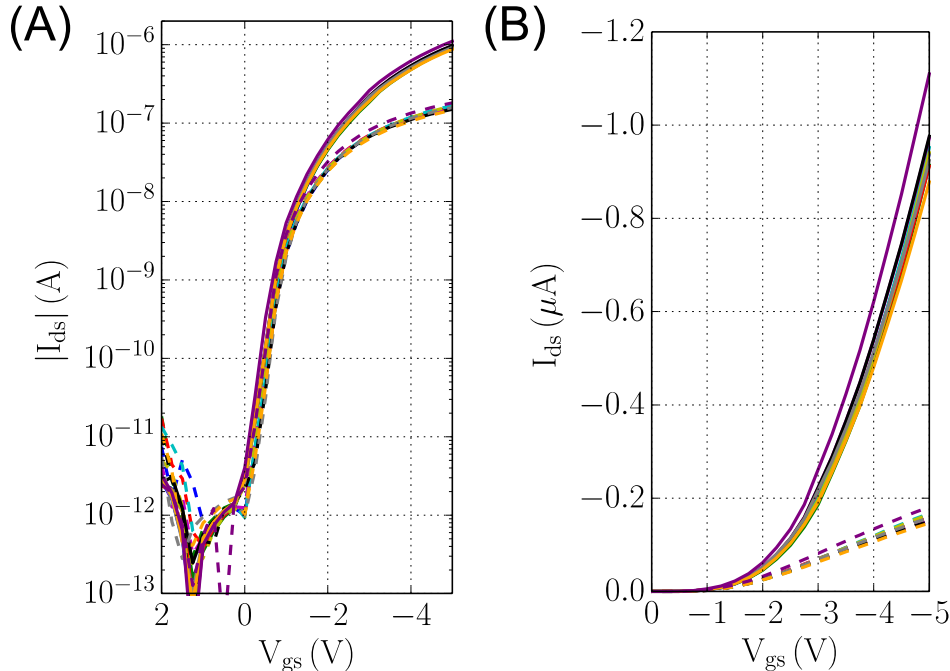


Figure 49 Field-effect transistors for signal multiplexing (A) Semilog plot of transfer characteristics for 10 printed FETs taken at $V_{ds} = -0.5$ V (dotted lines) and $V_{ds} = -5$ V (solid lines). (B) Linear plot of transfer characteristics for 10 printed FETs taken at $V_{ds} = -0.5$ V (dotted lines) and $V_{ds} = -5$ V (solid lines).

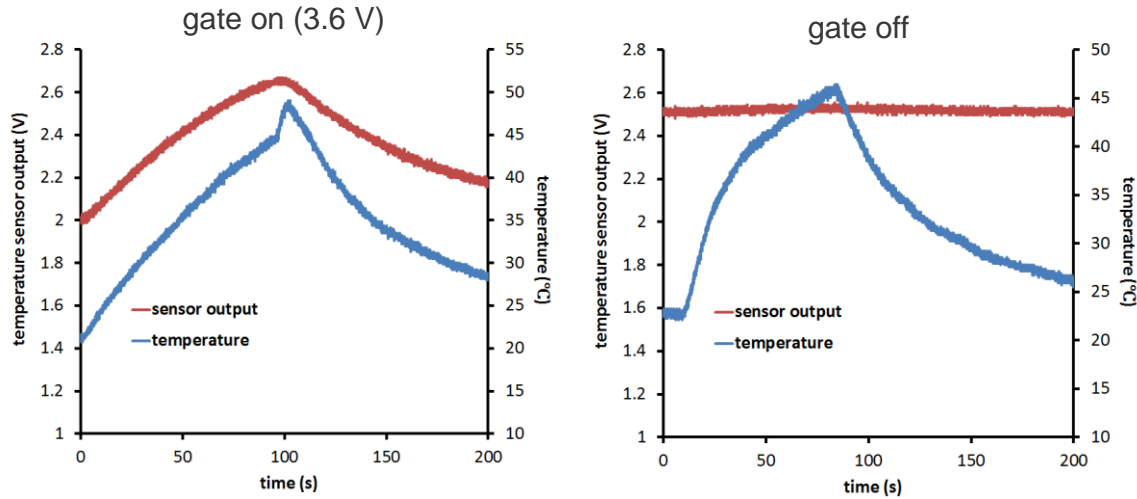


Figure 50 Control of sensor signal using printed TFTs. Left plot shows the temperature sensor output (red line) and temperature (blue line) when the TFT gate is turned on (3.6 V). The right plot shows the temperature sensor output (red line) and temperature (blue line) when the TFT gate is turned off.

Passives

A number of passive devices are also required for the sensor system. This includes a 13.56 MHz antenna, resistors for the photosensor divider, pull up resistors, and a capacitor for the antenna network.

In order to maximize the antenna performance, the total coil resistance should be $< 50 \Omega$. Coils fabricated using ink-jet printing showed resistances higher than this ($\sim 100 \Omega$), primarily due to the low thickness of the ink-jet printed traces ($0.5 - 2 \mu\text{m}$). As the line width of the antenna is relatively large, lower resolution printing techniques can be used (such as extrusion). We found that extrusion printing of a silver paste was appropriate for antenna fabrication as it can readily provide thicker traces (10s of μm), which gave an antenna resistance of $< 50 \Omega$ (typically $\sim 25 \Omega$). Tests with this antenna gave a maximum reading distance of $\sim 7 \text{ cm}$. Figure 51 shows an example of a printed antenna as well as a simulation indicating the effect of increasing trace thickness (decreasing resistance) on the antenna characteristics.

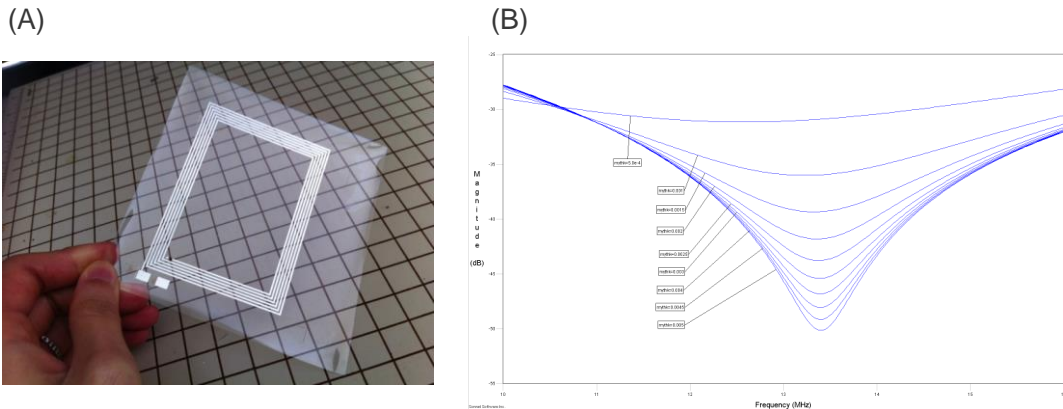


Figure 51 (A) Image of printed antenna. (B) Simulation showing the effect of increasing trace thickness (decreasing resistance) on the antenna resonance.

A number of other passive components are needed. These include a capacitor for the antenna that was fabricated using the transistor dielectric sandwiched between two printed silver electrodes. The resistor for the photosensor divider requires a fairly high resistance ($\sim 1.5 \text{ M}\Omega$) was ink-jet printed from a carbon nanoparticle ink (which allows for thin, finely patterned higher resistance traces), and the lower resistance ($\sim 4.7 \text{ k}\Omega$) pull-up resistors were ink-jet printed from a silver nanoparticle ink using a serpentine design.

PCB Test Setup

In order to test the circuit layout, the printed components and to program the chips a PCB version of the sensor system was designed and built, and demonstrated full system functionality (Figure 52 and Figure 53).

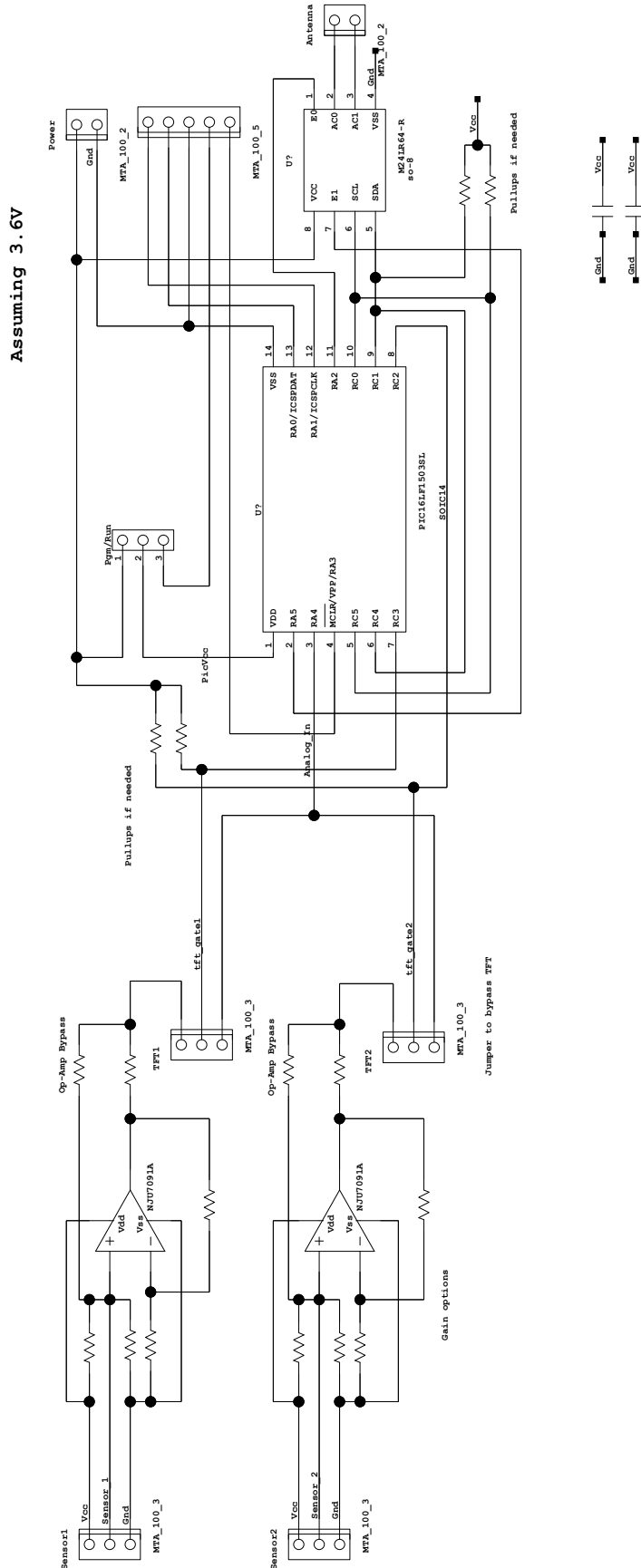


Figure 52 PCB tester schematic

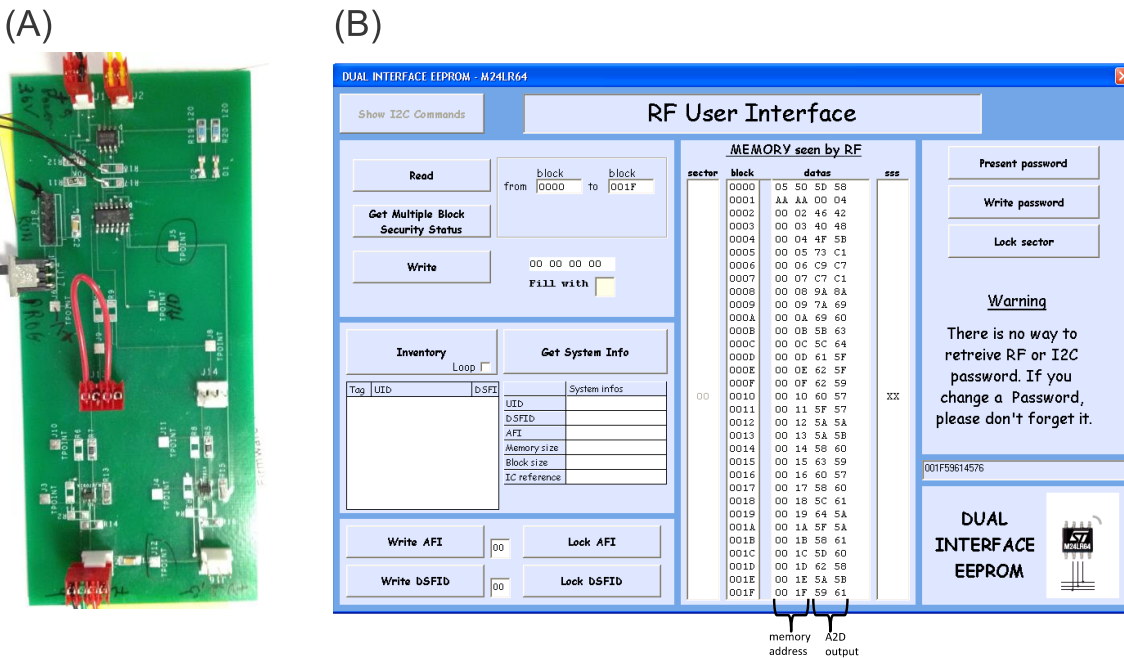


Figure 53 (A) Test board. (B) Software interface for reading RF chip memory.

System Fabrication

Integration of the printed components was completed by first printing the interconnect layout onto a PEN master substrate using extrusion printing of a conductive silver ink. Where necessary cross-overs were provided using kapton tape to isolate the underlying interconnect, followed by connection using silver paint. Once the master layout was complete pre-programmed chips and pre-tested printed components were adhered to the master substrate using epoxy adhesives and interconnected using silver paint. All components were attached to the same face of the PEN substrate except the antenna which will be placed on the opposing face, and attached to other circuits using a via interconnect through the substrate. A list of the individual components and their fabrication methods is shown in Table 10.

A number of methods were evaluated for attaching the chips to the PEN surface, including anisotropic conductive adhesives (which provide for both attachment and interconnection) as well as using a non-conductive epoxy adhesive to fix the chip to the surface. Ultimately, the latter approach was used as the anisotropic conductive adhesive proved unreliable as an interconnect (occasional open circuit between the printed interconnects and the chips). Figure 54 shows an example of a PIC adhered to a PEN substrate.

For this project 2 systems were produced. This second pass was necessary since the PIC needed to be reprogrammed multiple times in order to correct the timing of the gate pulses to the multiplexing TFTs (longer gate pulses were required in order to reduce cross-talk between the two sensors). Repeated removal and reattachment of the PIC onto the 1st sensor system caused damage and required a 2nd (final) device to be built (this 2nd system was delivered to JPL) (Figure 55).

Table 10 Fabrication methods and materials for the various components of the sensory system.

Component	Purpose	Fabrication Method	Active Material
<i>Active components</i>			
Field effect transistor	Sensor signal multiplexing	Ink-jet printed	Organics
Photosensor	Light sensing	Stencil Printed	Organics
Thermistor	Temperature sensing	Screen printed	Si nanoparticles
PIC microcontroller	A2D conversion, data processing	Pre-fabricated	Si CMOS
RF chip	Wireless communication, memory	Pre-fabricated	Si CMOS
<i>Passive components</i>			
Capacitor	Antenna impedance matching	Ink-jet printed	Organics
kΩ resistor	Pull-up resistors	Ink-jet printed	Ag nanoparticles
MΩ resistor	Sensor signal conversion	Ink-jet & screen printed	C particles
Antenna	Wireless communication	Extruded	Ag particles
<i>Others</i>			
Conductive tracks	Electrical interconnection	Extruded	Ag particles

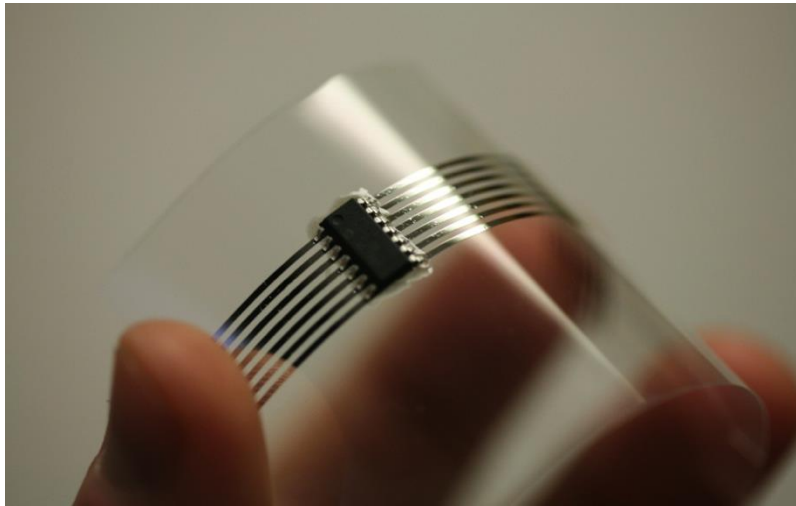


Figure 54 PIC on PEN surface with printed interconnects.

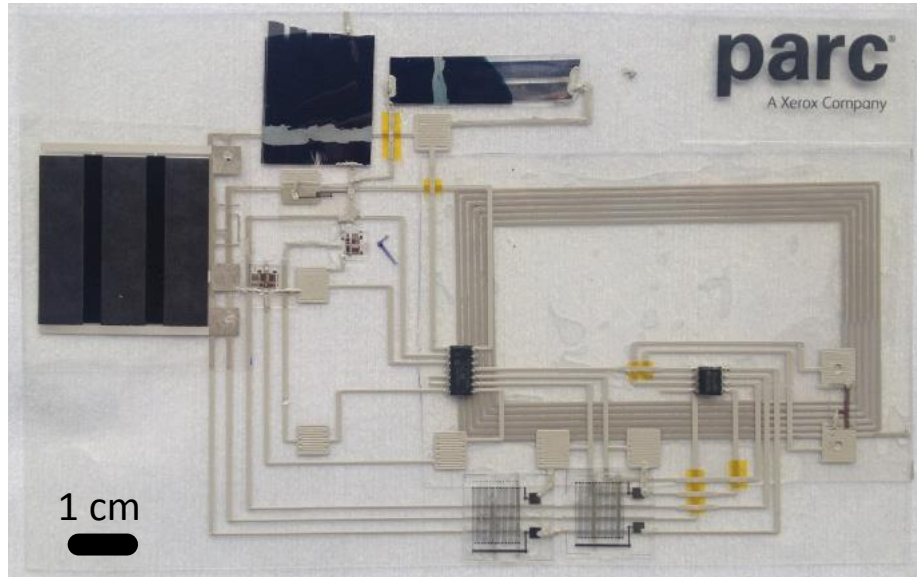


Figure 55 Image of the completed sensor system.

System Testing

The completed sensor system operates as follows 1) Start up and initialization. 2) 300 ms 3.6 V pulse applied to the gate of the multiplexing TFT of sensor 1. 3) At the end of the pulse 4 readings taken sequentially for sensor 1. 4) Average of these 4 sensor 1 measurements recorded to memory. 5) brief wait. 6) 300 ms 3.6 V pulse applied to the gate of the multiplexing TFT of sensor 2. 7) At the end of the pulse 4 readings taken sequentially for sensor 2. 8) Average of these 4 sensor 2 measurements recorded to memory. 9) Wait until 1 s since previous measurement set was taken (~300 ms). 10) repeat steps 2-9 for duration of experiment. 11) Wirelessly read data from the RF chip. 12) Process data. See Figure 56 for an illustration of the gating signals.

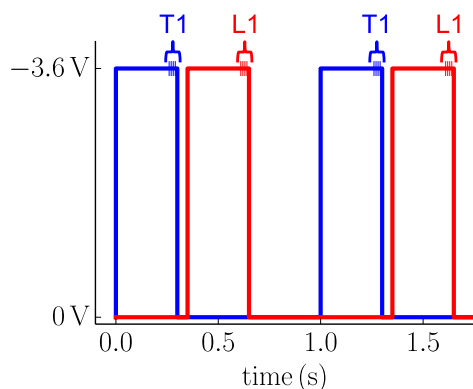


Figure 56 Gating signals for the multiplexing TFTs for the temperature sensor (blue line) and the photosensor (red line) T1 & T2 are the 1st and 2nd measurements taken from the temperature sensor and L1 & L2 are the 1st and 2nd measurements taken from the photosensor.

The system was tested and calibrated by running experiments where the sensor system was exposed to heat and light (broadband incandescent source through a 500 nm filter), of various levels over the course of about 20 minutes. After the experiment was complete the data was read

off wirelessly from the system. Data from one such experiment is displayed in Figure 57 and shows that the system is operating as expected with minimal cross-talk between the sensors. Assuming a linear response over the irradiance and temperature range gives a sensitivity for the system of $\sim 0.7\text{ }^{\circ}\text{C}$ and $2.5\text{ }\mu\text{W cm}^{-2}$.

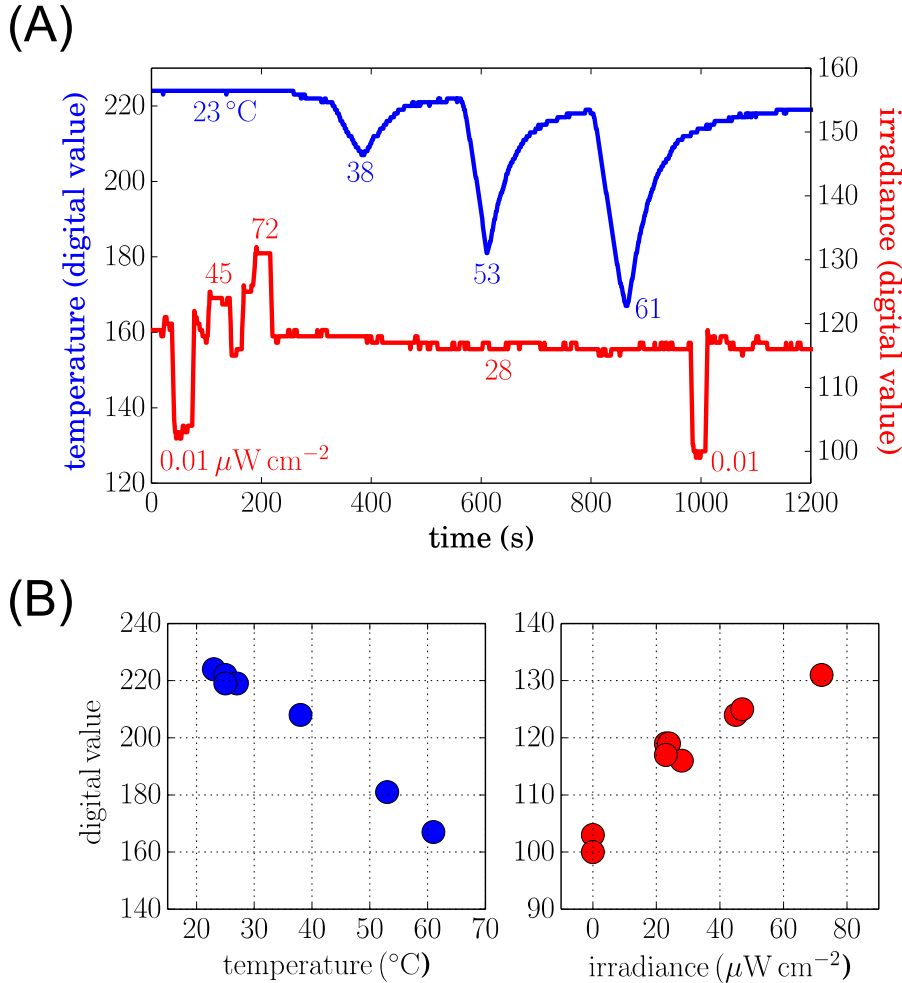


Figure 57 Sensor system characteristics (A) Irradiance (500 nm light, red line) and temperature (blue line) data taken from sensor system. (B) Calibration data for temperature (blue points) and irradiance (500 nm light, red points).

Summary

This study developed and demonstrated a sensor system able to measure both temperature and irradiance with good accuracy using a wireless readout by following a hybrid approach that integrated printed electronic devices with pre-fabricated Si-CMOS components. This approach enabled fabrication of device with improved performance when compared with electronic system prepared entirely from solution based inks with little compromise in terms of form factor, weight and print manufacturability.

8 Environmental Testing

8.1 Motivation for test program.

Some of the most interesting places in the solar system also pose the most challenging environments. Methane atmospheres, caverns with no sunlight, liquid nitrogen temperatures, and crippling radiation. How robust are the materials and construction of common printed electronics to the demands of space? Environmental compatibility with these harsh demands represents a critical aspect of the technical feasibility of printed electronics in space. The effects of these extreme conditions on basic survivability, mechanical and electrical properties and device performance are largely unknown. For some of the basic materials, vacuum outgassing properties or physical properties over temperature ranges can be found, specifically high temperature performance as that is driven by the demands of curing during fabrication. However, little data can be found for some of the materials at the low temperatures required for space mission applications. Additionally at the device level, very little is known about the adequacy of the inter-layer adherence or device performance under vacuum, thermal cycling and radiation. A literature search was performed using the technical documentation services at JPL which confirmed the scarcity of the necessary data set in the public domain to validate the technical feasibility of printed electronics longevity in the space environment.

There has been some radiation testing done of thin-film transistors (TFTs) under space radiation environments. In one report by Dr. Erik Brandon at JPL, he discussed the performance of two types of TFTs on polyimide substrates using hydrogenated amorphous silicon (a-Si:H) and pentacene under radiation conditions. The devices were exposed up to 1 Mrad total dose after which mechanical and electrical properties were characterized, then the devices were annealed at high temperature and re-characterized. Channel carrier mobility and threshold voltages for the different devices were determined from the data. The results indicated that shifts in the a-Si TFT parameters do occur upon irradiation, but that performance can be recovered via thermal annealing. For the pentacene TFTs, the data indicates that the normalized mobility decreased up to 50% upon exposure to the x-ray radiation.⁴⁷ The data generated from Dr. Brandon's testing is valuable in that it augments the sparse data set that exists for the radiation effect on flexible thin film electronics. This is especially true for the emerging field of organic printed electronics.

8.2 The Test Program

The test program conducted as part of the NIAC task intended to show whether there are fundamental survivability issues with the printed elements and materials in the STANLE platform under the driving environmental conditions of the reference mission at Mars. Common ink/substrate combinations are considered as well as some representative functional devices. If after exposure to relevant environment, the device functionality has shifted, it indicates an area deserving further experimentation. The intent is to use the limited data set generated from the NIAC test program to inform subsequent testing and materials developments. The test conditions and testing protocol shown in Figure 58 Environmental Testing Protocol was established to be representative of the condition the STANLE lander would see during the reference mission. The critical driving environments for a Mars lander would be the exposure to vacuum during cruise, the diurnal thermal cycling on the surface and ultimately exposure to absorbed radiation.

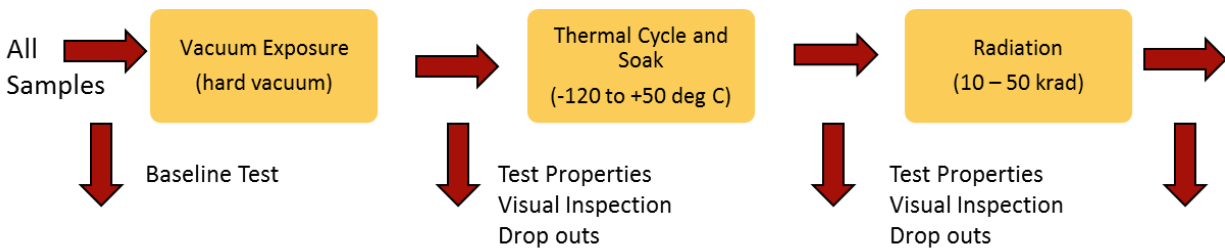


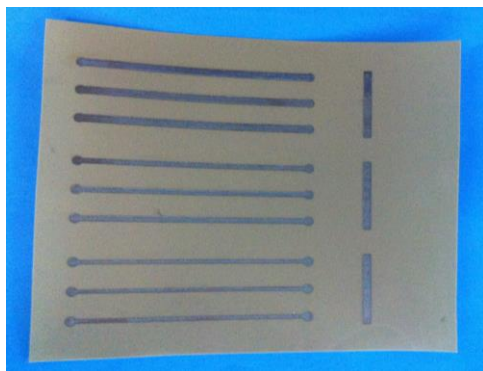
Figure 58 Environmental Testing Protocol

Jeff Duce, from Boeing Research and Technology, was responsible for conducting the test program. Due to their own internal research, development and applications in printed and direct write electronics, they have significant experience with testing printed systems for “extreme environments”. Boeing possesses the on-site facilities and equipment needed to perform the tests required for this program including the Boeing Radiation Effects Laboratory (BREL) for radiation exposure. Instrumentation and test equipment are available within all Boeing labs and research facilities. Boeing has a long history and is considered a world leader in materials characterization and testing.

A peer review was held prior to fabricating the test samples and initiating the test program. Technical experts from JPL and Caltech in materials, radiation testing, electronics, and mechanical test labs participated. Jeff Duce and the Boeing test lab staff participated. The peer review confirmed we had a sound program. Two recommended changes were to increase the time in vacuum to “overnight” and to stop the radiation exposure at 10 krad for a visual inspection and then proceed to 50 krad for extreme survivability.

8.3 Test Samples

Both materials coupons and functional elements were included in the test. The materials samples were fabricated in Dr. Sergio Pellgrino’s lab at CalTech by John Steeves. Three substrates and two inks were used to make six materials test coupons. Each fabricated coupon had multiple ink traces of various widths, as well as some cutaway patches for use in the mechanical stiffness testing. A representative photograph of a PEEK sample is shown in Figure 59.



Coupon #	Substrate	Ink
#1	PEN 250µm thick	Methode 9104 (Ag)
#2	PEN 250µm thick	Methode 3804 (Carbon)
#3	PEEK 200µm thick	Methode 9104 (Ag)
#4	PEEK 200µm thick	Methode 3804 (Carbon)
#5	Kapton 125µm thick	Methode 9104 (Ag)
#6	Kapton 125µm thick	Methode 3804 (Carbon)

Figure 59 Materials Test Sample Coupons (PEEK/9104 shown in photograph)

All materials samples were all fabricated on a Dimatix DMP-2831 piezoelectric ink jet printer. Substrate materials included Victrex PEEK (APTIV 1000), Tejin Dupont Teonex Q51 PEN, and Dupont Kapton (HN). The inks were both from Methode – M9104 silver nano-particle conductive ink and M3804 carbon nano-particle resistive ink. Three print layers were used for each trace. The M9104 ink was applied at 1 pL/drop whereas the M3804 ink was applied at 10pL/drop. The materials coupons were cured at 200 degC for an average of 90 minutes to achieve adequate electrical properties. It is noted that 200 degC is higher than the glass transition temperature of the PEEK and PEN, but no notable material changes were observed upon removal from the oven.³

The functional device samples were provided by PARC. Four of the PST thermal sensors from the prototype build lot were provided. Three arrays of the low voltage field effect transistors similar to those used in the prototype build were provided. Two organic solar cells were fabricated and furnished by USC. Two IGZO transistors on a Si wafer were supplied. The functional samples were characterized by PARC prior to the test program. At the time of this publication, the post exposure characterization is still on-going. Results are expected to be published when the data is available. The solar cells were exposed only to the radiation environment to isolate its effect on performance.

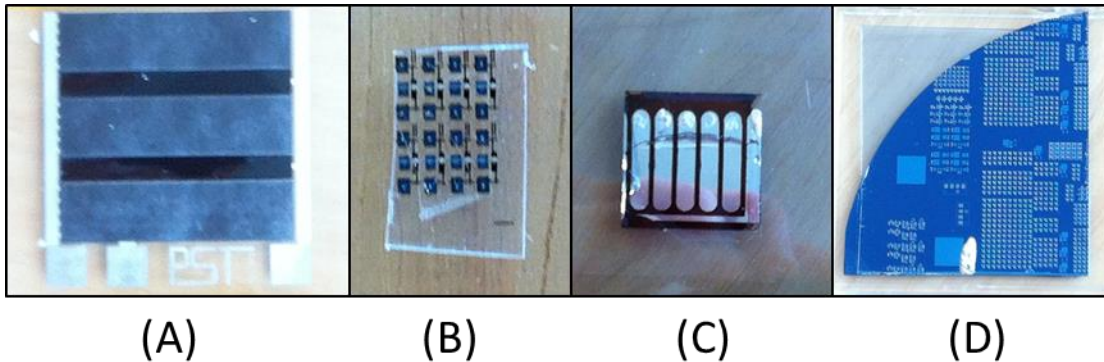


Figure 60 Functional Test Samples (A) temperature sensors (B) transistor arrays (C) organic solar cells (D) IGZO transistors

8.4 Results

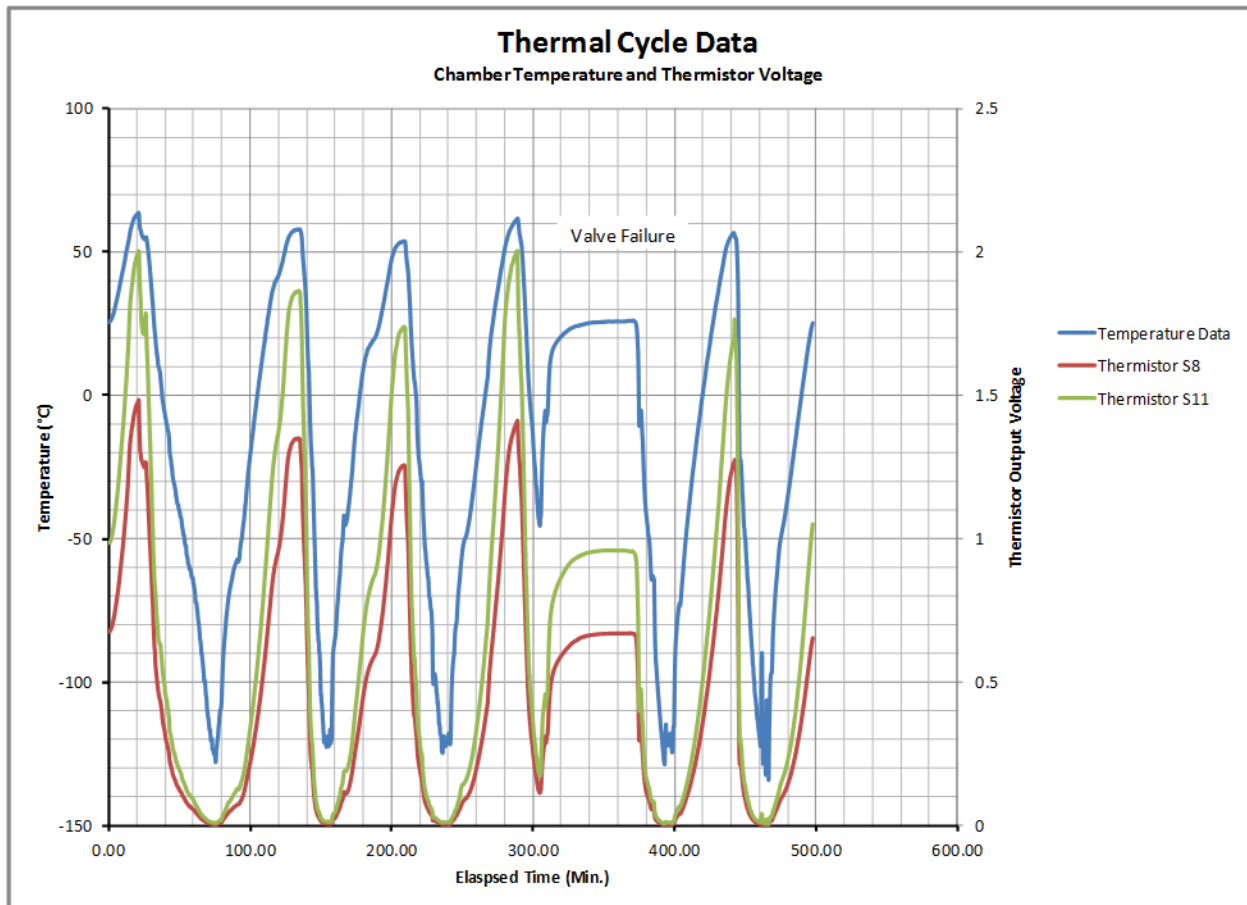
The full test program final report furnished by Boeing, complete with photographs, data and graphs, is included as an appendix in this report. Summarized results and conclusions are included here in this Chapter.

Vacuum Exposure: The samples, not including the solar cells, were exposed to vacuum conditions for a total of 15 hours. There was no noticeable visible change in the samples. There was no significant change in resistance of the materials samples (-0.3%).

³ Manufacturing notes supplied by John Steeves, Caltech.

Thermal Cycling: The samples, not including the solar cells and IGZO transistors, were exposed to thermal cycle testing between -120 deg C and +50 deg C. Sample were held at each temperature extreme for 5 minutes each cycle. A total of 5 cycles (high and low) were applied. A couple test anomalies occurred. The PST temperature sensors were wired up during the test to measure and correlate their output to the test chamber thermistor. During test set up, some of the leads disbonded from the substrate and pulled the printed pad from the substrate. Also, during the fourth cycle the coolant valve on the chamber froze. Once the ice was removed, testing continued. As can be seen in the plot, the two thermistors tracked the chamber temperature cycle with good correlation, however, the absolute measurement values differ between the PST sensors and the chamber. This could be attributed to gradients in the chamber or humidity effects on the sensor material.

The resistance measurements showed very little change due to thermal cycling. The ink on one of the Kapton substrates started to disbond upon application of pressure with the measurement probes.



Radiation Exposure: All samples, including the solar cells and IGZO transistors, were exposed to gamma radiation levels up to 50 krad. The samples were removed after 10 krad for a visual inspection and then were re-exposed to reach total dose of 50 krad. Other than the expected discoloration on the Si wafers, no visual or physical degradation was noted in the samples (e.g.

further disbonding of inks) after exposure to radiation. Also, very little change in resistance was measured in all traces except one. Trace #1 on Coupon #6 saw an increase of 11% in its resistance measurement. No obvious source for this anomalous reading could be detected.

Tensile Tests: Initial tensile tests were performed on patch samples of each of the substrates with and without an ink trace prior to exposure to any environments. These tests were repeated after exposure to all environments. Almost all tensile test coupons saw a reduction in stiffness after exposure to the environments, ranging from almost negligible to over a 12% reduction. One sample saw a slight increase in stiffness. The presence or absence of an ink trace did not have a consistent effect on the amount of reduction nor did the thickness of the substrate.

Table 8-1: Stiffness Measurements

Coupon	Pre-test		Post Test		Percent Change
	Average Stiffness (N/m)	Average Stiffness (lbf/in)	Average Stiffness (N/m)	Average Stiffness (lbf/in)	
#1 w/ Trace	666,900	3,808	627,810	3,585	-5.9%
#1	679,679	3,881	673,991	3,849	-0.8%
#2 w/Trace	681,702	3,893	636,549	3,635	-6.6%
#2	681,171	3,890	615,088	3,512	-9.7%
#3 w/Trace	240,061	1,371	225,163	1,286	-6.2%
#3	252,743	1,443	235,999	1,348	-6.6%
#4 w/Trace	202,898	1,159	203,526	1,162	0.3%
#4	240,527	1,373	213,515	1,219	-11.2%
#5 w/Trace	327,766	1,872	325,350	1,858	-0.7%
#5	314,395	1,795	334,280	1,909	6.3%
#6 w/Trace	343,849	1,963	340,657	1,945	-0.9%
#6	389,366	2,223	340,657	1,945	-12.5%

Conclusions: It appears that no single environmental variable caused dramatic changes to either the substrate or the conductive traces. Stiffness seems to have reduced nominally. When looking at the total trace resistance difference between pre-test and post-test, there does seem to be some significant change in resistance especially in the wider traces, but it is not a consistent change. Some have increased resistance and some decreased, there doesn't seem to be any clear patterns.

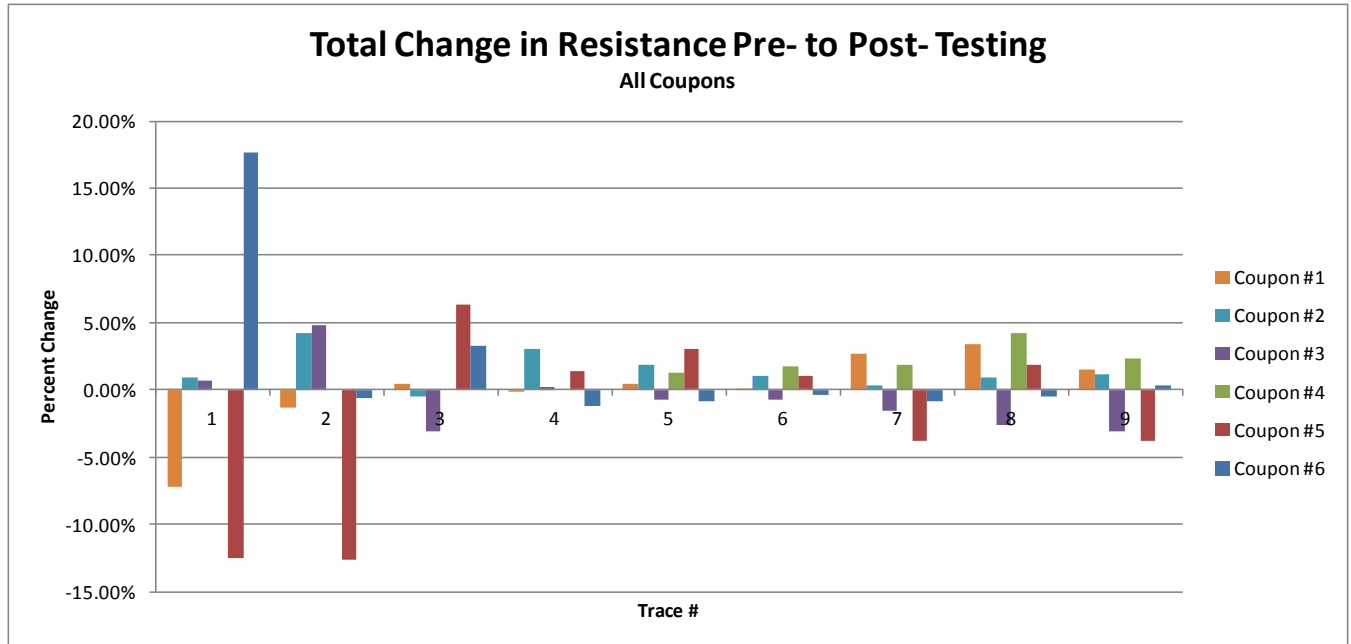


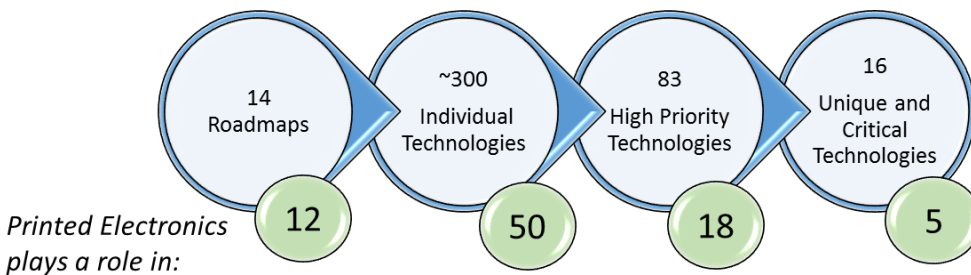
Figure 61: Total Resistance Change After Testing

In conclusion, printed electronics could feasibly be used to create devices which would survive the space environment. More research would be required to ensure that entire printed systems would also survive and function as expected. More test coupons, functional systems during exposure and a broader test regime would be a good next step in the development of printed spacecraft. Recently, Ian Markon from South Dakota School of Mines and Technology was selected as a NASA Space Technology Fellow working with JPL to continue to expand the materials evaluation and test program for printed electronics in the space environment.

9 Roadmaps

9.1 NASA Technology Roadmaps and Applications for Printed Electronics

Roadmaps are critical tools to help guide and motivate the progress of any technology. NASA has a well-constructed set of 14 Technology Area Roadmaps recently analyzed and prioritized by the National Research Council.⁶¹ This NIAC report began with the word “universal”. In looking at the NASA roadmaps, the word becomes even more apropos. In their assessment, the NRC mapped the roughly 300 “level 3” technologies against the NASA exploration goals and synthesized these 300 technologies into two tiers of importance. The first grouping represents 83 technologies considered “high-priority”. The second group boils this down even further to 16 unique and critical technologies. Looking at this comprehensive set of needs and technology solutions, printed electronics could be part of the solution in a surprisingly large number of areas.



9.2 Printed Electronics Technology Area Roadmap

The NASA roadmaps are defined by functional areas (e.g. space power and energy storage) with specific technologies (e.g. low mass solar power) that would address the global advancement in that functional area. Coming from the other direction, a different kind of roadmap can be constructed with an integrated view of a specific technology and the advancements needed to serve many functional areas. Examples would be a composite structures roadmap, an electric propulsion roadmap, or a printed electronics roadmap. The field of printed electronics (for space) is built on a foundation of several major themes: sensors, materials compatibility, device level functionality, manufacturing and verification. Advancing some or all of these areas will deliver capabilities that can be integrated and applied to find specific solutions to many problems whether they are smart habitats, dexterous manipulation, or lightweight solar power. These major themes make up the “swim lanes” of a technology area roadmap focused on advancing the general field of printed and flexible hybrid electronics for space (see

The following Figures are 11x17 fold outs provided at the end of the report

Figure 62).

The first swim lane is sensors. It’s all about measuring something – an environment, feedback for closed loop control, or structural health to avert failure. There is already a broad suite of sensors developed for terrestrial applications. The NASA investment would be to make the sensitivity, stability and robustness in line with the space application needs. Also, there are unique instruments that may not have a commercial drive. A light weight ground penetrating

radar may not be cost effective on Earth, but when every kilogram counts in launch mass, it may be very cost effective for NASA.

Materials compatibility is critical for this roadmap. Without the fundamental knowledge of design allowables and limitations designs for printed system cannot be optimized. Government investments into materials databases and registry to generate and disperse data in the extremes for the space environment is critical. Materials compatibility testing and development make up the second swim lane.

The third swim lane is engineering device performance. This is most certainly a collaborative effort across the field with all players in printed and flexible electronics – government, industry academia. Leveraging the advances made by others and finding the niche for NASA would represent the right way to focus critical funds.

Manufacturing and inspection is an important part of any roadmap. To fully realize the promise of low cost systems, more effort needs to be put into examining the tradeoff between an optimized manufacturing approach for a specific device versus a globally optimized solution. Experimentation with manufacturing reliably and in-process inspections and verification are important. This area is also one for significant partnership. With the US government focus on advanced manufacturing initiatives, NASA is in a unique position to be the “public” in Public-Private partnerships. Another critical component of the manufacturing swim lane is the in-space manufacturing. Printed electronics offers the same promise as the 3D additive manufacturing for in-situ production. It can produce a plethora of devices from a common set of stock materials. It offers the same responsiveness to need that is required for efficient logistics in support of human exploration. Development and testing of in space variants of the printed and direct write manufacturing tools represent a critical element of this piece of the roadmap.

Other critical elements of a focused roadmap, and shown at the top of Figure 62, include application development and design methods and standards. A healthy part of keeping a technology program relevant is to keep in touch with the applications and customers you are trying to serve. While it’s not a technology development, it is an important activity that can help guide the specific investments. In addition, system integration and design methods are valuable contribution the government can make. In such an “immature” industry where everyone is trying to gain a foothold, there hasn’t been a push to develop design standards or even part standardization. Design rules and best practices would certainly move the collective industry forward. For example, what are the best practices for designing around the variability in the TFT performance due to ink deposition anomalies? However, that kind of knowledge can be viewed as a competitive edge and is not shared openly. Government derivation of this information makes it more broadly available to a wider set of stakeholders improving capabilities across the board.

9.3 STANLE Mission Roadmap

In order to implement the STANLE mission, there are many things that need to mature in the concept and advance the technology of the flexible printed and hybrid science platform. A roadmap of activities, funding sources and advancements needed, specifically for STANLE, will help set the pace of activities in order meet the goal of technology readiness (TRL6) by 2020.

The roadmap that has been developed for the STANLE mission is shown in Figure 63. If the STANLE mission isn't the mission worth pursuing, this roadmap can be easily morphed into one specific for a different mission by following the same construct but substituting the challenges specific to that opportunity.

The STANLE roadmap is also divided into the same basic swim lanes as the technology area roadmap, but each activity is specifically focused on a key area, all of which contribute synergistically to reaching the goal of an implementable mission in the 2024 timeframe. The first swim lane is called "Science Mission Development". This is absolutely critical. Because no "printed spacecraft" mission is on the books for any program (planetary, mars, astrophysics), science advocacy needs to be developed. Science advocacy includes not only establishing the appropriate science objectives and traceability to program goals and instrument measurements, but also to craft the appropriate scale of the target mission. The reference mission was assessed as moderate class mission, frankly, because of the availability of comparative data. But as was seen through that assessment, a single entry vehicle standalone mission may not be the right target and a multi-probe mission or mission of opportunity or secondary payload may be more suitable. The other part of science mission development is the demonstration of some of the more unusual aspects of the mission concept: the release, descent and landing of the flutter landers. The roadmap must include maturation of this critical functionality.

The second focus area, is the development of sensors and instruments. The technology gap table in Chapter 5 illustrated that the sensors and measurements have a ways to go from the lab demonstration to a calibrated and reliable instrument. This piece of the roadmap would include continued investment and development of the sensors themselves as well as considering alternatives that are compatible with the platform form factor. Other aspects of the sensor development include field testing to ensure the integrity of the measurement in the context of the platform architecture (can you accurately detect the atmosphere and surface temperatures from the platform resting on the surface). Another important aspect is the "backend electronics". Most science instruments today do a significant amount of data processing and calculations on board to derive the measurement of interest. The "low performance" printed platform is more compatible with recording "raw data" digital representations of the analogue measurements.

Space compatibility is the third general area of the roadmap. The mission specifics dictate a particular environment. As we saw from the environmental testing conducted under this NIAC task, the Mars environment may not be too challenging for the common material choices for substrates inks and devices. A broader suite of test samples is needed along with testing functionality at temperature rather than just after exposure. Life testing also is needed. Because it is likely that the overall platform will consist of separately applied elements, the adhesives to choose for this integration step need to be evaluated too.

Platform performance is an area that will need a focus from NASA. The area of top priority is the RF communications. It is unlikely that the commercial sector will pursue an RF system compatible with the needs of the UHF relay link for the STANLE mission. NASA will need to step up and leverage the investments already made in flexible electronics for RF and radar elements to produce a universal wireless printed communications relay system. Other

advancements in device performance can certainly be beneficial to the platform design and should be pursued and tracked synergistically with industry.

The last swim lane is the manufacturing. While in most missions, the attention is put on the performance of the design, for this mission manufacturing can make or break the value proposition. As we saw in the cost comparison, with a multiplier factor of thousands, any network mission needs to drive the unit manufacturing costs down. This means compatible materials, simplified layering designs and as automated processing as possible. Compatibility with roll to roll manufacturing would be ideal. Pilot production lines can be configured for the unique needs of the STANLE platform. This approach needs to be design and prototype as part of the technology readiness.

The following Figures are 11x17 fold outs provided at the end of the report

[Figure 62 - Printed Electronics Technology Focus Roadmap](#)

[Figure 63 - STANLE Mission Roadmap](#)

10 Summary and Conclusions

10.1 Summary

We believe we have addressed the NIAC program goals to study major feasibility issues of the technology with results that provide a sound basis for NASA to consider the concept for further development. By looking closely at the technical and programmatic challenges, we assessed the utilization of printed electronics in space. We specifically considered the technology in a mission context by producing a point design and a detailed analysis for the STANLE reference mission. To address the technical challenge of system integration, we designed and fabricated a hybrid printed platform that includes the functions of continuous sensor measurements, data processing and conversion and storage, and RF wireless transmission. To address the technical challenge of space environment survivability, we tested common materials and printed devices under conditions representative of space (vacuum, thermal cycling, radiation). The printed materials samples showed no substantial degradation nor did the temperature sensors. Other devices are still undergoing post-test characterization. To address programmatic feasibility, we investigated the benefits to a reference mission in terms of cost and mass. We were able to show that replacing a traditional lander with the equivalent mass of printed flutter landers saved significant cost and risk. To provide guidance on a path forward, we formulated two roadmaps - one to bring the reference mission to maturity and one to invest in progressing the technology in general. The Printable Spacecraft phase two effort accomplished everything it set out to do and more. One might be able to claim that as a result of the prototype build and environmental testing the “printable spacecraft” has moved forward from TRL 2 to a state between TRL 3 and 4. This task also inspired four successfully funded follow-on activities:

- A Rocksats-X sounding rocket demonstration of the STANLE printable spacecraft working with a student team at Northwest Nazarene University
- A NASA EPSCoR Research Initiation Grants (RIG) on printable spacecraft with Dr. Dmitri Anagnostou and Dr. Grant Crawford at South Dakota School of Mines and Technology (SDSMT)
- A NASA Space Technology Research Fellow, Ian Markon from SDSMT, who will expand the materials testing and characterization program
- A Flex Tech Alliance task awarded to Xerox PARC on integrated sensor platforms (building on the NIAC design) for terrestrial applications.

10.2 Conclusions

Conclusion can be drawn at various levels within the context of this task. On one level, the general viability of printed electronics in space, we conclude that this is a technology worth pursuing. Printed electronics should be a tool in the toolbox as commonplace as composite structure, wire EDM manufacturing, 3D printing, ASICs, cCPI backplanes, etc. It is there to offer advantages when it makes sense. While technical performance may be limiting the near term functionality, the benefits of light weight, low volume, and low cost make it valuable to pursue further.

On a second level, we can draw conclusions about the feasibility of a printed spacecraft. In the Introduction we said the answer to “can you build an entire spacecraft out of printed electronics” was yes, more or less. A printed spacecraft is an idea that redefines the term *spacecraft*. It boils it down to the basic functionality and survivability. If a printable spacecraft is defined as a multifunctional system made from printed flexible electronics, then yes it is feasible. Near term applications may start with simple engineering sensors, with more moderate term opportunities evolving into a self-contained science platform for secondary payloads or technology demonstrators. However, if you are expecting to launch a printed spacecraft off a rocket and have them orient and propel themselves to their intended destination in the solar system, then that may be a ways off.

The third level of conclusion is a critical underlying piece of the technology - the manufacturing. In essence, printed electronics is all about the manufacturing. No one is inventing new electronics, they are inventing different ways to manufacture them – digital, additive, low cost, and flexible. These are advantages that any program can align with. These new features of the manufacturing are compatible with the desires of the human space exploration program as well and offers great promise for in-situ/in-space manufacturing. Many devices can be made on demand from common stock materials – a necessity for human expansion into the solar system.

11 Acknowledgements

A significant number of people contributed to the Printable Spacecraft task and all deserve recognition and gratitude.

First we would like to thank the leadership team within the NIAC program. Jay Falker, Jason Derleth, Kathy Reilly and Ron Turner. They all should be commended for running such a valuable program, and doing it in a way that is fun, engaging and real.

The accomplishments in this task would not have been possible except for the remarkable intelligence, creativity and flexibility of the industry partners. Greg Whiting and the PARC team did an excellent job to develop such a challenging system on a shoe string budget. The team at PARC (Gregory Whiting, Brent Krusor, David Schwarz, Bob Krivacic, Tse Nga Ng, Sasha Tuganov, Janos Veres) plus partners (PST sensors, UCB, USC) did a fantastic job pulling it all together. Jeff Duce and Boeing pulled off the test program under budget and produced encouraging results. We appreciate the quality of the engineering and test facility staff personnel.

We would like to thank Dr. Sergio Pellegrino at CalTech and his student team members, John Steeves and Yamuna Phal. They were instrumental in fabricating the material test samples as well as providing other advice and guidance.

Margaret Tam and Kathleen Reising did a nice job of evaluating the aerodynamic behavior of the flutter landers and other shapes which helped inform the right choices in the point design.

At JPL, the advice and mentoring of Greg Davis and Andrew Shapiro kept us on the right path and encouraged us to keep marching. Carolyn Barela and Elly Ponce were instrumental in the financial management and placing countless procurements on a moment's notice. Emmanuel Onyegam was with us for a brief summer but was key in getting the PARC prototype set up and functional in the JPL lab facility.

Graphics support is always critical and you can never have enough talented and creative people. We would like to thank PARC for the astronaut graphic, Dan Goods and Joseph Harris for mission concept imagery. We would also like to thank Aidan Schmitgal for developing our custom "Printable Spacecraft" font used on the cover page.

12 References

1. NASA Mars Advanced Planning Group, “Robotic Mars Exploration Strategy 2007-2016”, Dan McCleese (chair and editor), March 2006.
2. “Vision and Voyages for Planetary Science in the Decade 2013-2022”, Committee on the Planetary Science Decadal Survey Space Studies Board, National Research Council, 2011.
3. Mars Meteorology Network Workshop, March 10-12, 2009, Boulder, Colorado.
4. The Value of Landed Meteorological Investigations on Mars: The Next Advance for Climate Science, 17 July 2009 (Rev. 5), Scot C. R. Rafkin and Robert M. Haberle, a report for consideration by the NRC Space Studies Board in the development of the next Planetary Science Decadal Survey.
5. IEEE 1152 Transducers’11, Beijing, China, June 5-9, 2011. “Flexible Polymer Humidity Sensor Fabricated by InkJet Printing” *E. Starke*, A. Türke, M. Krause, and W.-J. Fischer.*
6. Thesis for the degree of Licentiate Sundsvall, 2008. “Characterization of Low Cost Printed Sensors for Smart Packaging”, Tomas Unander, Electronics Design Division Department of Information Technology and Media, Mid Sweden University, SE-851 70 Sundsvall, Sweden ISBN 978-91-86073-18-3.
7. PARC presentation “Flexible and Printed Electronics for Sensors, Displays, and photovoltaics” International Workshop on Flexible and Printed Electronics, Sept 8-10, 2010, Korea. Jurgen Daniel.
8. “The Rationale for a Long-lived Geophysical Network Mission to Mars” Submitted to The Mars Panel, NRC Decadal Survey for the Planetary Sciences Division, SMD, NASA Phil Christensen, Chair; Wendy Calvin, Vice Chair.
9. Proc. Eurosensors XXV, September 4-7, 2011, Athens, Greece “Fully Printed Flexible Humidity Sensor” A.S.G. Reddy a* B.B. Narakathua, M.Z. Atashbara,b, M. Rebrosov, E. Rebrosovab, M.K. Joyce.
10. “Transparent, Optical, Pressure-Sensitive Artificial Skin for Large-Area Stretchable Electronics”, *Marc Ramuz, Benjamin C-K. Tee, Jeffrey B.-H. Tok, and Zhenan Bao, Adv. Mater.* 2012, 24, 3223–3227.
11. “Highly sensitive flexible pressure sensors with microstructured rubber dielectric layers”, Stefan C. B. Mannsfeld¹, Benjamin C-K. Tee², Randall M. Stoltenberg³, Christopher V. H-H. Chen¹, Soumendra Barman¹, Beinn V. O. Muir¹, Anatoliy N. Sokolov¹, Colin Reese¹ and Zhenan Bao^{1*}, *Nature Materials*, PUBLISHED ONLINE: 12 SEPTEMBER 2010 | DOI: 10.1038/NMAT2834.
12. “Invention allows clear photos in dim light”, Jun 3 2013, Singapore.
13. “Printed Optical Sensors : A Disruptive Technology for Industry 4.0 and Internet-Of-Things, Connected and Smart Objects, Innovative User Interfaces for Display and Consumer Products.” Presentation by ISORG at Printed Electronics 2014 Conference, Berlin April 2014.
14. “Printed Image Sensors Can Be Flexible Says Plextronics”, web article, Electronics Weekly.com
15. “ γ -Radiation Dosimetry Using Screen Printed Nickel oxide Thick Films”, K Arshak, O. Korostynska, and J. Harris. PROC. 23rd INTERNATIONAL CONFERENCE ON

-
- MICROELECTRONICS (MIEL 2002), VOL 1, NIŠ, YUGOSLAVIA, 12-15 MAY, 2002. 0-7803-7235-2/02
16. "ROVER ENVIRONMENTAL MONITORING STATION FOR MSL MISSION.", J. Gomez-Elvira, et al.
 17. "Low-cost flexible thin-film detector for medical dosimetry applications", P. Zyganski, C. Abkai, Z. Han, Y. Shulevich, D. Menichelli, J. Hesser. JOURNAL OF APPLIED CLINICAL MEDICAL PHYSICS, VOLUME 15, NUMBER 2, 2014
 18. BOUNDARY LAYER CONDUCTANCE AND LOW WIND SPEED MEASUREMENT SENSOR (WS01). Data Sheet. HuksefluxUSA Thermal Sensors.
 19. "Thinfilm Printed Ferro-Electric Memories and Integrated products", Christer Karlsson and Peter Fischer, 978-3-9815370-2-4, 2014 Design, Automation and Test in Europe Conference and Exhibition.
 20. "A 4b ADC Manufactured in a Fully-Printed Organic Complementary Technology Including Resistors", Sahel Abdinia1, et al. ISSCC 2013 / SESSION 6 / EMERGING MEDICAL AND SENSOR TECHNOLOGIES.
 21. "CEA-Liten claims first ever printed ADC made on plastic foil", web article, EETimes Europe, February 28, 2013 // Julien Happich.
 22. "The First Plastic Computer Processor", MIT Technology Review, Tom Simonite, March 25, 2011.
 23. "The Plastic Processor – Europeans announce the first organic microprocessor", IEEE Spectrum, Joseph Calamia, February 21, 2011.
 24. "An 8-Bit, 40-Instructions-Per-Second Organic Microprocessor on Plastic Foil", Kris Myny, Erik van Veenendaal, Gerwin H. Gelinck, Jan Genoe, Wim Dehaene, and Paul Heremans, IEEE JOURNAL OF SOLID-STATE CIRCUITS, VOL. 47, NO. 1, JANUARY 2012.
 25. FleX-MCU™ Microcontroller Data Sheet, American Semiconductor, May 23, 2013.
 26. FleX-RFIC™ Microcontroller Data Sheet, American Semiconductor, May 23, 2013.
 27. FleX-ADC™ Microcontroller Data Sheet, American Semiconductor, May 23, 2013.
 28. "The Mars Environmental Survey (MESUR) Network and Pathfinder Mission", McNamee, John, Cook, Richard. AIAA Conference Proceedings, 1993.
 29. "THE PASCAL MARS SCOUT MISSION", R.M. Haberle, Mars Atmosphere Modelling and Observations Workshop, January 13 - 15, 2003, Granada, Spain
 30. "MetNet Network Mission to Mars" A.-M. Harri, S. Alexashkin, I. Arrugeo, W. Schmidt, L. Vazquez, M. Genzer, and H. Haukka, Eighth International Conference on Mars (2014)
 31. "Planning for the Scientific Exploration of Mars by Humans", By the MEPAG Human Exploration of Mars Science Analysis Group, MEPAG Human Exploration of Mars Science Analysis Group (HEM-SAG), James B. Garvin (co-chair), Joel S. Levine (co-chair), January 31, 2008.
 32. "Inkjet-printed energy storage device using graphene/polyaniline inks", Yanfei Xu, et al., Journal of Power Source, Journal of Power Sources 248 (2014) 483-488.
 33. "Performance Characterization of Flexible Printed Supercapacitors", Hiong Yap Gan, Cheng Hwee Chua, Soon Mei Chan and Boon Keng Lok, IEEE 11th Electronics Packaging Technology Conference, 2009.

34. "Printed supercapacitors on paperboard substrate", Jari Keskinena,, Eino Sivonen, Salme Jussila, Mikael Bergelin, Max Johansson, Anu Vaari, Maria Smolander, *Electrochimica Acta* 85 (2012) 302– 306.
35. "Design and Characterization of Novel Paper-based Inkjet-Printed UHF Antennas for RFID and Sensing Applications", Amin Rida*, Li Yang, and Manos M. Tentzeris, 1-4244-0878-4/07 IEEE.
36. "UHF RFID Antenna: A Printed Dipol Antenna with CPS Matching Circuit and Inductively Coupled Feed", Nenad Popović, Predrag Manojlović, IEEE, Telsiks October 2009.
37. "Printed RF tags and sensors: the confluence of printing and semiconductors", Vivek Subramanian, Frank Liao, and Huai-Yuan Tseng, Proceedings of the 5th European Microwave Integrated Circuits Conference, 27-28 September 2010, Paris, France.
38. "All additive inkjet printed humidity sensors on plastic substrate", F. Molina-Lopez*, D. Briand, N.F. de Rooij, *Sensors and Actuators B: Chemical*, 2012.
39. "Printed and Flexible Sensors Forecasts, Players and Opportunities 2012-2022", Dr Harry Igbenehi and Raghu Das, IDTechEx Publication, 2011.
40. "REMS: The Environmental Sensor Suite for the Mars Science Laboratory Rover", J. Gómez-Elvira, et al., *Space Science Review*, 10 July 2012.
41. "Inkjet-Printed Nanocrystal Photodetectors Operating up to 3 μm Wavelengths", *Michaela Böberl, Maksym V. Kovalenko, Stefan Gamerith, Emil J. W. List, and Wolfgang Heiss**, *Advanced Materials*. 2007, 19, 3574–3578.
42. RFI-RQKM-2014-0022, INSTITUTES FOR MANUFACTURING INNOVATION Request for Information (RFI), Contracting Office: Department of the Air Force, Air Force Research Laboratory (AFRL) - Wright Research Site.
43. "CPI Printable Electronics - The National Printed Electronics Centre", Tom Taylor, presentation at the CIKC Event December 2012.
44. "The Pascal Discovery Mission: A Mars Climate Network Mission", Haberle, R.M. et al. NASA Technical Reports, July 2000.
45. "A Micro-Meteorological mission for global network science on Mars: a conceptual design", Steven C. Merrihew, Robert M. Haberle and Lawrence G. Lemke3, *Planetary Space Science.*, Vol. 44, No. 11, pp. 1385-1393, 1996.
46. "Aerodynamic Design for a 3-D Printable Mars Surface Lander" Kathleen Riesing and Margaret Tam, Department of Mechanical and Aerospace Engineering, Princeton University, May 2, 2013.
47. "Flexible electronics for space applications", Erik Brandon, William West, Lisong Zhou, Tom Jackson, Greg Theriot, Rod A.B. Devine, David Binkleg, Nikhil Verma and Robert Crawford.
48. Aperturen, published by Acreo AB, a part of Swedish ICT Research, 2006.
49. "Mars' Surface Radiation Environment Measured with the Mars Science Laboratory's Curiosity Rover", Donald M. Hassler, et al., *Science* 24 Vol 343 no. 6169, January 2014.
50. "γ- radiation Sensor Using Optical and Electrical Properties of Manganese Phthalocyanine (MnPc) Thick Film", A. Arshak, S Zleetni, K Arshak, *Sensors* 2002 2(5) 174-184, 2002.
51. Supposed to be the oxide radiation sensor article but the file has a copy of ref 50.
52. Thinfilm Ferro-electric Memory, Thinfilm web article, <http://www.thinfilm.no/technology-innovation/technology/>.

-
53. “Scalable, ambient atmosphere roll-to-roll manufacture of encapsulated large area, flexible organic tandem solar cell modules”, Thomas R. Andersen et al., *Energy & Environmental Science*, 2014, 7, 2925.
 54. “NREL, UCLA Certify World Record for Polymer Solar Cell Efficiency”, National Renewable Energy Laboratory News Release NR-1412, February 29, 2012
 55. “Ultrathin and lightweight organic solar cells with high flexibility”, Martin Kaltenbrunner, Matthew S. White, Eric D. Glowacki, Tsuyoshi Sekitani, Takao Someya, Niyazi Serdar Sariciftci, Siegfried Bauer, *Nature Communications*, Published 3 Apr 2012.
 56. Blue Spark Technologies data sheet, HD Series Printed Batteries, 2009.
 57. Infinite Power Solutions data sheet, Thinergy MEC100 Series, 2011.
 58. Infinite Power Solutions data sheet, Thinergy MEC200 Series, 2012.
 59. “Mars UHF Relay Telecom: Engineering Tools and Analysis”, Bradford W. Arnold, David J. Bell, Monika J. Danos, Peter A. Ilott, Ricardo Mendoza, Mazen Shihabi, 978-1-4577-0557-1/12 2012 IEEE.
 60. “Imprint Energy Secures \$6M Series A Financing Led by Phoenix Venture Partners”, web article, PRWeb, June 16, 2014.
 61. “NASA Space Technology Roadmaps and Priorities: Restoring NASA's Technological Edge and Paving the Way for a New Era in Space”, Steering Committee for NASA Technology Roadmaps; National Research Council of the National Academies, National Academies Press, 2012.
 62. “Printable Spacecraft: Flexible Electronic Platforms for NASA Missions”, Kendra Short and David Van Buren, September 2012, Phase One Report submitted to the NASA NIAC program office.
 63. Acreo Press Release, web article, <https://www.acreo.se/media/news/new-printed-low-cost-device-for-uv-light-monitoring>.

13 Appendix A – Environmental Test Report

Appendix A contains the full text, photographs and data plots of the environmental testing performed at Boeing Research and Technology.